AFOSR-TR- 89-0131

(2)

VISUAL REPRESENTATIONS OF TEXTURE

Final Report AFOSR Grant 85-0359
(September 1, 1985 - November 30, 1988)

Part I

Jacob Beck

Department of Psychology
University of Oregon
Eugene, OR 97403

Part II

Kent A. Stevens

Department of Computer and Information Sciences
University of Oregon
Eugene, Or 97403

UNCLASSIFIED

SECURITY CLASSIFICATION OF THIS PAGE

REPORT DOCUMENTATION PAGE

1a. REPORT SECURITY CLASSIFICATION	1b. RESTRICTIVE MARKINGS
2a. SECURITY CLASSIFICATION AUTHORITY	3. DISTRIBUTION / AVAILABILITY OF REPORT
2b. DECLASSIFICATION / DOWNGRADING SCHEDULE	Approved for public release; distribution unlimited.
4. PERFORMING ORGANIZATION REPORT NUMBER(S)	5. MONITORING ORGANIZATION REPORT NUMBER(S) AFOSR-TR- 89-0131
6a. NAME OF PERFORMING ORGANIZATION: Department of Psychology, University of Oregon / 6b. OFFICE SYMBOL (If applicable)	7a. NAME OF MONITORING ORGANIZATION: AFOSR/NL
6c. ADDRESS (City, State, and ZIP Code): Eugene, OR 97403-0237	7b. ADDRESS (City, State, and ZIP Code): Bldg 410, Bolling AFB DC 20332-6448
8a. NAME OF FUNDING / SPONSORING ORGANIZATION: AFOSR/NL / 8b. OFFICE SYMBOL (If applicable): NL	9. PROCUREMENT INSTRUMENT IDENTIFICATION NUMBER: AFOSR-85-0359
8c. ADDRESS (City, State, and ZIP Code): Building 410, Bolling AFB DC 20332-6448	10. SOURCE OF FUNDING NUMBERS: PROGRAM ELEMENT NO. 61102F; PROJECT NO. 2313; TASK NO. A5; WORK UNIT ACCESSION NO.
11. TITLE (Include Security Classification): Visual Representations of Texture — UNCLASSIFIED	
12. PERSONAL AUTHOR(S): Jacob Beck, Kent A. Stevens	
13a. TYPE OF REPORT: Final / 13b. TIME COVERED: FROM 9/1/85 TO 11/30/88	14. DATE OF REPORT (Year, Month, Day): December 15, 1988 / 15. PAGE COUNT: 117
16. SUPPLEMENTARY NOTATION	

17. COSATI CODES		
FIELD	GROUP	SUB-GROUP

18. SUBJECT TERMS (Continue on reverse if necessary and identify by block number): Vision, texture perception, texture segmentation

19. ABSTRACT (Continue on reverse if necessary and identify by block number)

Our research is concerned with understanding both the computational and neurophsiological bases of texture segregation. During the grant period we have (a) conducted a series of experiments investigating the interaction of size and contrast in texture segregation, (b) compared our experimental results with the calculated outputs of a 2D Gabor model of simple-cell-like spatial-frequency channels, (c) established that the function describing perceived segregation of a texture resulting from lightness differences of the texture elements is not the same as the function describing the perceived lightness differences of the elements. We also showed that the outputs of spatial frequency channels that predict the perceived segregation of texture regions fail to predict the perceived salience of a line composed of disconnected shapes embedded in a background of the same shapes.

The second part of the report describes work by Stevens on the earliest levels in the extraction of geometric structure. The work has involved a computational and psychophysical study of the role of retinal and cortical spatial frequency filters in the extraction (over)

20. DISTRIBUTION / AVAILABILITY OF ABSTRACT: ☒ UNCLASSIFIED/UNLIMITED ☐ SAME AS RPT. ☐ DTIC USERS	21. ABSTRACT SECURITY CLASSIFICATION: Unclassified
22a. NAME OF RESPONSIBLE INDIVIDUAL: John Tangney	22b. TELEPHONE (Include Area Code): (202) 767-5021 / 22c. OFFICE SYMBOL: AFOSR/NL

DD FORM 1473, 84 MAR — 83 APR edition may be used until exhausted. All other editions are obsolete.

SECURITY CLASSIFICATION OF THIS PAGE

21 DEC 1988

19. Abstract (cont)

of contour information. The specific areas reported concern: i) the differential roles of radially-symmetric and elongated receptive fileds on the Cafe wall illusion, a pattern that is useful for the induction of illusory brightness bands and orientation, ii) a strategy for parsing of band-pass filtered images to differentiate line-like versus edge-like luminance changes, iii) asserting orientation between discrete items, and iv) connecting contour fragments across liminance gaps. Across these areas one common theme is the importance of spatial gating nonlinearity.

CONTENTS

Part I

1. ABSTRACT

Our research is concerned with understanding both the computational and neurophysiological bases of texture segregation. During the grant period we have (a) conducted a series of experiments investigating the interaction of size and contrast in texture segregation, (b) compared our experimental results with the calculated outputs of a 2D Gabor model of simple-cell-like spatial-frequency channels, (c) established that the function describing perceived segregation of a texture resulting from lightness differences of the texture elements is not the same as the function describing the perceived lightness differences of the elements. We also showed that the outputs of spatial frequency channels that predict the perceived segregation of texture regions fail to predict the perceived salience of a line composed of disconnected shapes embedded in a background of the same shapes.

The trade-off between size and contrast follows from the hypothesis that strong preattentive texture segregation occurs when spatial-frequency channels yield a large difference in mean or modulated activity to two textures. Though overall the results of our experiments were consistent with the hypothesis that texture segregation occurs as a result of the differential stimulation of spatial-frequency channels, aspects of the results from experiments in which the fundamental frequency of the texture was varied, textures containing elements of opposite contrast-sign, and textures containing balanced elements with no energy at their fundamental frequency were not consistent with the hypothesis. These discrepancies suggest that our model was not making sufficient use of information in the higher harmonic channels. One way in which the information in the higher harmonics may be used involves a more complicated spatial-frequency channels model. In this model, each channel contains in addition to an initial linear-filtering, a nonlinear rectification followed by a second linear-filtering. Both filterings are selective for spatial-frequency and orientation. We call these "channels complex" to both distinguish it from the simple channels and because this kind of channel is similar to current models of complex cells. The complex channel model taking into consideration the effects of light adaptation is able to account qualitatively for all our discrepancies.

A striking finding is that we have been able to construct texture displays composed of elements differing clearly in lightness which fail to yield perceived segregation. Equal lightness differences can lead to markedly different degrees of perceived segregation depending on the ratio of the background luminance to the high-luminance square. The functions describing the perceived lightness differences of the squares and the perceived segregation of the texture displays are not the same functions. Our experiments show that segregation ratings are a

function of the ratio of the contrasts of the high- to low-contrast squares. Contrast is defined as the difference between the luminance of the square and the luminance of the background, divided by the luminance of the background. The relevant variable for texture segregation is therefore the luminance increment ratio of the target to the background. For perceived lightness, the relevant variable is instead the luminance ratio of the target to the background.

In a display composed of disconnected shapes, a line may sometimes popout even though the shapes in the line do not differ from the other shapes in the display and do not occupy a disjoint region. The spacing between the shapes in the line and in the background are also similar. The difference is that the shapes in the line are approximately aligned and there is a greater density of shapes in the direction of the line. In our texture patterns, the arrangement of local properties is different in different regions so that if the display is suitably filtered by convolving the appropriate property at each point, or by performing some equivalent filtering process in the Fourier domain, the regions in the filtered display differ in different regions. This type of computation does not appear to be able to account for the global popout of lines of disconnected shapes in which the line does not occupy a disjoint region of the display.

2. RESEARCH SUMMARY

2.1 Introduction

Models of texture segregation fall into three classes. In one class of models, texture segregation is based on the geometric features of a texture pattern. Beck (1972, 1982) and Marr (1976) proposed that texture segregation is based on differences in first-order statistics of simple features of a texture pattern such as the slopes and sizes of texture elements or of their component parts. Julesz (1981) has labeled such features textons and proposed that there are three kinds: elongated blobs (e.g. line segments), terminators (e.g. line terminations), and intersections (e.g. crossings of line segments). In a second class of models, the primitives for texture segregation are not geometric features but the outputs of receptive-field-like operators. In many of the models in this class, texture segregation is based on differences in image statistics following convolution of a texture with local, linear filters that have weighting functions like the receptive fields of simple cells. A number of investigators have proposed that texture segregation is, at least sometimes, directly based on differences in the outputs of spatial-frequency channels (e.g. Beck, Sutter, & Ivry, 1987; Caelli, 1985; Daugman, 1987; Ginsburg, 1984; Graham 1981; Grossberg & Mingolla, 1985; Turner, 1986). Spatial-frequency channels are quasi-independent, parallel channels composed of local receptive fields that are distributed

throughout the visual field and are alike in their sensitivity to spatial frequency and orientation. The evidence that the visual system analyzes a stimulus into a set of spatial-frequency channels, and their usefulness in visual modeling has been reviewed elsewhere (e.g., Graham 1980, 1981, 1985).

In a third class of models, texture segregation is based on differences in second-order statistics of the luminances at different points in the texture. The second-order statistics of a region are based on the joint probability distribution that a pair of points separated by a given distance and orientation have particular gray levels. Julesz's original conjecture (1975) considered two gray levels and the extension of this conjecture to patterns containing many gray levels must be done carefully (Klein and Tyler, 1986). Julesz (1975) conjectured that textures with the same global second-order statistics do not segregate, but counter-examples to Julesz's conjecture have been found (Julesz, Gilbert & Victor, 1978; Victor & Brodie 1978). Gagalowicz (1981) pointed out that the counter-examples involve patterns in which local second-order statistics are not the same throughout the pattern and differ from the global second-order statistics. He hypothesized that textures which have the same local second-order statistics throughout will fail to segregate. It should be noted that if texture segregation is a function of only the amplitudes and not the phases of the spatial frequencies, then the spatial-frequency channel approach is closely related to models based on second-order statistics.

Beck, Sutter, and Ivry (1987) investigated texture segregation in a three-part (tripartite) pattern in which each part contains approximately equal numbers of two different elements (large and small squares in Figure 1). The textures to be segregated differed in the arrangement of the two elements. In the top and bottom regions, the two elements were arranged in vertical stripes. In the center region, the elements were arranged in a checked pattern. They reported four important findings: (1) Size and contrast are not independent attributes but can cancel each other. For example, large and small squares of equal contrast yielded strong texture segregation. However, texture segregation was reduced greatly if the contrast of the small square was increased so that the areal contrasts (area x contrast) of the large and small squares were equal. (2) A difference in sign of contrast yields strong texture segregation. Squares of equal size whose luminances were above and below the background luminance yielded strong texture segregation even when the ratio of background luminance to square luminance was very close to 1.0. (3) Texture segregation does not vary directly with the lightness difference of the squares. Equal size squares differing by a large lightness difference failed to give texture segregation, while the same squares differing by a smaller lightness difference yielded strong texture segregation depending upon the background luminance. (4) Hue is a weak feature for texture segregation. In the absence of size and contrast

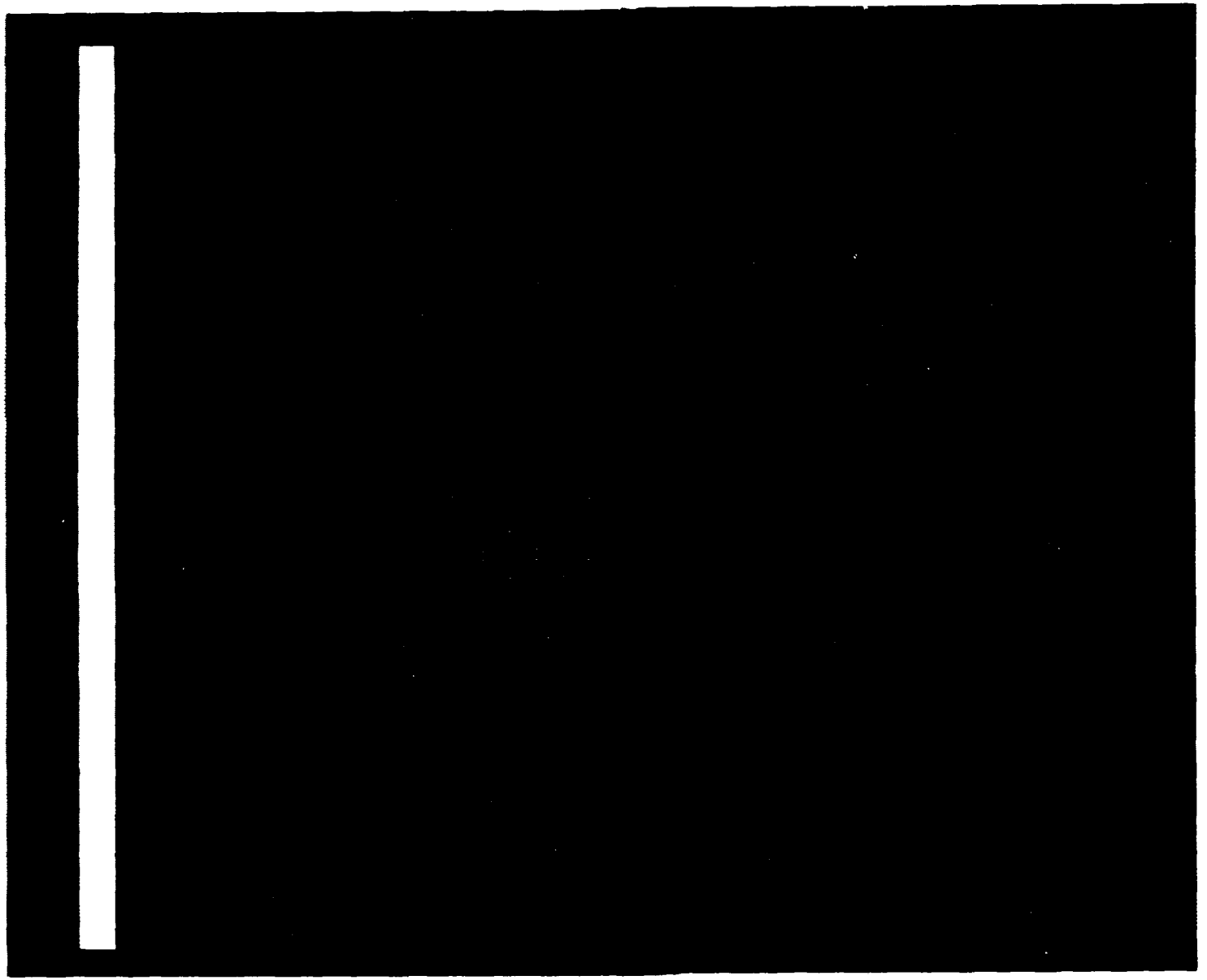

FIGURE 1

differences, hue differences failed to yield strong spontaneous texture segregation. Our research has focused on investigating in detail the first three of the above findings.

2.2 Spatial-frequency channels in texture segregation

When viewing the pattern in Figure 1, subjects reported spontaneously segregating it into two textures-stripes in the top and bottom regions and a checked region in the center (a perception that we call ''tripartite segregation''). The segregation of the pattern into three regions is not surprising and is explainable in many ways. Of interest is what happened when the large and small squares differed in contrast as well as size. Figure 2 shows the same display with the contrast of the small squares increased. As the contrast of the small squares increases starting at a value equal to that of the large squares, perceived segregation decreases. After sufficient increase in contrast, perceived segregation reaches a minimum and then starts increasing again. [Some results are shown in Figs. 7-9 and Beck, Sutter, & Ivry (1987).] The minimum tends to occur when the areal contrasts (area x contrast) of the large and small squares were made equal.

2.2.1 *How spatial-frequency channels might explain the area x contrast trade-off*

This trade-off between contrast and area suggested that perceived texture segregation occurs strongly when a spatial-frequency channel or channels yield a large difference in activity to the striped and checked regions of the tripartite pattern. The tripartite pattern is periodic repeating itself every two columns. The left panel in Figure 3 shows a pattern having unequal-size squares and equal contrast; the middle panel shows the output of a vertically oriented spatial-frequency channel tuned to the fundamental frequency of the striped region; and the right panel the output of a higher spatial-frequency channel. Specifications of the channel properties are given in Section 2.1.2. When the excitatory region of a receptive field tuned to the fundamental frequency of the pattern is centered over a column of large squares, the receptive field is strongly stimulated by the large squares and weakly inhibited by the small squares. When the excitatory region is centered over a column of small squares, the receptive field is weakly stimulated by the small squares and strongly inhibited by the large squares. Thus, the middle panel shows strongly modulated activity with high outputs at the center of the large-square columns and low outputs at the center of the small square-columns.

When the excitatory region of a vertically oriented receptive field is centered over either a large or a small square in the checked region of the pattern, the amounts of excitation and inhibition are approximately equal. Thus, the output at each

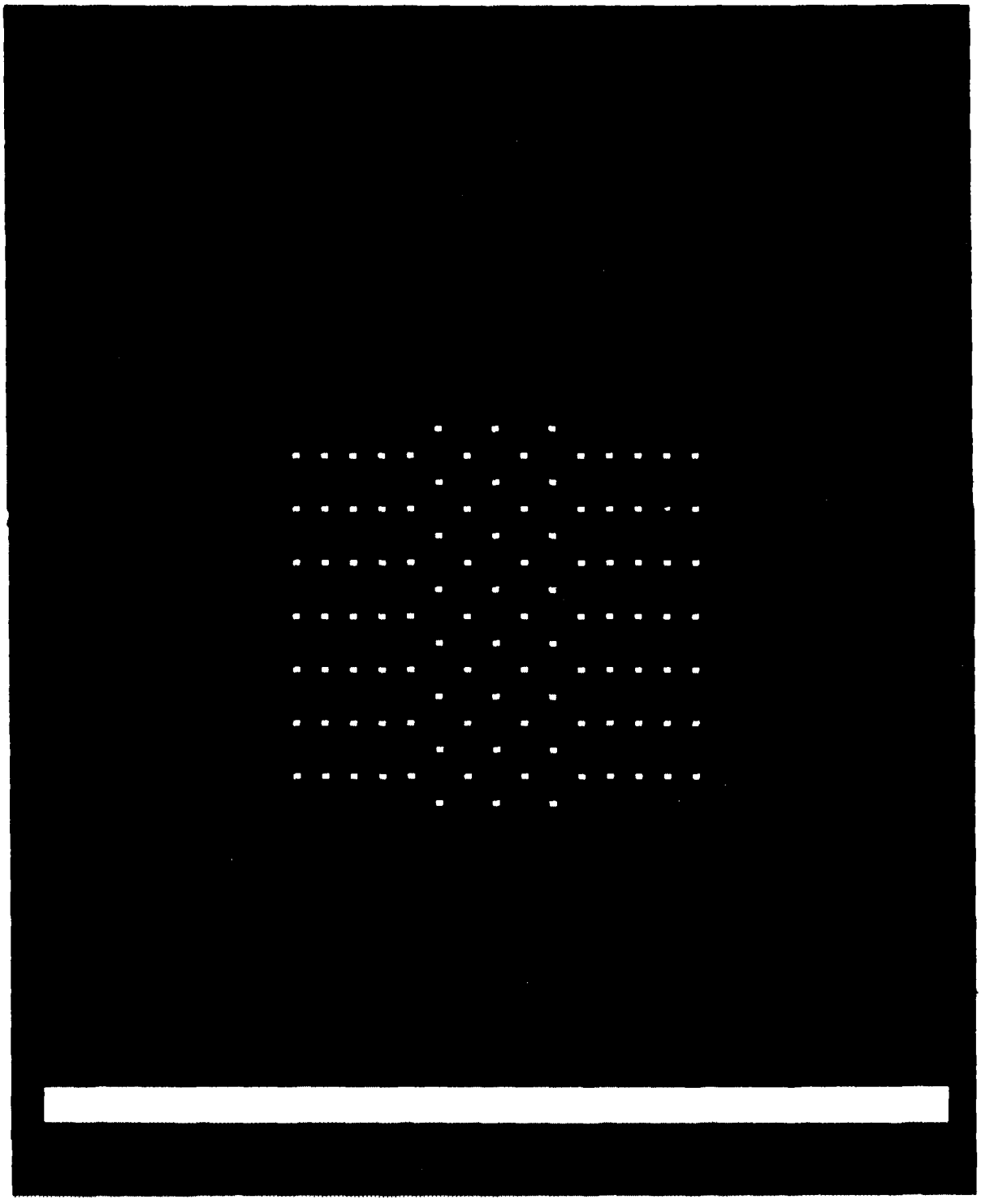

FIGURE 2

Element Type: Solid Squares

Area Ratio 4 Contrast Ratio 1

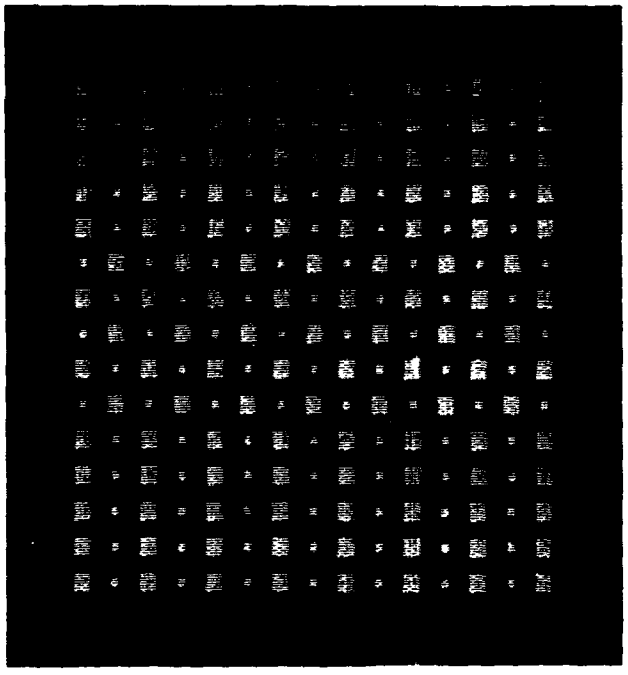

PATTERN

Vertical Fundamental

~ 1 c/deg

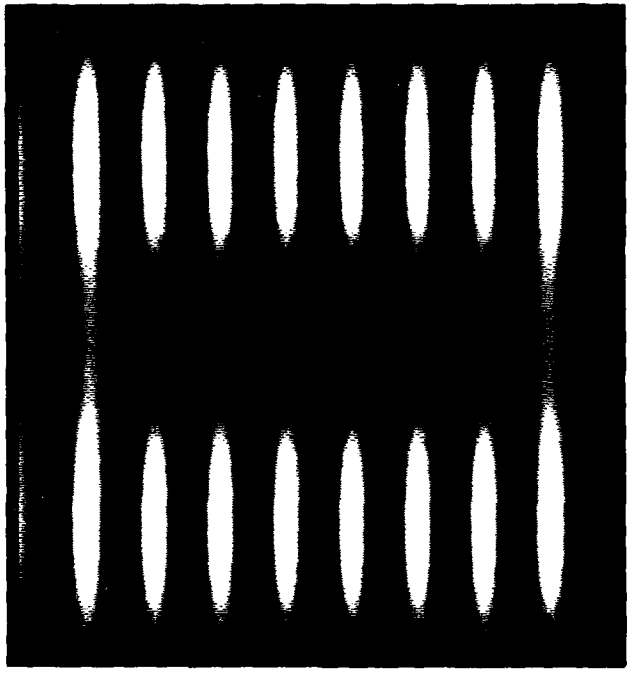

FILTER

Vertical

1 c/deg

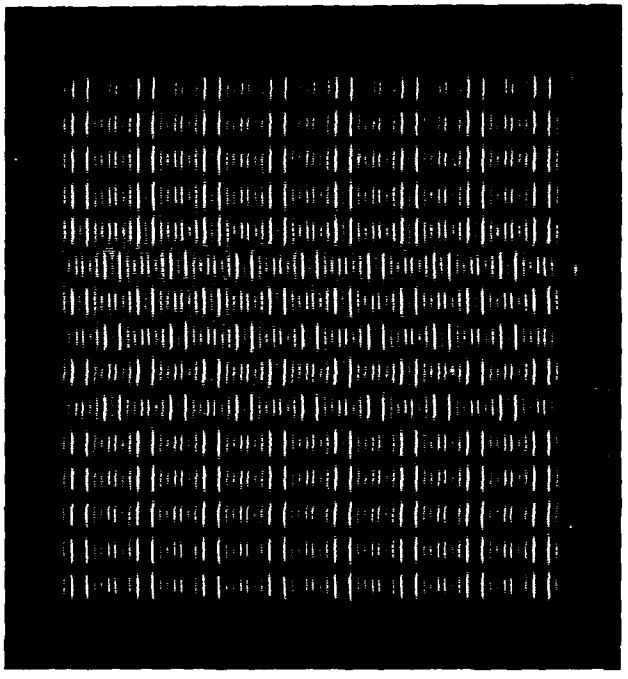

FILTER

Vertical

11.3 c/deg

FIGURE 3

spatial position is about the same, and there is little modulated activity (see middle region of output in middle panel of Figure 3). Channels tuned to higher harmonics of the pattern (right panel of Figure 3), respond to the edges of the squares in the pattern. Though there is a difference in the spatial arrangement of the outputs in the striped and checked regions, there is no difference in the amount of overall activity.

Figure 4 is like Figure 3 except that the contrast of the small squares in the pattern is now 4 times that of the large squares (so the areal contrasts are equal). Now when the excitatory region of a receptive field from the channel tuned to the fundamental frequency is centered over either a large or small square in either the striped or checked regions, the output is about the same since the greater contrast has balanced out the smaller size of the squares. The output of the higher-harmonic channel (right panel) looks much like that in Figure 3.

We conjectured that spontaneous strong texture segregation occurs only when there are differences in the mean or modulated activity of a channel or channels to the striped and checked regions of the tripartite pattern.

2.2.2 *Simple spatial-frequency channels model*

The challenge was to find a quantitative model that will predict the observer's ratings of perceived segregation. To do so requires, at the least, considering the responses of all the filters. These responses are displayed in summary form in Figure 5 by taking a period from the middle of the checked region on any one filter's outputs (as in Figure 3) and another period from the middle of the striped region of any one filter's outputs and then displaying this pair of periods for each of the different filters. Figure 5 shows the outputs of 39 filters resulting from the combination of thirteen different spatial frequencies (from left to right in 13 columns in Figure 5) and three different orientations-vertical, 45 degrees oblique, and horizontal (from top to bottom in three pairs of two rows each).

Figure 5 shows responses to the unequal-size equal-contrast pattern in Figure 1. (The large square is 4 times the area of the small square and the contrasts of the squares are equal.) As discussed in the previous sections, the vertically oriented channels sensitive to spatial frequencies near the fundamental frequency of the pattern (1.0 and 1.41 cycles/deg) show strongly modulated activity in the striped region and little modulated activity in the checked region. Strong modulated activity occurs in the checked region for channels sensitive to the fundamental oblique frequency (greater by the square root of 2 than the fundamental vertical frequency-1.41 and 2.0 cycles/deg) and little modulated activity in the striped region. For lower spatial

Element Type: Solid Squares

Area Ratio 4 Contrast Ratio 1/4

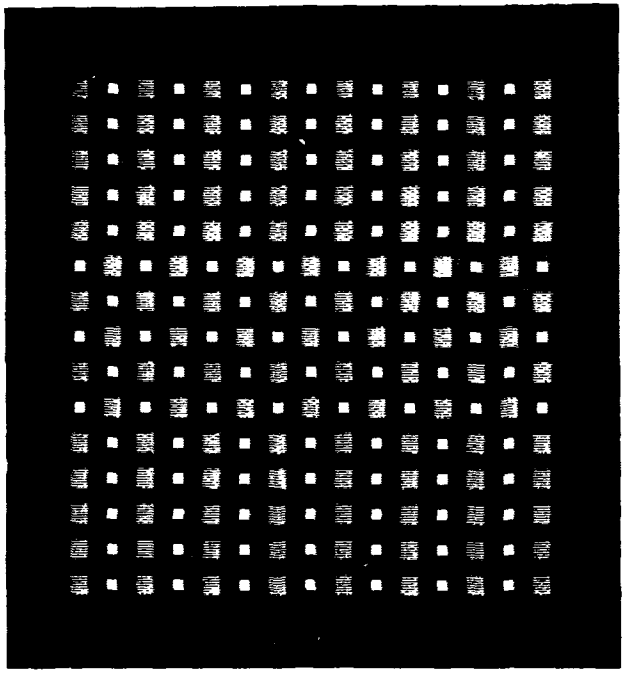

PATTERN

Vertical Fundamental

~ 1 c/deg

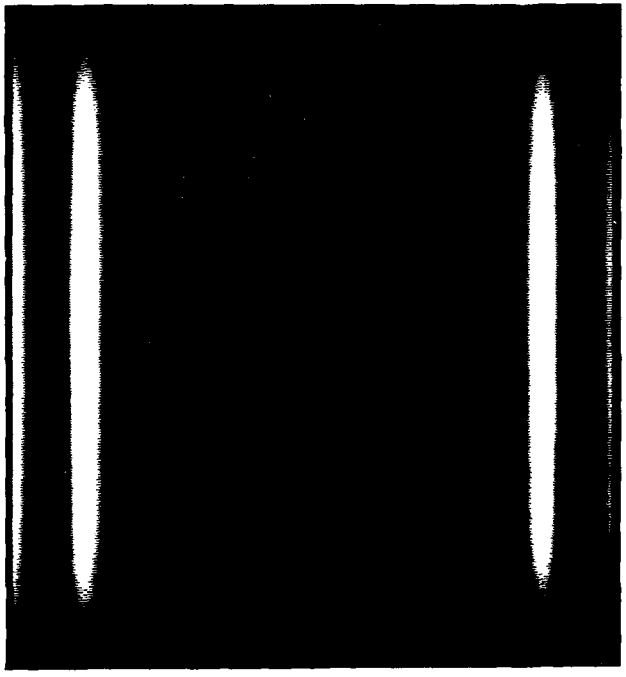

FILTER

Vertical

1 c/deg

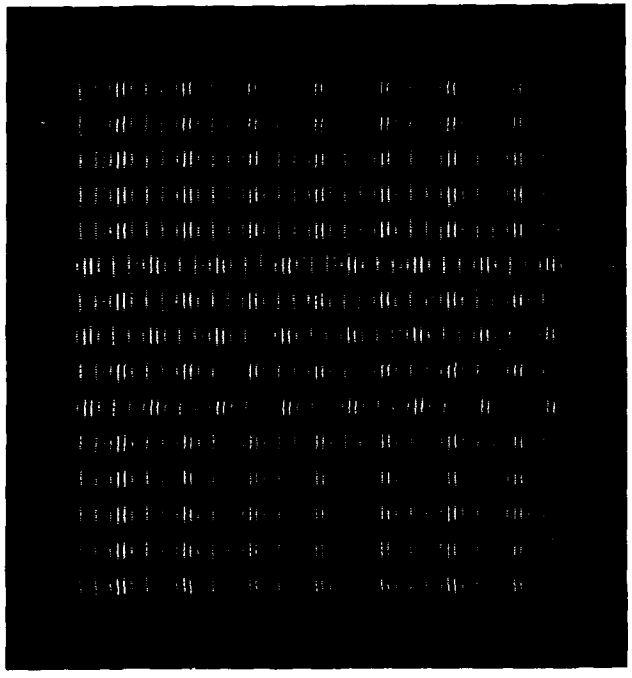

FILTER

Vertical

11.3 c/deg

FIGURE 4

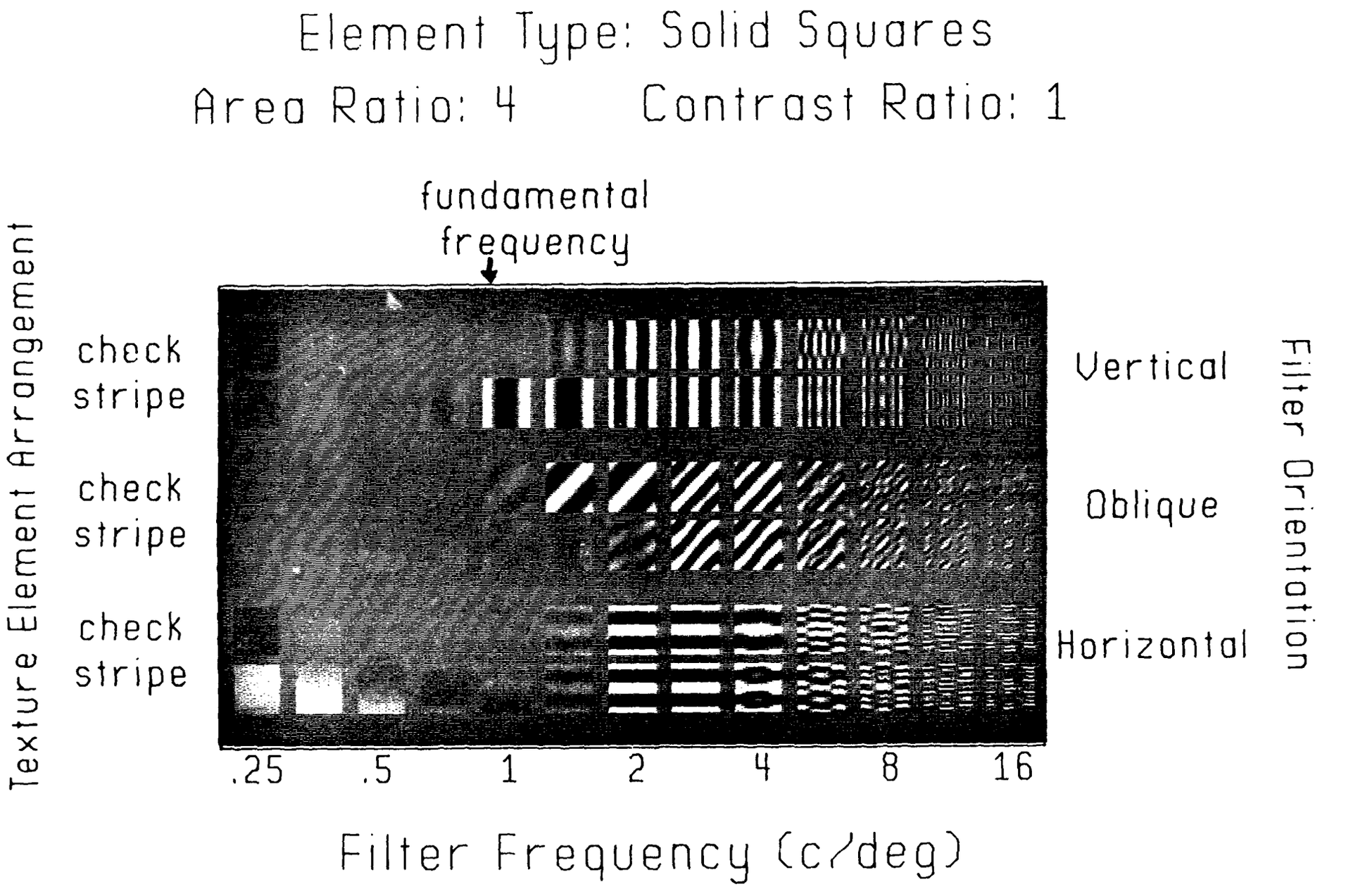
Element Type: Solid Squares
Area Ratio: 4
Contrast Ratio: 1
fundamental frequency
Texture Element Arrangement
check stripe
check stripe
check stripe
Vertical
Oblique
Horizontal
Filter Orientation
.25
.5
1
2
4
8
16
Filter Frequency (c/deg)
each patch = one square period of the pattern

FIGURE 5

frequencies whose periods are larger than the fundamental period, there is little response to either the checked or striped regions by either the vertical or oblique channels. The receptive fields are so large that they average over adjacent rows and columns of squares. (Some slight mean output differences between checks and stripes are visible-especially in the lower left of Figure 5. These are responses by very large receptive fields to the edges of the tripartite pattern. The differences are caused because striped patterns were always near the horizontal edges of the filtered patterns.) Spatial frequencies whose period is smaller than the fundamental period respond near the edges of all the squares in the pattern. Although the pattern of the activity is distributed differently in the striped and checked regions, the amounts of modulated activity to the striped and checked regions by the vertical and diagonal channels are similar.

Figure 6 shows the filtered outputs to the pattern in Figure 2 in which the products of the areas x contrasts of the large and small squares are equal. (The large square is 4 times the area of the small square; the small square is 4 times the contrast of the large square.) As discussed in the previous subsection, the vertical 1.0 and 1.41 cycles/deg and the oblique 1.41 and 2.0 cycles/deg channels show no modulated response to either the checked or striped regions of this pattern. There is no information in the amount of modulated activity for segregating the tripartite pattern into distinct regions.

Characteristics of Channels.--Each channel is assumed to be a linear, translation-invariant filter. We modeled the receptive-field weighting functions by two-dimensional Gabor functions (as used, for example, by Daugman, 1985; Watson, 1983). The weighting function in one direction is a Gaussian multiplied by a sinusoid and in the perpendicular direction a Gaussian. The parameters of the model we have implemented follow Watson (1983) in that the spatial-frequency half-amplitude bandwidth is one octave and the orientation half-amplitude bandwidth is 38 degrees. In Figures 5 and 6, the variation in sensitivity with spatial frequency is not represented but is in the calculations of the model. Our model is less complete than that of Watson in two respects: the fields have even symmetry, and we have not incorporated the decrease in acuity occurring with retinal eccentricity.

Combining the Outputs of Many Channels to Predict the Observer's Rating.--We now wanted to turn these channel outputs into a quantitative prediction of the observer's ratings of perceived texture segregation. Our first attempt is a crude measure of the degree to which there are gross difference between the outputs of one or more filters to the two different texture regions. This simple model can be seen as an elaboration of Julesz's (1972) original statistical conjecture and is rather in the spirit of recent attempts by a number of investigators (e.g., Caelli, 1982; Daugman, 1987; Turner, 1986) to use spatial-frequency filters to predict results from a number of early texture patterns. It differs from this earlier theoretical

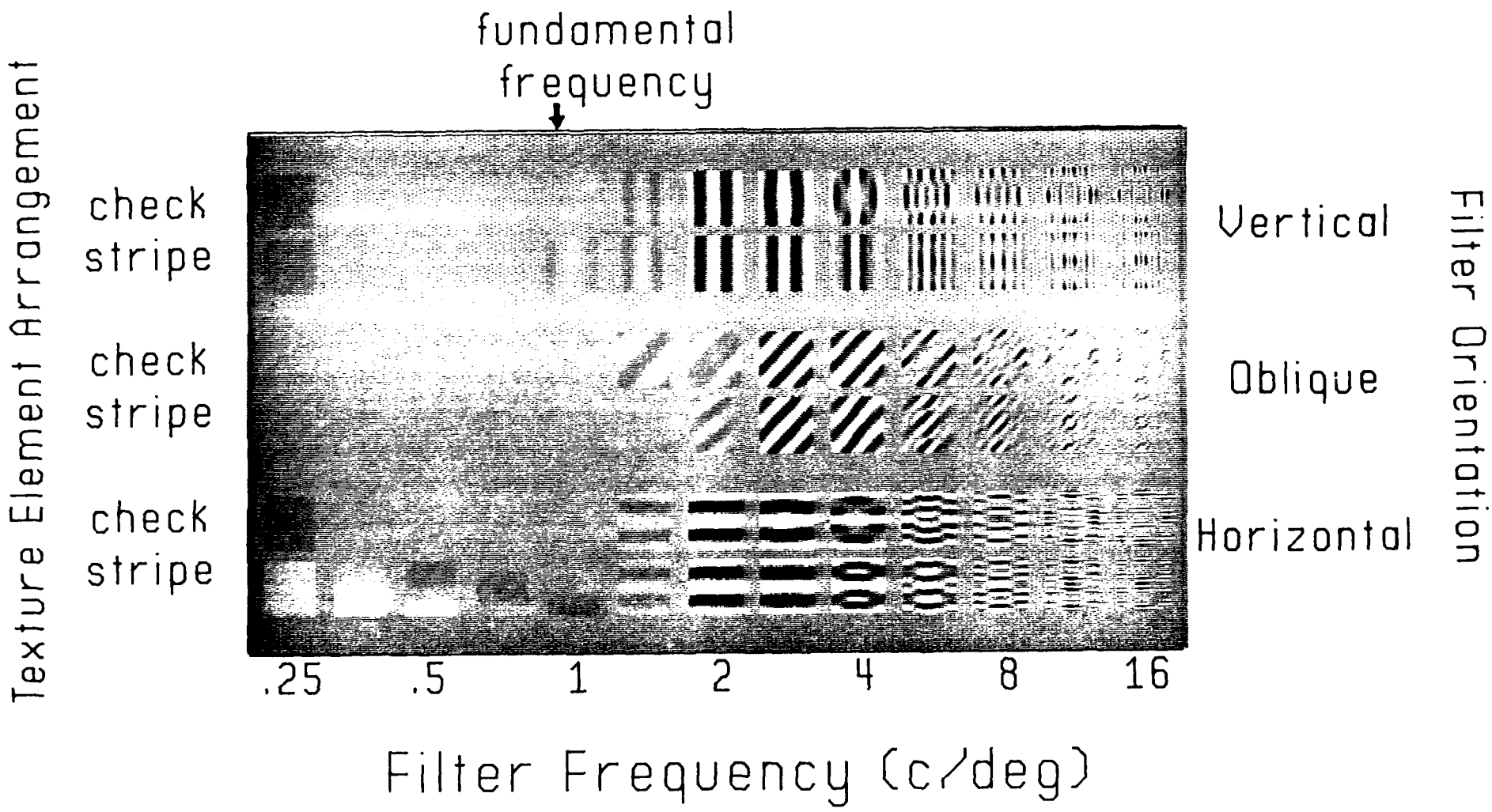
Element Type: Solid Squares
Area Ratio: 4
Contrast Ratio: 1/4
fundamental frequency
Texture Element Arrangement
check stripe
check stripe
check stripe
Vertical
Oblique
Horizontal
Filter Orientation
.25
.5
1
2
4
8
16
Filter Frequency (c/deg)
each patch = one square period of the pattern

FIGURE 6

work in attempting to generate quantitative predictions of the strength of perceived texture segregation (rather than just distinguishing textures that would segregate from those that wouldn't at all) so that these quantitative predictions can be compared to empirical results in a rigorous way.

(i) Our simple model first computes the output of channels that are linear, translation-invariant filters tuned to many different spatial frequencies and orientations as described above. Let the output at position (x,y) of the channel tuned to the i^{th} frequency and the j^{th} orientation be called O_{ij} (x,y).

(ii) The model then computes a spatially-pooled response of each channel to the checked and to the striped region; in particular, the standard deviation of the outputs at different spatial position is computed. For example, the spatially pooled response of the ij^{th} channel to the checkerboard region is

$$R_{ij}(ch)^2 = \sum_{\substack{x \\ \text{in checked} \\ \text{region}}}^{N_x} \sum_{y}^{N_y} \frac{\left(O_{ij}(x,y) - E(O_{ij})\right)^2}{N_x \cdot N_y}$$

where N_x N_y are the numbers of spatial positions in the x and y directions in one period of the pattern and the summing is done over the checked region. The model then takes the difference between each filter's spatially-pooled response to the checked and to the striped region yielding a within-filter difference for the ij^{th} filter of

$$Diff_{ij} = R_{ij}(ch) - R_{ij}(st)$$

(iii) The model combines (pools) these within-filter differences cross many spatial frequencies and orientations of filters, weighting the differences according to the observers' sensitivity to different orientations and spatial frequency: So, the predicted value equals a pooled weighted sum of within-filter differences. In particular, the predicted value equals the following quantity:

$$\sqrt{\sum_{i}^{N_f} \sum_{j}^{N_o} \left(\text{Diff}_{ij} \cdot S_{obs}(f_i, O_j)\right)^2}$$

where S_{obs} (f_i, O_j) is the sensitivity of the observer to the i^{th} frequency and j^{th} orientation, N_f is the number of frequencies (13--from .5 to 16 cycles/deg in square-root-of-two steps) and N_o is the number of orientations (3--vertical,

45-degrees, and horizontal).

(iv) Finally the model assumes that the observer's ratings of perceived segregation are monotonically related to the predicted value shown above.

Note. We tried exponents of 1, 3, 4 in the above equations (both for spatial-pooling and for pooling across channels) as well as using the maximum, the minimum, or the maximum-minus-minimums. Conclusions using any of them were identical to those illustrated here with an exponent of 2. It should also be noted that the model we are investigating specifies the information for texture segtregation but does not provide a procedure for locating texture boundaries since it does not address the question of how the information is used to segment a pattern into regions. This is a problem discussed by Caelli (1985), Grossberg & Mingolla (1985), and Grossberg (1987).

2.3 Experiments compared to predictions of simple model

Methods and Procedures.--The procedure and instructions were similar to Beck, Sutter, & Ivry (1987). Except where noted the background luminance was set at 16.1 ft.-L and appeared gray. The intensity of one kind of texture element (e.g., the large squares in Figures 1 or 2) was kept constant while the intensity of the second kind of texture element (e.g., the small squares in Figures 1 or 2) was varied. When the texture elements differed in size, the constant-luminance element was always the larger element and the variable-luminance element the smaller element. Except where noted the fundamental frequency of the patterns was about 1 c/deg (the period was 56 pixels and at the viewing distance of 6 feet, 1 pixel subtends 1.08 minutes). In each experiment, 10 subjects rated the perceived texture segregation of each pattern 5 times on a 5-point rating scale. Each pattern was shown for 1 second. In between patterns the screen was at the background luminance. All the patterns in a given experiment were randomly intermixed.

The contrast of an element is defined here to be the luminance of the element minus the luminance of the background divided by the luminance of the background. (This is the quantity that Shapley & Enroth-Cugel 1985 called Weber contrast.) The horizontal axes in all the figures show the contrast ratio of the variable-intensity to fixed intensity elements.

2.3.1 *Area-ratios and background luminances*

Three experiments investigated texture segregation as a function of contrast and background luminance. In one experiment (Sutter, 1987), the textures were composed of either two 16-pixel squares or of one 16- and one 8-pixel squares. Thus, the element

area-ratios in the first experiment were 1:1 and 4:1. The squares were presented on a white (32.3 ft.-L) and on a black (.05 ft.-L) background. The luminance of fixed-intensity squares was set at values close to the background (28.1 ft.-L. for the white background and .26 ft.-L. for the black background) or far from the background (24.06 ft.-L. for the white background and 2.44 ft.-L for the black background). The luminances of the variable-intensity squares were always equal to or below the white background (.2 to 28.1 ft.-L for the close condition and .2 to 24.06 ft.-L. for the far condition) and always equal to or above the black background (.62 to 6.72 ft.-L. for the close condition and 2.44 to 32.2 ft.-L. for the far condition). Figure 7 presents the results with a white background and Figure 8 with a black background. The results are consistent with the earlier findings of Beck, Sutter, and Ivry (1987) and are in accord with the predictions of the simple model. For the textures composed of the 16 and 8 pixel squares, segregation was a u-shaped function, with a minimum around the point at which the squares were of equal areal contrast. For the textures composed of equal size squares (both squares 16 pixels), segregation increased steadily as the luminance of one square increased. The increase was slower on a background than on a white background. A possible reason for this difference is that because of early response compression the effective contrast of the squares on a black background reaches a maximum which does not increase with further increases in luminance.

Two further experiments (Sutter, Beck, & Graham 1988) investigate the interaction of contrast and size in texture segregation by using four different element area-ratios: 1:1 (both squares were of the same size--16 pixels or approximately 16 minutes on a side), 1.78:1 (16 x 16 pixels and 16 x 12 pixels), 4:1 (16 x 16 and 8 x 8) and 16:1 (16 x 16 and 4 x 4). In the first experiment (results shown in top panel of Figure 9), the patterns were presented on a black background of .05 ft.-L and the luminance of the fixed-intensity squares was set at .26 ft.-L. The variable-intensity squares were always above the background and ranged from .26 ft.-L. to 32.2 ft.-L. In the second experiment, the patterns were presented on a gray background of 16.1 ft.-L, and the luminance of the fixed-intensity squares was held constant at 2 ft.-L. above or below the background (18.1 or 14.1 ft.-L., respectively). The variable-intensity squares were presented above (middle panel of Figure 9) and below (bottom panel of Figure 9) the background. The luminance of the variable squares was set at 1 of 7 values ranging from .03 to 14.1 ft.-L. for the squares below the background and from 18.1 to 32.2 ft.-L. for the squares above the background. The element contrast ratios varied in steps of 2^{-1}.

Figure 9 shows that perceived segregation is, in general, a u-shaped function with the minimum depending on the relative size of the square and shifting to larger contrast ratios as the element area-ratio increased. For an area-ratio of 1, the minimum

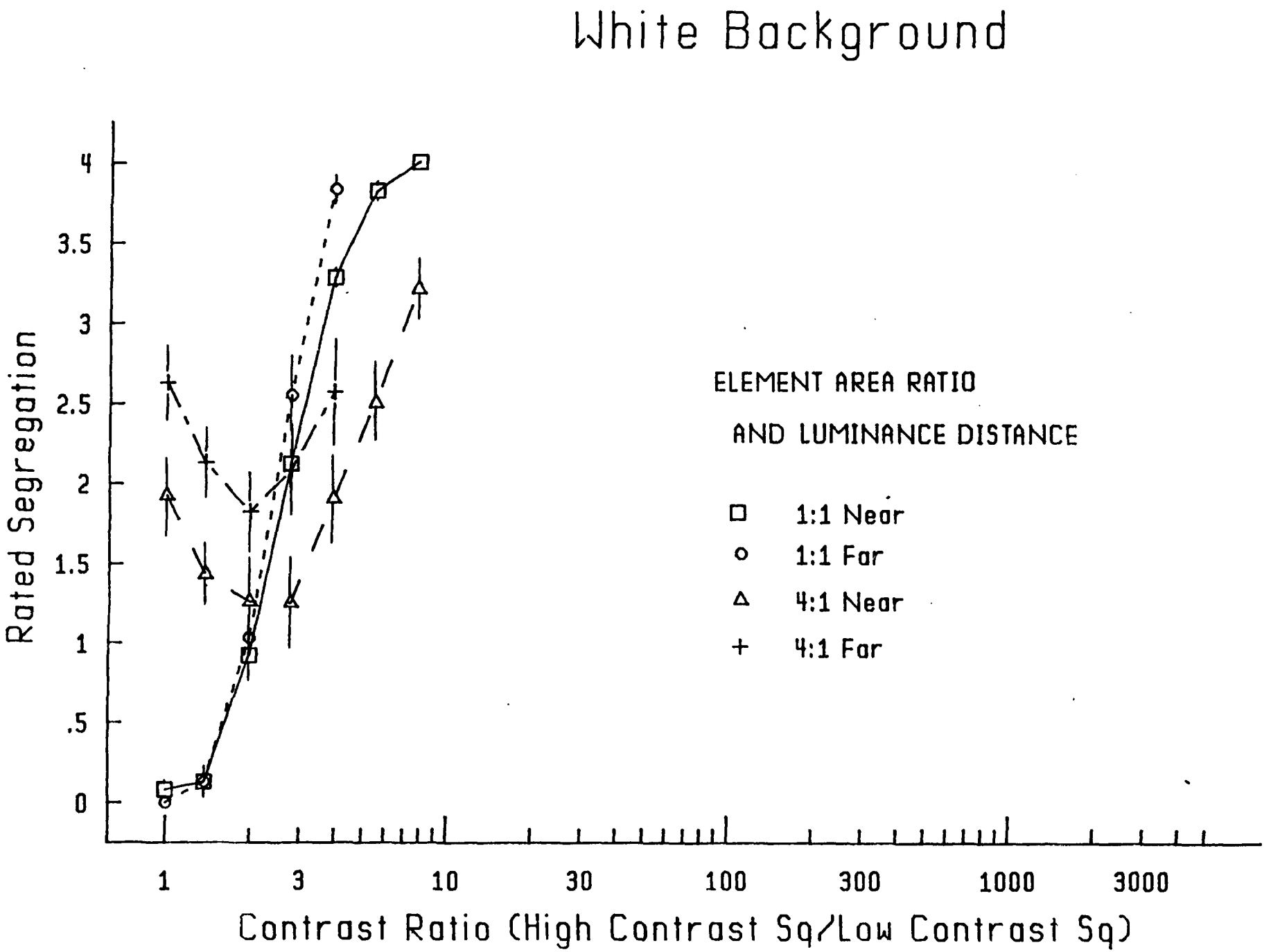
White Background
Rated Segregation
4
3.5
3
2.5
2
1.5
1
.5
0
1
3
10
30
100
300
1000
3000
Contrast Ratio (High Contrast Sq/Low Contrast Sq)
ELEMENT AREA RATIO
AND LUMINANCE DISTANCE
1:1 Near
1:1 Far
4:1 Near
4:1 Far

FIGURE 7

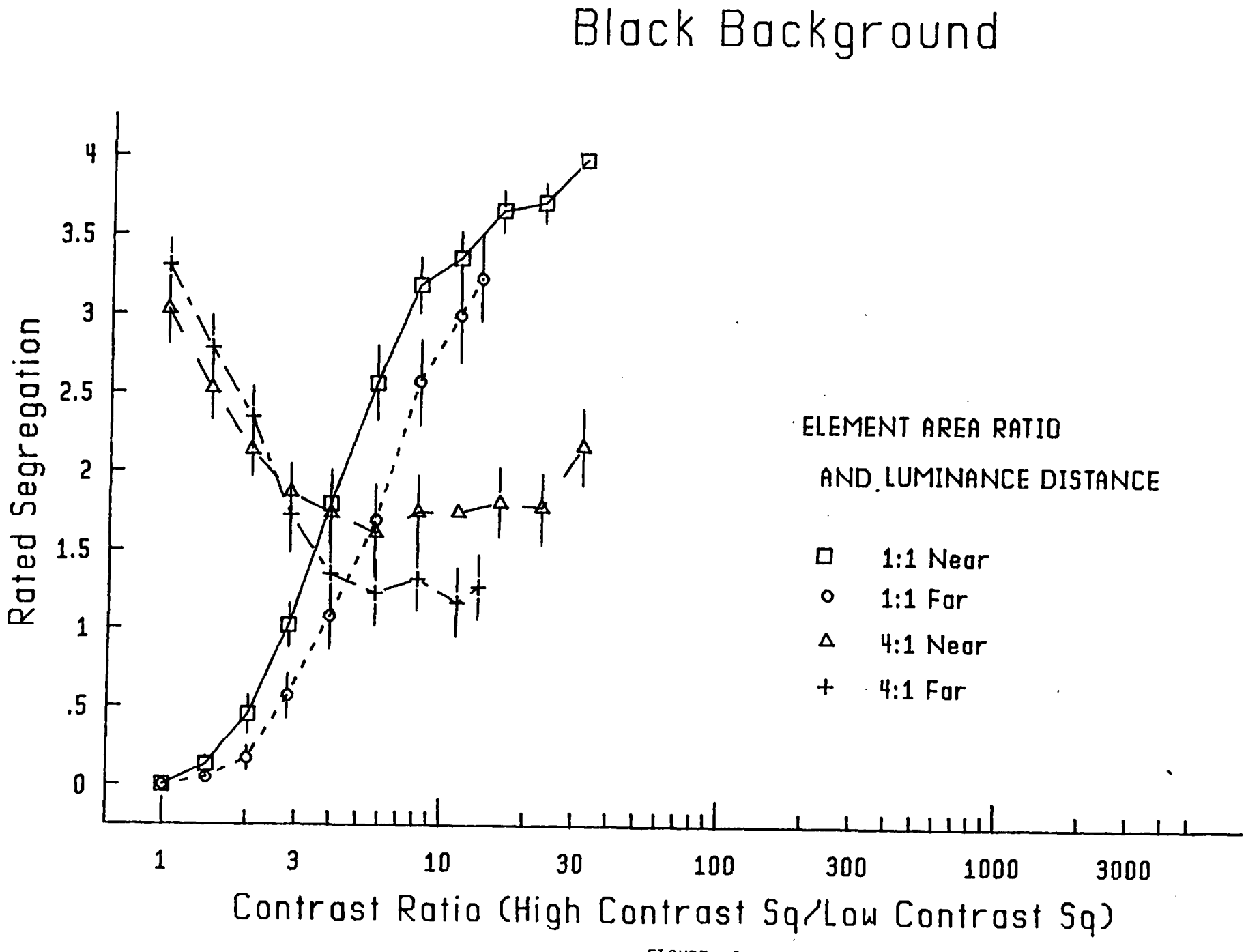
Black Background
Rated Segregation
4
3.5
3
2.5
2
1.5
1
.5
0
1
3
10
30
100
300
1000
3000
Contrast Ratio (High Contrast Sq/Low Contrast Sq)
ELEMENT AREA RATIO
AND LUMINANCE DISTANCE
1:1 Near
1:1 Far
4:1 Near
4:1 Far

FIGURE 8

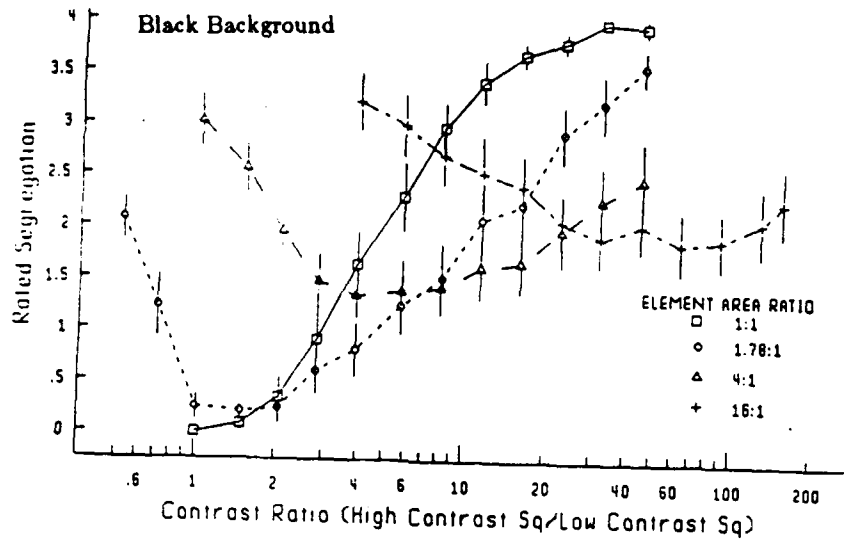

Squares Above the Background

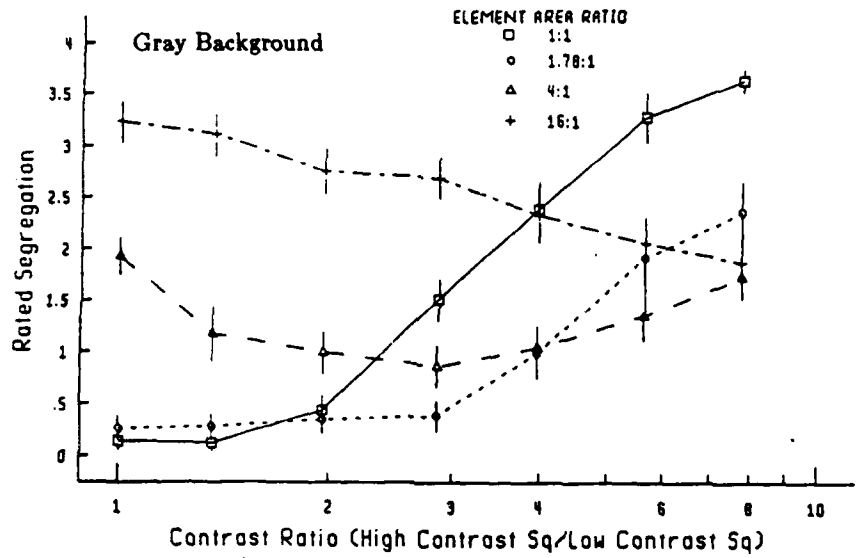

Squares Below the Background

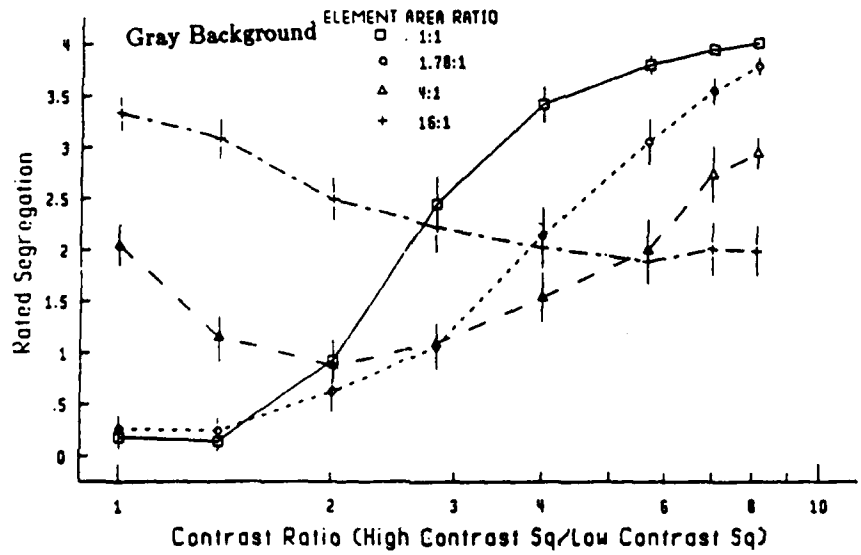

FIGURE 9

perceived segregation occurred when the contrast ratio was 1. For an area-ratio of 1.78:1, the minimum occurred between 1 and 2. For 4:1, the minimum occurred between 2 and 4, and for 16:1, the minimum occurred at approximately 20:1. This pattern of results is consistent with the simple model. (The minimum is not predicted to occur precisely at the point of equal a real contrast for these patterns because the large squares were larger than the space between them.)

Note that the size difference of the squares also affected texture segregation. For example, the perceived segregation at the minimum in the top panel (black background) increased as the element area-ratio increased ranging from .20 for the 1:1 area-ratio to 1.85 for the 16:1 area-ratio. That is, the steepness of the trough decreased as area-ratio increased. This dependence is not consistent with the simple model; it predicts that functions for all area-ratios should dip down to approximately the same very low value. We will return to this dependence in our discussion of the complex model (page 22).

Some minor differences among the three panels of Figure 9 may be other effects of response compression for luminances far above the background luminance. For example, perceived segregation increased for contrast ratios higher than that at the minimum except for the 16:1 condition where the luminance of the small square was becoming extremely high by the time the perceived segregation reached a minimum.

2.3.2 *Lines vs. square elements*

This experiment investigated whether there are differences in perceived segregation as a function of whether the texture elements are squares or lines (Sutter, Beck, & Graham (1988). Four patterns composed of squares and four composed of lines were presented. In the textures composed of squares, the fixed-intensity elements were always 16 x 16 pixel squares. The variable-intensity elements were 16 x 16, 11 x 11, 8 x 8, or 4 x 4 pixel squares. (Each pixel is approximately 1 minute of visual angle.) In the textures composed of lines, the fixed-intensity elements were always lines of width 2 pixels and height 16 pixels. The other elements were all lines of width 2 pixels; the heights could be 16, 11, 8, or 4 pixels. The center-to-center separation of the squares and lines was 28 pixels. The variable-intensity elements were always above the background. The luminances of the background and the fixed- and variable-intensity elements were the same as in the gray background experiment in Section 2.3.1 (page 11).

Figure 10 shows the mean ratings of the textures composed of squares (top) and lines (bottom). As in the earlier experiments, and as predicted by the simple spatial frequency model, perceived

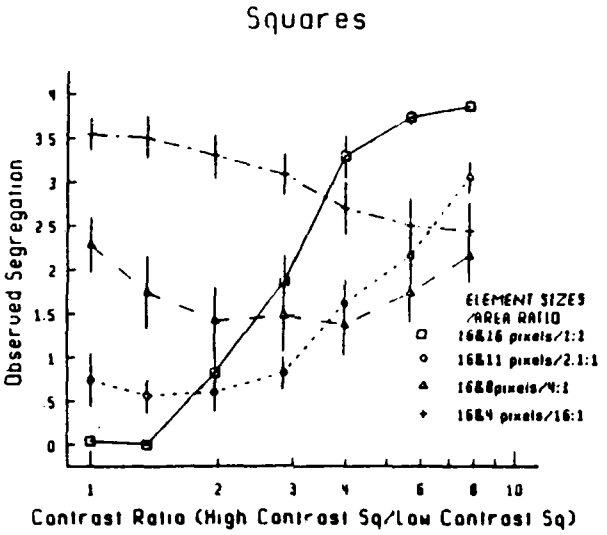
Squares
Observed Segregation
Contrast Ratio (High Contrast Sq/Low Contrast Sq)
ELEMENT SIZES
/AREA RATIO
16&16 pixels/1:1
16&11 pixels/2.1:1
16&8pixels/4:1
16&4 pixels/16:1

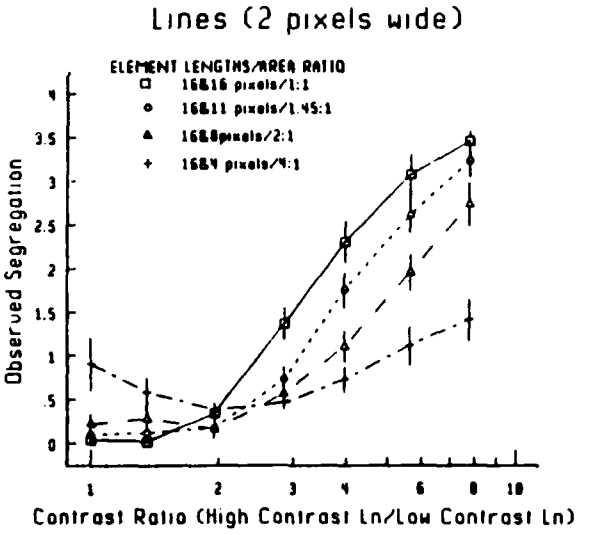
Lines (2 pixels wide)
ELEMENT LENGTHS/AREA RATIO
16&16 pixels/1:1
16&11 pixels/1.45:1
16&8pixels/2:1
16&4 pixels/4:1
Observed Segregation
Contrast Ratio (High Contrast Ln/Low Contrast Ln)

FIGURE 10

segregation depends on differences in areal contrast (contrast times area) between the texture elements with minimal segregation occurring at the point where the areal contrasts of the large and small elements are approximately the same. Patterns composed of squares produced better segregation than patterns composed of lines. This result was also found by Beck, Prazdny and Rosenfeld (1983) and is predicted by the simple spatial-frequency model. It follows from the fact that the lines occupied a smaller area of the pattern than the squares and activation of the spatial frequency channels was thus "diluted" by the background.

The interaction of element area and contrast supports the argument that the segregation of patterns composed of different arrangements of lines is not attributable to "emergent" features of the elements. If segregation of the line patterns had depended on the linking of the longer (16 pixel) lines into emergent, even longer lines, segregation should have been an increasing function of the contrast ratio between the elements, regardless of their area-ratio, since greater differences in contrast would have increased the linking of lines based on similarity of contrast.

For the textures composed of squares, the size difference of the squares affected perceived segregation. Figure 10 (top) shows that the minimum segregation ratings increased with the size differences between the squares in the pattern. This result is not explained by the simple model. For the textures composed of lines, however, Figure 10 (bottom) shows that the size difference of the lines did not yield different minimum segregation ratings. This is in accord with the simple model. A reason for this difference in results will be proposed when we present the complex model (page 23).

2.3.3 *Pattern density (duty-cycle)*

Seventy patterns were constructed through the combination of 2 element area-ratios (1:1 and 4:1), 5 large-square-sizes (12, 10, 8, 6, and 4 pixel squares), and 7 contrast-ratios.Thus, for the 1:1 element area-ratio condition, the patterns were composed of two sets of equal size squares of 12, 10, 8, 6, or 4 pixels on a side (12.96, 10.80, 8.64, 6.48, and 4.32 min, respectively). In the 4:1 element area-ratio condition, the patterns were composed of 12 pixel and 6 pixel squares, 10 pixel and 5 pixel squares, 8 pixel and 4 pixel squares, 6 pixel and 3 pixel squares, or 4 pixel and 2 pixel squares. The center-to-center element spacing was held constant at 14 pixels (15.12 min), thus creating patterns that were approximately 4 degrees in width and height. The variable-intensity elements were always above the background. The luminances of the background and the fixed- and variable-intensity elements were the same as in the gray background experiment in Section 2.3.1 (page 11).

Figure 11 (top panel) shows the mean segregation ratings for

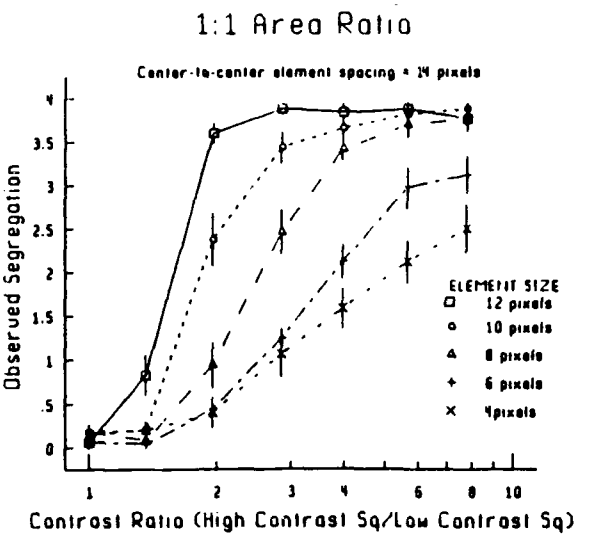
1:1 Area Ratio
Center-to-center element spacing = 14 pixels
Observed Segregation
Contrast Ratio (High Contrast Sq/Low Contrast Sq)
ELEMENT SIZE
12 pixels
10 pixels
8 pixels
6 pixels
4pixels

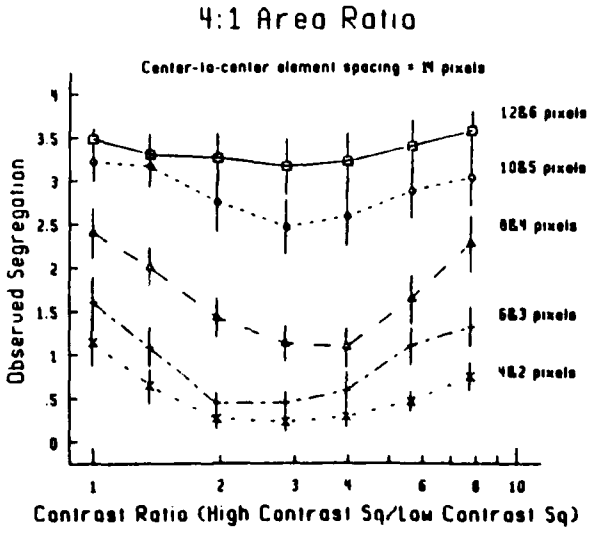
4:1 Area Ratio
Center-to-center element spacing = 14 pixels
Observed Segregation
Contrast Ratio (High Contrast Sq/Low Contrast Sq)
12&6 pixels
10&5 pixels
8&4 pixels
6&3 pixels
4&2 pixels

FIGURE 11

the 1:1 element area-ratio condition, and Figure 11 (bottom panel) shows the mean ratings for the 4:1 element area-ratio. As in previous experiments, perceived segregation for the 4:1 element area-ratio was a u-shaped function and minimal at or around the point at which the areal contrasts of the large and small squares were equal. For both the 1:1 and 4:1 element area-ratios, perceived segregation decreased with decreasing density (decreasing element size). This result is consistent with our simple model. Decreasing element density dilutes the effect of contrast differences between the elements because there is more background space. This would result in greater uniformity in the outputs of spatial-frequency channels corresponding to the fundamental period of the striped and checked regions. This should, and in fact did, produce poorer segregation. However the basic tradeoff between area and contrast remains. As in previous experiments, one aspect of the results was not predicted by the simple model. Texture segregation was also a function of the size difference between the large and small squares. The u-shaped functions are shallower as the size difference between the large and small squares increased.

2.3.4 *Varying the fundamental frequency (scaling)*

Normally texture patterns scale in the sense that perceived segregation remains constant with changes in the visual angle subtended. Wertheimer (1923) observed that the grouping of a set of elements does not change with viewing distance or the magnification of the pattern. Green, Wolf, and White, (1959) also found that, as long as the relative element sizes and separations remain constant the absolute size of the pattern does not affect texture discrimination. In contrast, Beck, Prazdny and Rosenfeld (1983) found that patterns like Figure 1 fail to scale. When the sizes and separations of the squares were reduced by one-half, perceived segregation increased. This indicates that segregation depends on the absolute sizes of the elements and their separations.

This observation is consistent with the view that perceived segregation is mediated by the outputs of spatial frequency channels. Contrast sensitivity is generally highest at a spatial frequency ranging from 3-10 cycles/deg, depending on experimental conditions. The standard tripartite pattern (Figures 1 and 2) had a period of 56 pixels (the distance between the centers of two columns of the same type of square), which translates to approximately 1 cycle/degree. Figures 5 and 6 show that the spatial frequency channel that gives the best information for segregation is one that matches the period of the pattern. For the standard tripartite pattern, this channel would have peak output at a spatial frequency of around 1 cycle/degree. By either increasing the viewing distance or proportionately decreasing the sizes of the elements and their separations, the period of the pattern can be decreased, thus increasing the spatial frequency

which carries the most information about differences between the striped and checked regions of the pattern. Reducing the period of the pattern should increase perceived segregation, up to the point where the fundamental frequency component of the pattern has a spatial frequency at the peak of the contrast sensitivity function. Further reduction of the period of the pattern should lead to a decrease in perceived segregation because the fundamental frequency component of the pattern will be of a spatial frequency that is higher than that at the peak, thus entering a range where contrast sensitivity decreases.

We tested this prediction of the spatial frequency model. The period of the tripartite pattern was reduced by decreasing the sizes and separation of the squares making up the pattern. The effects of contrast differences between the two types of squares were investigated under 3 element area-ratio (1:1, 4:1, and 16:1) and 4 fundamental frequency conditions (1, 2, 4, and 8 cycles/degree).

Seventy-seven stimuli were constructed through the partial combination of 3 element area-ratios (1:1, 4:1, and 16:1), 4 fundamental-frequencies (1, 2, 4, and 8 cycles/degree), and 7 contrast-ratios. The 3 element area-ratio conditions were equal-size squares (1:1 element area-ratio), unequal-size squares with a ratio of areas of 4:1, and unequal-size squares with a ratio of areas of 16:1. The 4 fundamental-frequencies were 1, 2, 4, and 8 cycles/degree, which corresponded to center-to-center element separations (one-half periods) of 28 pixels (30.24 min), 14 pixels (15.12 min), 7 pixels (7.56 min), and 4 pixels (4.32 min), respectively. The center-to-center element separation was held constant at 1.75 times the width of the largest square in the pattern. The 4 largest square sizes were 16, 8, 4, and 2 pixels on a side (17.28, 8.64, 4.32, and 2.16 min, respectively). The effect of reducing the element size and separation was to decrease the size of the whole pattern, as well as its period. The patterns with a fundamental frequency of 1 cycle/degree measured 7.56 degrees in height and width. The patterns with fundamental-frequencies of 2, 4, and 8 cycles/deg measured 3.78, 1.89, and 1.08 degrees, respectively, in height and width. The variable-intensity elements were always above the background. The luminances of the background and the fixed- and variable-intensity elements were the same as in the gray background experiment in Section 2.3.1 (page 11).

The results are presented in Figure 12 for the 1:1, 4:1, and 16:1 element area-ratios. As in the previous experiments, perceived segregation is a u-shaped function of contrast ratio, with a minimum around the point at which the areal contrasts of the two texture elements are equal. Figure 13 shows the predicted segregation values produced by the simple spatial frequency model. A comparison of the predicted and observed segregation curves shows that the general shapes of the observed segregation curves for each

Observed Segregation

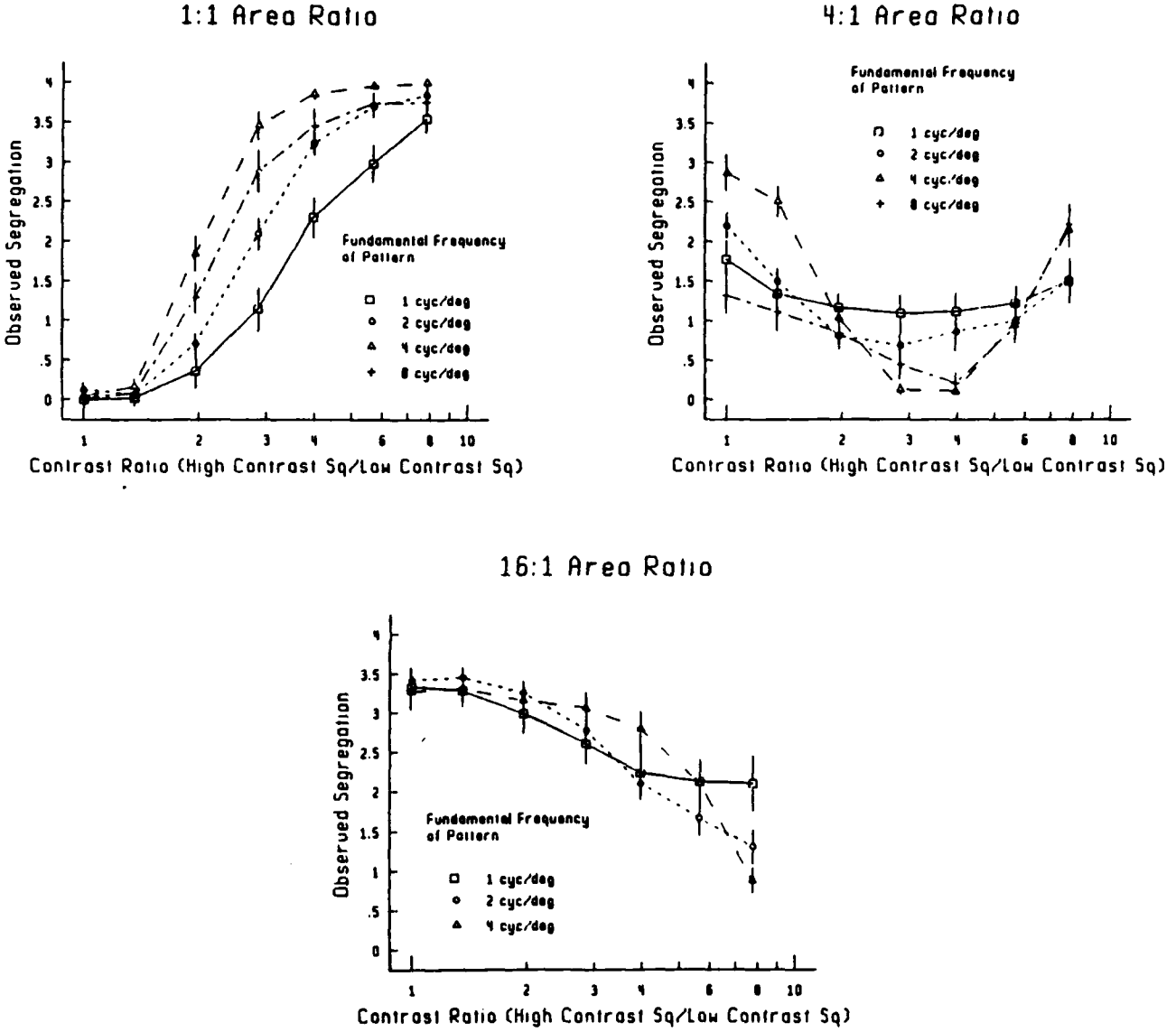

FIGURE 12

Predicted Segregation

1:1 Area Ratio

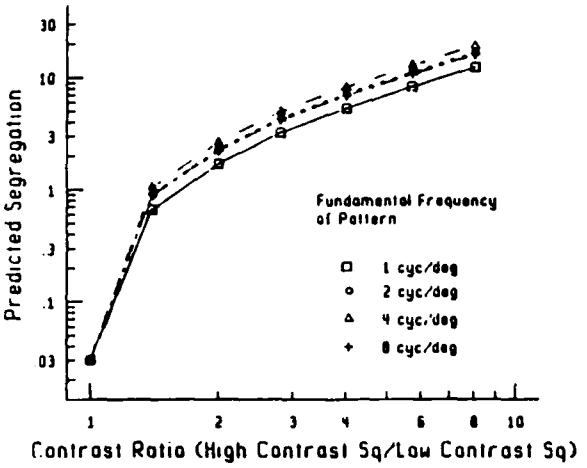

4:1 Area Ratio

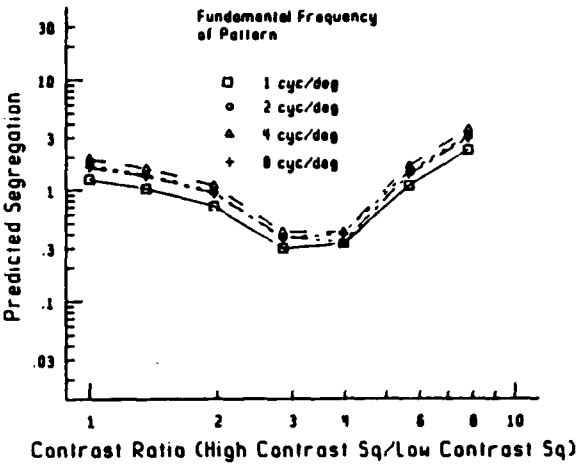

16:1 Area Ratio

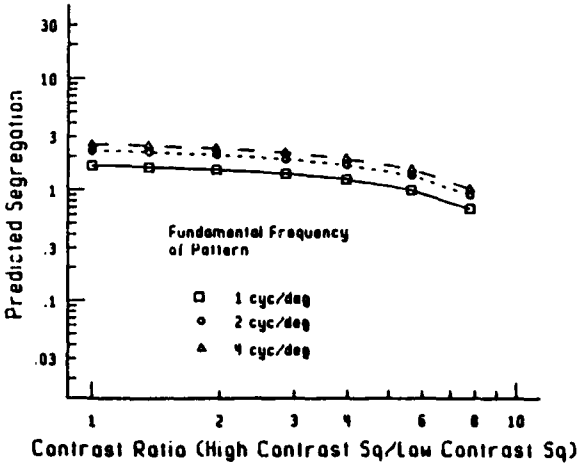

FIGURE 13

element area-ratio are fairly well predicted by the model, as are the contrast ratios at the points of minimum segregation for the three element area-ratios.

Figures 12 shows that perceived segregation of the patterns varies with their period. Some aspects of this variation in perceived segregation are predicted by the simple spatial frequency model (Figure 13). According to the model, the pattern which should be most easily segregated, at a given contrast ratio, is that whose fundamental spatial frequency component is approximately 4 cycles/degree. Patterns with higher or lower fundamental frequency components should be more difficult to segregate. This prediction is consistent with many of the observed segregation ratings, with a few striking exceptions in the 4:1 and 16:1 element area-ratio conditions. The effects of changing the fundamental frequency were also found with patterns of constant size. Instead of reducing the overall size of the patterns, the overall size of the patterns was maintained by increasing the number of rows and columns of elements (Sutter 1987).

The contrast-ratio at which minimum observed segregation occurs in these conditions is well-predicted by the model, but notice that the observed segregation curves cross-over dramatically, while the predicted curves just move up or down, for the most part, depending on fundamental frequency. For very low contrast ratios, the ordering of curves is roughly from the most visible on top to the least visible fundamental frequencies (as was built into the model by weighting the predictions by a particular sensitivity function). In the trough, however, the ordering is different; patterns having low fundamental frequencies still segregate quite well (contradicting the model) while patterns with high fundamental frequencies don't segregate at all (agreeing with the model).

This discrepancy between the simple model's predictions and the results of varying fundamental frequency is probably closely related to another discrepancy mentioned near the beginning of this section--namely, for patterns with a fundamental frequency of about 1 c/deg, the dip in the u-shaped function becomes less pronounced as the area-ratio becomes higher or, equivalently, as the difference between the sizes of the squares becomes larger. The relation between the two discrepancies will become clearer below when we propose the complex model (page 24). Roughly, the idea is this: for low fundamental spatial frequencies of textures, the information at the higher harmonics (transmitted by channels sensitive to the higher harmonics (e.g., the right hand side in Figures 5 and 6) is available to the observer and does help to segregate the patterns (although this kind of information is totally ignored by the simple model). At high fundamental spatial frequencies, however, the higher harmonics of the texture patterns are invisible to the observer so cannot contribute.

2.3.5 *Squares, circles, blobs, and aligned vs. non-aligned squares*

Perceived segregation of the tripartite pattern depends on the detection of the difference in the arrangement of elements in the striped and checked regions of the patterns. The channels showing strikingly different outputs to the different arrangement of elements in the striped and checked regions are at the fundamental period of the pattern. The outputs from the higher spatial-frequency channels have very little affect on perceived segregation. Although the pattern of activity is distributed differently in the striped and checked regions, the amounts of modulated activity in the striped and checked regions are similar at the higher spatial-frequencies. Channels tuned to the higher spatial-frequencies respond to the edges of the elements in a pattern. Therefore, altering the contours of the elements should only have a minor effect on the perceived segregation.

An alternative explanation proposed by Grossberg and Mingolla (1985) explains perceived segregation of the tripartite pattern as the result of complex interactions within a Boundary Counter System (BC) system. According to Grossberg and Mingolla, the boundaries generated by the BC system need not be visible. In the case of tripartite patterns, Grossberg and Mingolla argue that the BC system creates invisible elongated, vertical, boundaries in the top and bottom regions and invisible diagonal boundaries in the middle region of the tripartite pattern. These invisible boundaries are the basis for the perceived segregation of the tripartite pattern. Perceived segregation should, therefore, be significantly affected by changing the contours of the elements. The invisible boundaries formed in the BC system would be expected to be formed more strongly when the elements of the patterns are aligned than when they are not aligned.

Two experiments investigated the effect of element contour alignment on perceived segregation. In the first experiment, the elements were squares, circles, and blobs. Two area-ratios were investigated: 1:1 and 4:1. In the patterns composed of squares, the fixed-intensity square was 16 pixels on a side. The variable-intensity squares were either 16 or 8 pixels on a side. The circle and blob stimuli were equated in area to the squares. Figure 14 shows the 1:1 square, circle, and blob patterns. The center-to-center separation of the elements was 28 pixels. The variable intensity elements were always above the background. The luminances of the background and the fixed- and variable-intensity elements were the same as in the gray background experiment in Section 2.3.1 (page 11). (The patterns are shown on a dark gray background to facilitate copying.)

Figure 15 presents the mean segregation ratings for the 1:1 area-ratio (top panel) and the 4:1 area-ratio (bottom panel).

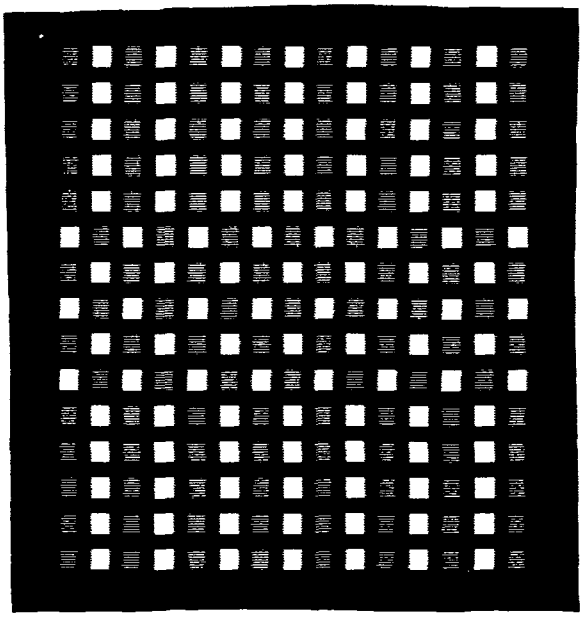

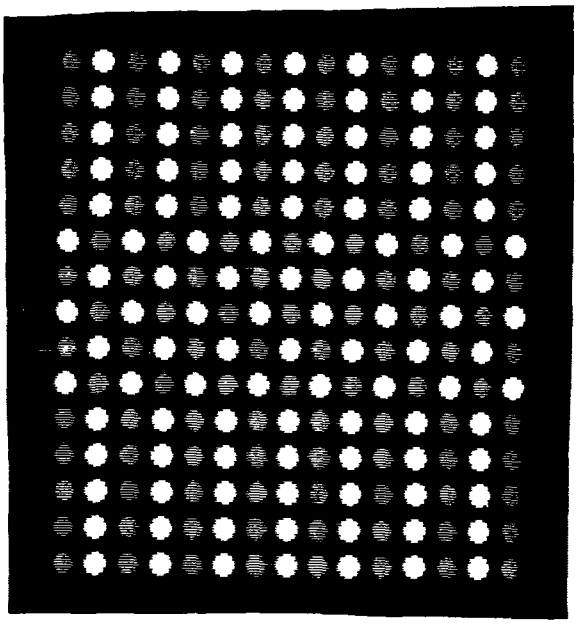

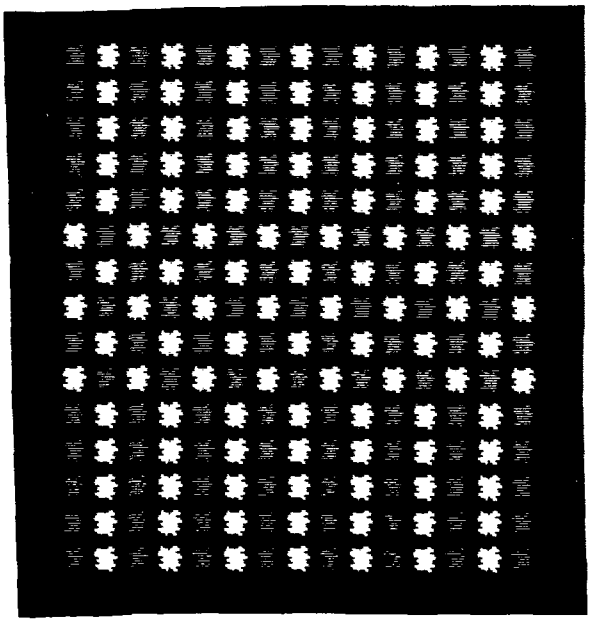

FIGURE 14

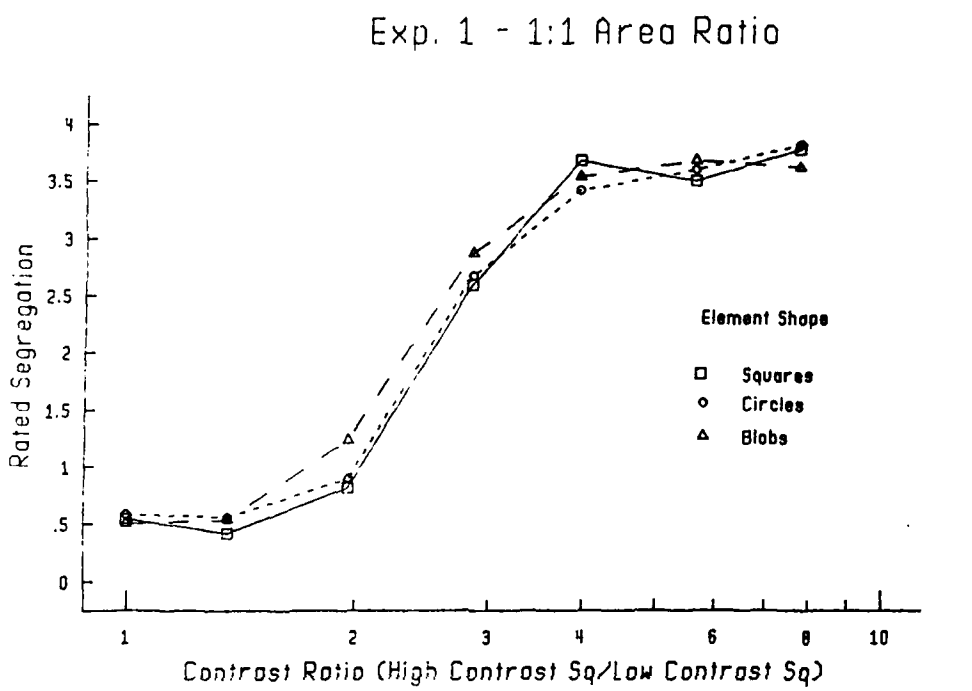
Exp. 1 - 1:1 Area Ratio
Rated Segregation
0
.5
1
1.5
2
2.5
3
3.5
4
1
2
3
4
6
8
10
Contrast Ratio (High Contrast Sq/Low Contrast Sq)
Element Shape
Squares
Circles
Blobs

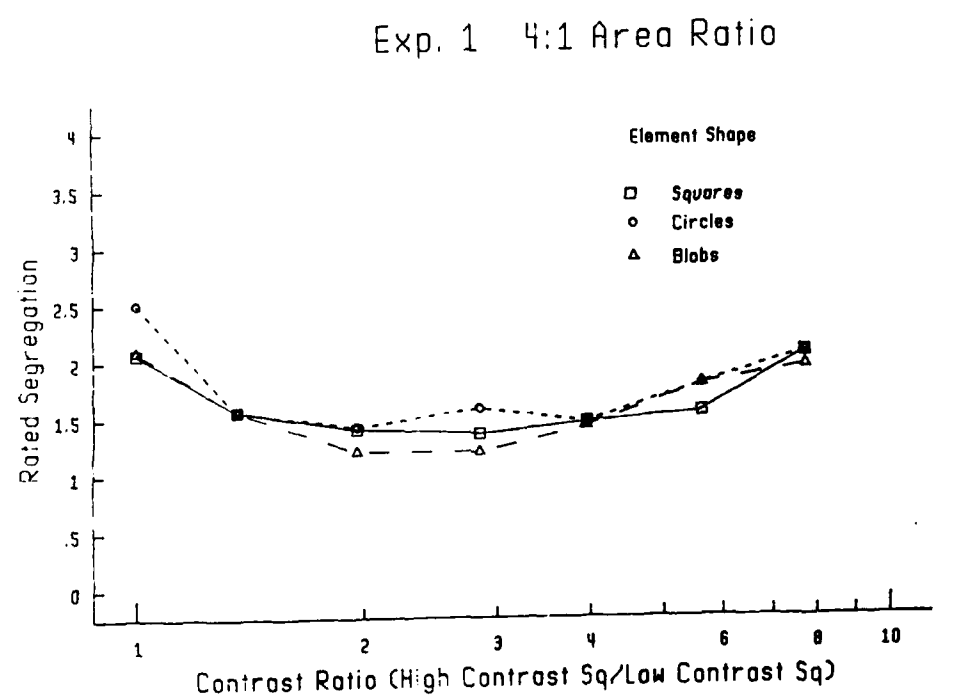
Exp. 1 4:1 Area Ratio
Rated Segregation
0
.5
1
1.5
2
2.5
3
3.5
4
1
2
3
4
6
8
10
Contrast Ratio (High Contrast Sq/Low Contrast Sq)
Element Shape
Squares
Circles
Blobs

FIGURE 15

Edge alignment failed to affect perceived segregation. The curves for the square, circle and blob elements are highly similar. The area x contrast tradeoff indicates that it is differences in the outputs of spatial-frequencies approximating the fundamental period of the pattern and not differences in the higher spatial-frequencies that are important for perceived segregation.

In the second experiment, the perceived segregation of aligned and non-aligned squares were compared. The textures were composed of squares 16 pixels on a side. Figure 16 shows examples of the aligned (top panel) and the non-aligned arrangements (bottom panel). The patterns were composed of one-element-only, opposite-sign-of-contrast, and same-sign-of-contrast elements. The elements composing the patterns, the luminance conditions, and the form in which the data are plotted is explained in Section 2.5 (page 21). Figures 17 and 18 present the results. No significant differences in perceived segregation occurred as a function of the alignment of the squares. If segregation occurred due to the contour interactions in the BC system, as suggested by Grossberg and Mingolla, perceived segregation should have been significantly reduced in the pattern composed of the non-aligned squares.

2.4 Patterns with no energy at the fundamental: results and predictions of simple model

In this experiment, the patterns contained elements that were either uniform squares (14 x 14 pixels) or were center-surround elements composed of a center square (10 by 10, pixels) surrounded by a square frame 2 pixels wide so that total dimensions of the element were 14 by 14. The center-to-center separation of the texture elements was 26 pixels. The contrasts of the centers and annuli of the center-surround elements were always equal but of opposite sign so that the average luminance of the center-surround element was the same as the background.

Some patterns-- called "opposite-sign-of-contrast patterns" below--were constructed so that the centers of the two types of texture elements were of opposite sign-of-contrast. In the case of center-surround elements (Figure 19 top) one element consisted of a higher intensity center and a lower intensity annulus; the other element of a lower intensity center and a higher intensity annulus. In the case of solid squares, one element consisted of squares brighter than the background and one of squares darker than the background. Other patterns--called "one-element-only patterns" below--contained only one kind of element (as shown in Figure 19 bottom). In this case that type could either have the center (which in the case of uniform squares implies the whole square) brighter than the background or dimmer than the background. We also used various unbalanced combinations which will not be discussed further although they might prove useful in testing our complex model. The background was set at 16.1 ft.-L.

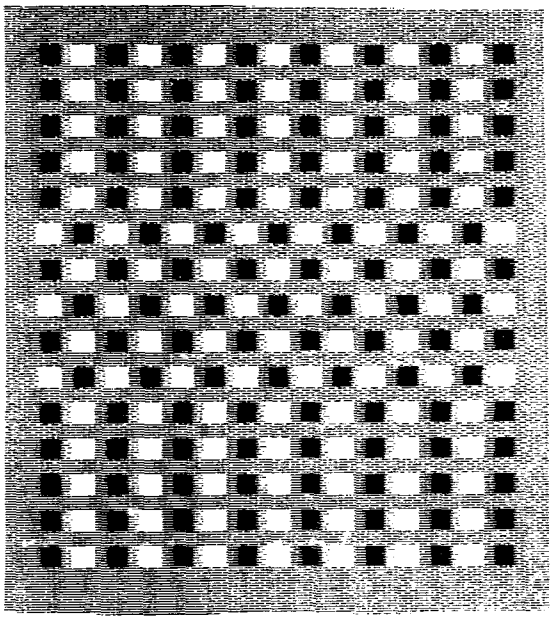

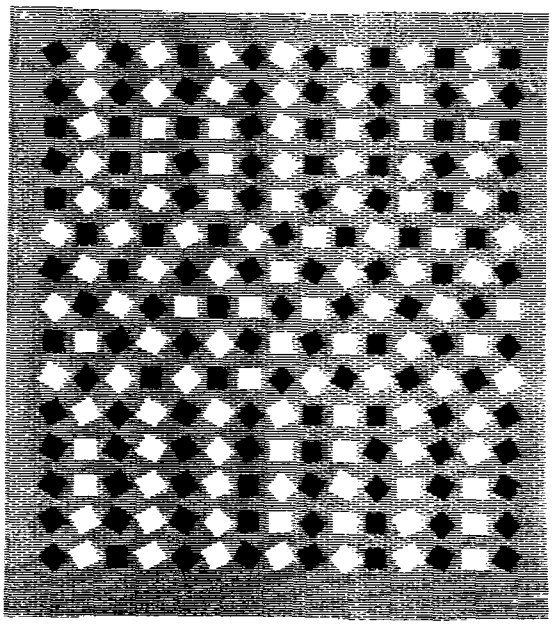

FIGURE 16

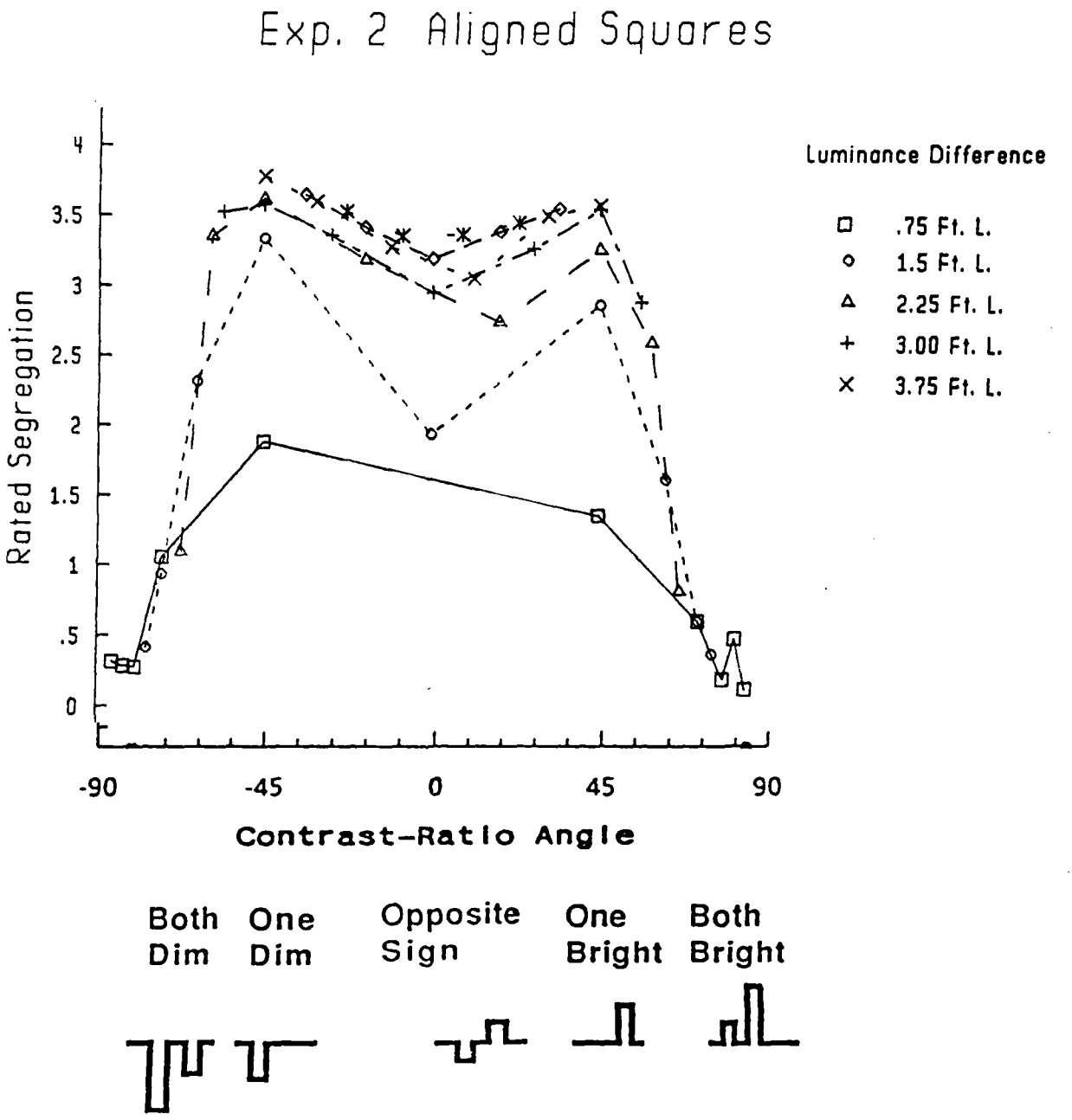
Exp. 2 Aligned Squares
Rated Segregation
4
3.5
3
2.5
2
1.5
1
.5
0
-90
-45
0
45
90
Contrast-Ratio Angle
Luminance Difference
.75 Ft. L.
1.5 Ft. L.
2.25 Ft. L.
3.00 Ft. L.
3.75 Ft. L.
Both Dim
One Dim
Opposite Sign
One Bright
Both Bright

FIGURE 17

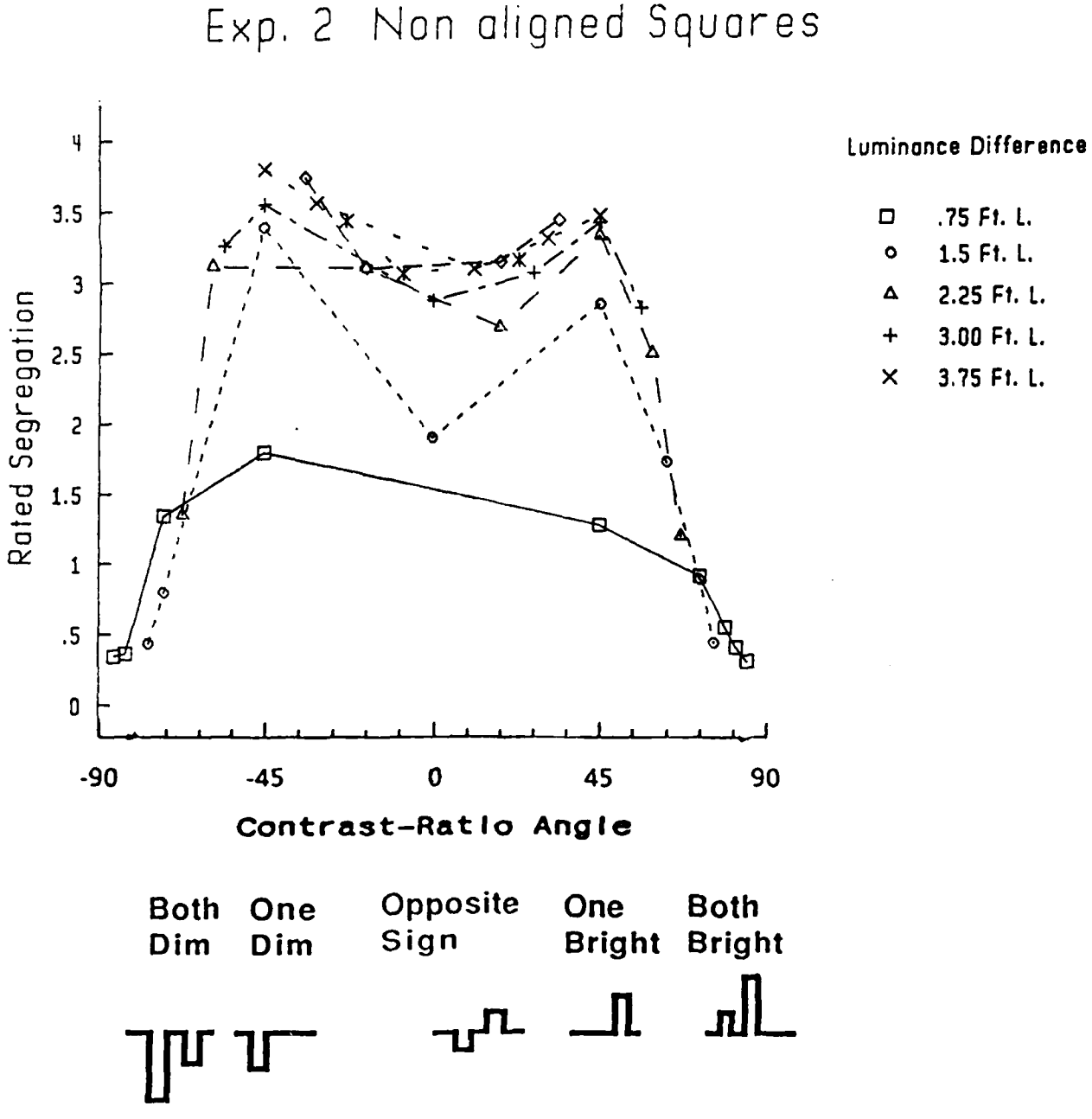
Exp. 2 Non aligned Squares
Rated Segregation
4
3.5
3
2.5
2
1.5
1
.5
0
-90
-45
0
45
90
Contrast-Ratio Angle
Luminance Difference
.75 Ft. L.
1.5 Ft. L.
2.25 Ft. L.
3.00 Ft. L.
3.75 Ft. L.
Both Dim
One Dim
Opposite Sign
One Bright
Both Bright

FIGURE 18

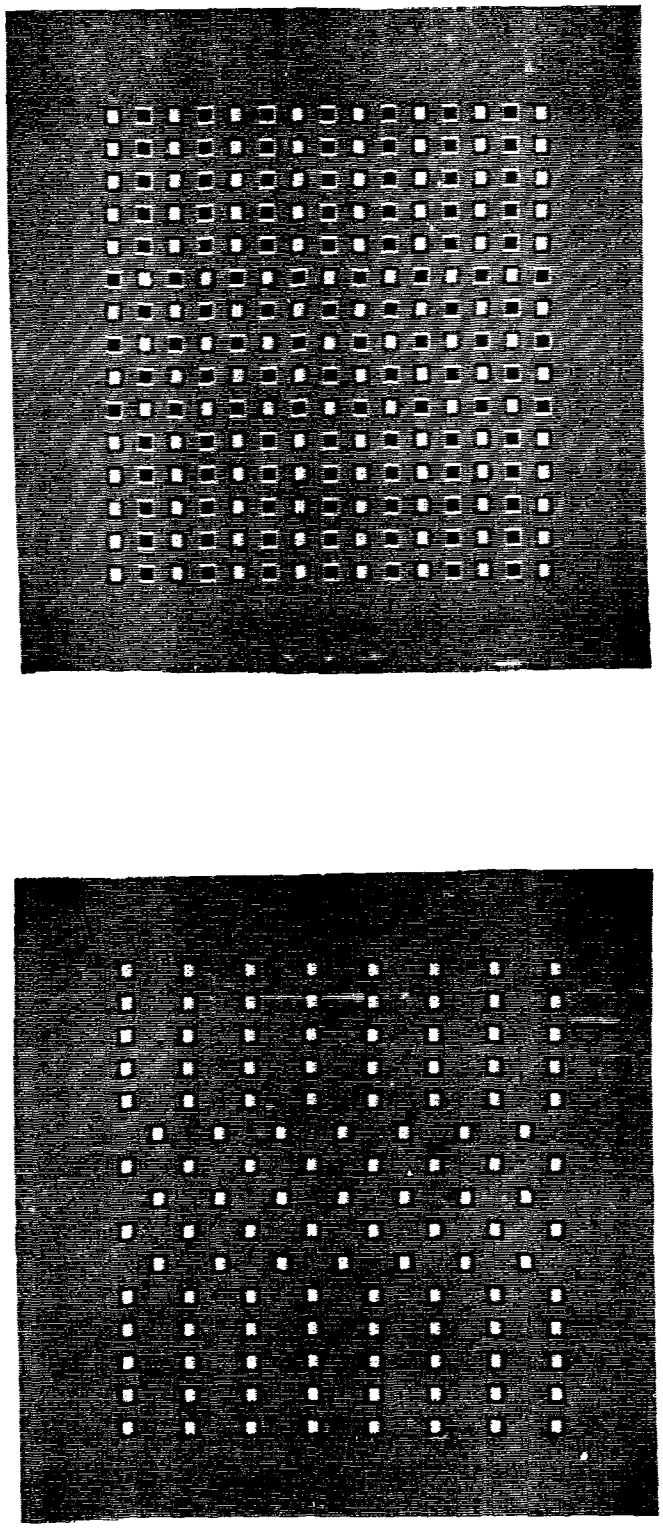

FIGURE 19

Some of the results are shown in Figure 20. The horizontal axis for each panel shows the difference in luminance between the center of an element (which in the case of the square was the whole square) and the background. For opposite-sign-of-contrast patterns using center-surround elements, segregation was poor, regardless of the level of contrast (Figure 20 upper left). When the elements were uniform squares of opposite sign of contrast (Figure 20 upper right), on the other hand, segregation was good (as previously reported by Beck, Sutter, & Ivry, 1987). For one-element-only patterns, perceived segregation was very good both for center-surround elements (Figure 20 lower left) and for solid squares (Figure 20 lower right).

These results are not in accord with the predictions of the simple model in several ways. The most dramatic is that, since the center-surround elements average out to the background luminance, no stimulus information is available at the fundamental frequency of the pattern. Thus, according to the simple model, no patterns based on center-surround elements should segregate well. However, the one-element-only patterns do. This shows that perceived segregation can occur based on information contained only in the higher harmonics of the texture pattern.

2.5 Patterns with same- and opposite-sign-of-contrast: results and predictions of simple model

An intriguing result that does not fit the framework of low-level channels without separate consideration of "on" and "off" responses is that patterns with squares of opposite-sign -of-contrast yield such good texture segregation compared to same-sign-of-contrast patterns (Beck, Sutter, & Ivry, 1987). One possibility is that sign of contrast is a feature, i.e. positive and negative contrasts are encoded in different feature maps. Perceived segregation of opposite-sign-of-contrast patterns should then be similar to one-element-only patterns. An experiment investigated whether the strong texture segregation that occurs when the squares are of opposite contrast-sign involve different mechanisms from those when the squares are same sign-of-contrast.

One-Element-Only, Opposite-sign-of-Contrast, and Same-sign-of-Contrast Solid Elements--Figure 21 shows portions from the luminance profiles of each of five different patterns. Each profile shows one of each of the two kinds of elements composing the texture. In all of these patterns both kinds of elements are squares of the same size. Also the background luminance is the same in all cases (16.1 ft.-L.). The element luminance changes from pattern to pattern but with the following important constraint: the difference between the luminances of the two squares is the same in all cases. Hence we will call the stimuli in Figure 21 a "constant-L_1-minimum-L_2" or "constant-difference" series of stimuli.

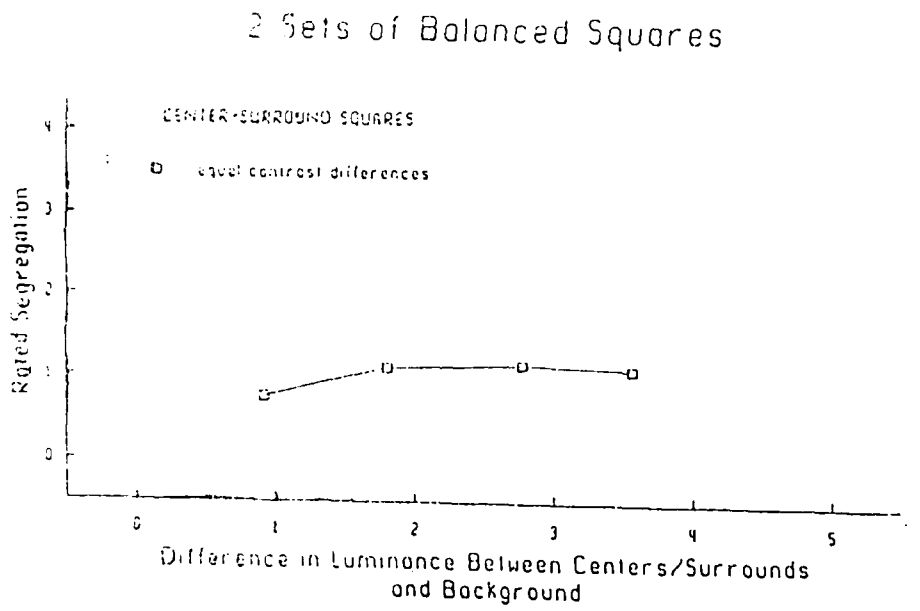
2 Sets of Balanced Squares
CENTER-SURROUND SQUARES
equal contrast differences
Rated Segregation
Difference in Luminance Between Centers/Surrounds and Background

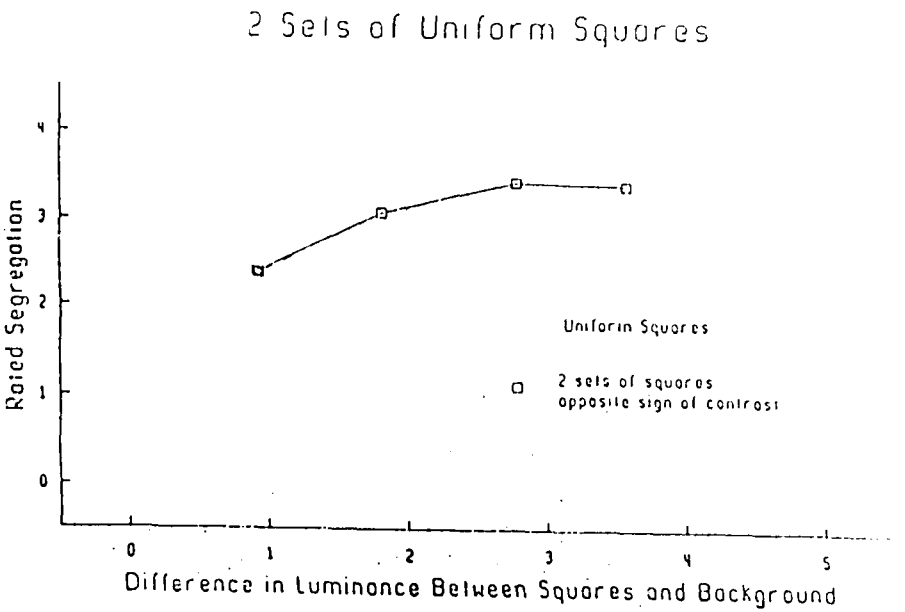
2 Sets of Uniform Squares
Uniform Squares
2 sets of squares opposite sign of contrast
Rated Segregation
Difference in Luminance Between Squares and Background

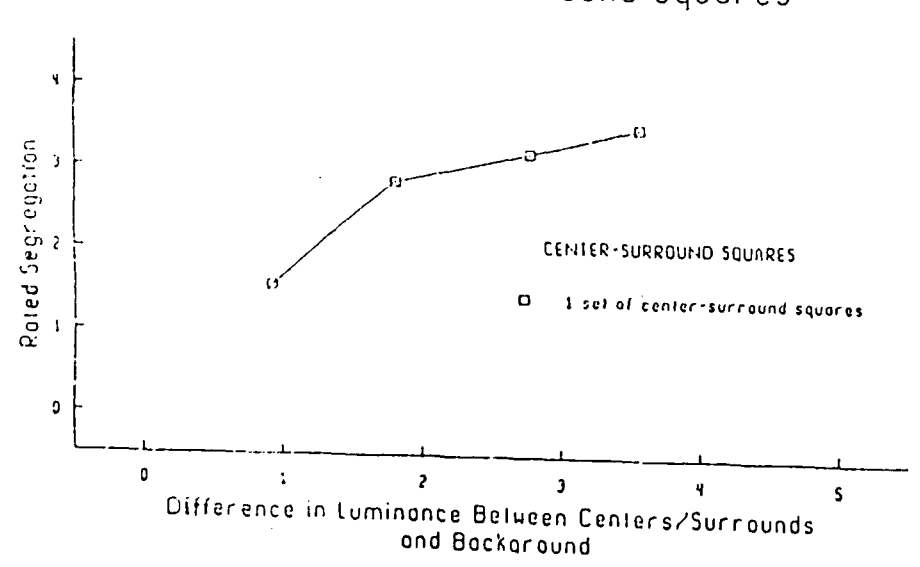
1 Set of Center-Surround Squares
CENTER-SURROUND SQUARES
1 set of center-surround squares
Rated Segregation
Difference in Luminance Between Centers/Surrounds and Background

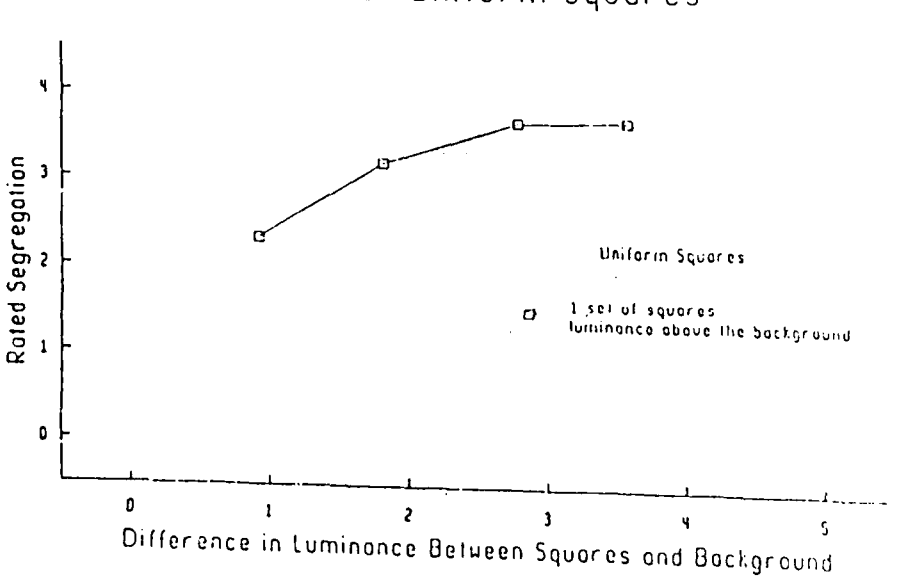
1 Set of Uniform Squares
Uniform Squares
1 set of squares luminance above the background
Rated Segregation
Difference in Luminance Between Squares and Background

FIGURE 20

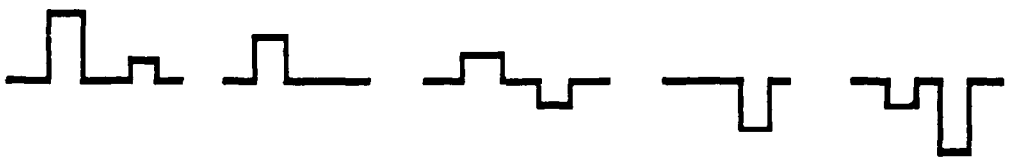

Both Bright	One Bright	Bright-Dark	One Dark	Both Dark
Same Sign of Contrast	One Element Only	Opposite Sign of Contrast	One element only	Same Sign of Contrast

FIGURE 21

In this experiment, we used 66 stimuli of the five types shown in Figure 21. The luminance difference between the squares could be 0.0, .75, 1.50, 2.25, 3.00, and 3.75 ft.-L. Figure 22 plots the mean ratings (except stimuli for which the difference was zero, all of which led to very low ratings between 0 and .16). The vertical axis shows the mean segregation ratings. Each curve connects the results for a constant-difference series of stimuli. The horizontal axis is simply a convenient monotonic transformation of contrast ratio into a quantity we called the contrast-ratio-angle. (The contrast-ratio angle is equal to 135 degrees minus arctan of contrast ratio.) A contrast-ratio angle of zero represents squares of opposite contrast-sign with the luminances of the two squares equally above and below the background. Points plotted between 0 and +45 degrees represent stimuli of opposite sign-of-contrast in which the contrast of the square above the background is increasingly greater than the contrast of the square below the background. At +45 degrees the luminance of the square below the background is equal to the background and a pattern was composed of a single square above the background. Points plotted between 45 and 90 degrees represent stimuli in which the luminances of both squares are above the background. As one moves towards 90 degrees the ratio of the contrasts of the two squares approach 1.0. At 90 degrees the contrasts of the two squares are equal.

Figure 22 shows that textures consisting of a single square segregated most strongly, followed by textures composed of elements of opposite-sign-of-contrast (thereby replicating the results in the right panels of Figure 20). Textures composed of elements of the same-sign-of-contrast segregated least. Figure 22 shows that the textures with a single square, squares of opposite-sign-of-contrast, and the squares of the same-sign-of-contrast all lie on a continuum. A small change in the stimulus produces a small change in perceived texture segregation. The continuity of the functions is consistent with the hypothesis that texture segregation is a function of the outputs of spatial-frequency channels rather than separate on and off mechanisms. Texture composed of single types of elements and of elements of opposite contrast-sign are not categorically different from textures composed of elements with the same contrast-sign. However, an examination of the output of the spatial-frequency channels shows that they cannot explain the data completely. Figure 23 (in the same form as Figure 22) shows the predictions of the simple model. As can be seen all stimuli in a constant-difference series are predicted to segregate to approximately the same extent. This occurs because the outputs of the most active channels (those tuned to frequencies near the fundamental) are the same to all stimuli in such a series. For these channels, the background falls equally on the inhibitory and excitatory portions of the receptive field so it is only the squares themselves that count. When the difference between the luminances of the squares is held constant, the modulated activity

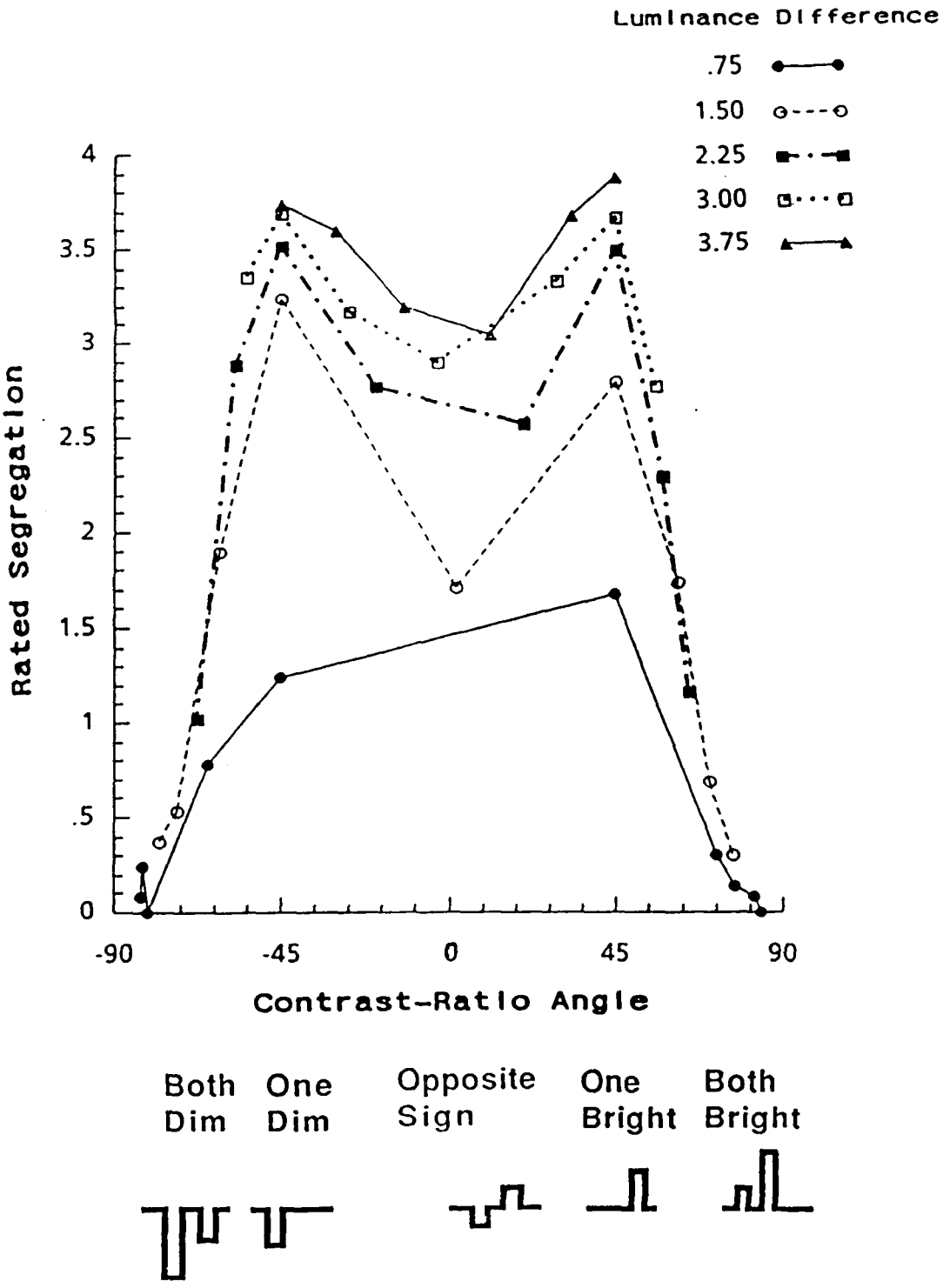
Luminance Difference
.75
1.50
2.25
3.00
3.75
Rated Segregation
4
3.5
3
2.5
2
1.5
1
.5
0
-90
-45
0
45
90
Contrast-Ratio Angle
Both Dim
One Dim
Opposite Sign
One Bright
Both Bright

FIGURE 22

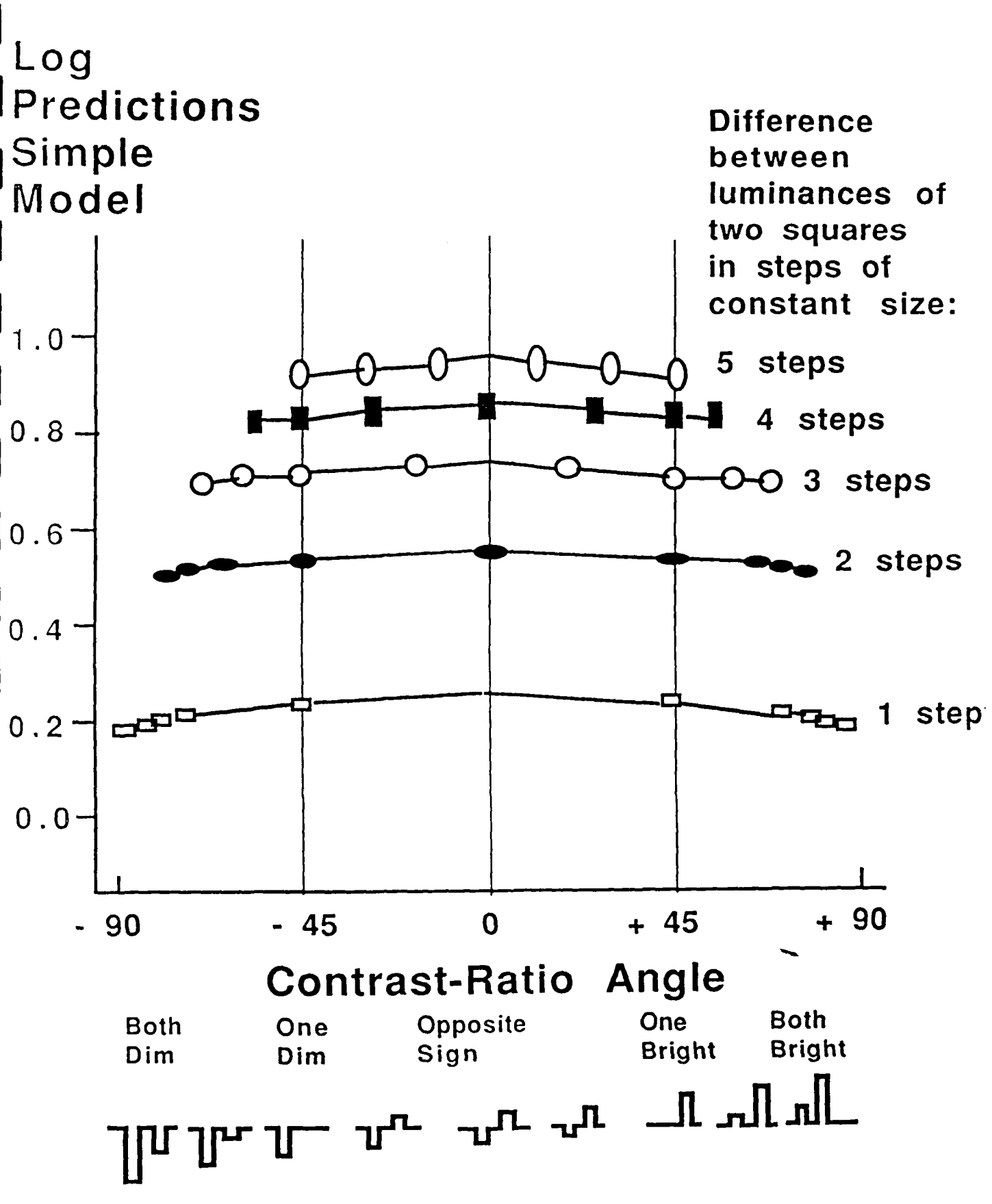
Log
Predictions
Simple
Model
Difference
between
luminances of
two squares
in steps of
constant size:
5 steps
4 steps
3 steps
2 steps
1 step
1.0
0.8
0.6
0.4
0.2
0.0
- 90
- 45
0
+ 45
+ 90
Contrast-Ratio Angle
Both
Dim
One
Dim
Opposite
Sign
One
Bright
Both
Bright

FIGURE 23

in the output of the channel is constant. The outputs of other channels are different for different members of the series, but these channels contribute very little to the predictions of the simple model. Thus, the greater perceived segregation of the one-element-only patterns than of the opposite-sign-of-contrast patterns and of the opposite-sign-of-contrast patterns than of the same-sign-of-contrast patterns is not consistent with the simple model.

Another discrepancy between predictions and results occurs for same-sign-of-contrast patterns (toward the left and right edges of Figures 23 and 22). Two patterns having the same contrast-ratio $(L_2-L_0)/(L_1-L_0)$ but different luminance differences L_2-L_1 are not predicted to segregate to the same extent; that is, the curves in Figure 23 are vertically displaced at the left and right edges as well as in the middle. But two such patterns did tend to segregate to the same extent in the experimental results--that is, the different curves in Figure 22 converge at the left and right edges of the figure so that for large luminance differences, the size of the luminance difference (which curve the pattern's point is on) ceases to affect perceived segregation; only contrast-ratio (the point's horizontal coordinate) does.

The two discrepancies just mentioned suggest two different modifications of the simple model may be necessary. As described earlier, the one-element-only advantage suggests using the information in the higher-harmonic channels. The second discrepancy suggests instead a modification of the assumption that each filter's output (and hence the simple-model's predicted value) is linear with luminance. Standard results on "light adaptation" make it clear, of course, that such modification is absolutely necessary in any complete model of the visual system. It is only in the case of patterns in which the range of luminances and contrasts is small enough that one can hope for linearity.

2.6 Complex spatial-frequency channels model

Two aspects of the results reported in Section 2.3 are different from those predicted by a simple spatial-frequency channels model, i.e., a linear pooling of within-filter differences weighted by the contrast sensitivity function (page 9). First, the fact that the minima in the functions in Figures 9, 10 (top panel), 11 (bottom panel), and 12 (right panel) is not the same for all area-ratios but varies with the size difference between the large and small squares making up a pattern. The minimum is less as the size difference between the large and small squares is larger. If areal contrast were the only factor affecting segregation, the segregation ratings should have been the same when the area x contrast between the large and small squares composing a pattern were equated. Second, the fact that the curves in Figure 12 (right panel) cross. Figure 13 shows that the functions predicted by the

simple model do not cross.

Further experiments with textures containing balanced elements with no energy at the fundamental frequency (Section 2.4) and with textures containing elements of opposite-sign-of-contrast (Section 2.5) also gave results which are not consistent with the simple model we proposed. These discrepancies suggest that the simple model does not make sufficient use of information in the channels sensitive to the higher-harmonics of the pattern. One way in which the information in the higher-harmonic channels may be used involves a more complicated spatial-frequency-channels model. This model is illustrated in Figure 24. Each channel in this model contains three stages: linear-filtering followed by a non-linear function such as a rectification, followed by a second linear filter. The filters in both stages are selective for spatial-frequency and orientation. A large number of such channels tuned to various spatial frequencies and orientations are assumed to exist. We call these channels "complex channels" to distinguish them from the simple channels of the earlier model, and because this kind of channel is similar to current models of complex cells, (e.g. Hochstein and Spitzer, 1985; and Hochstein, 1985a, b). Measures of pooled second-stage filter activity (analogous to that in the simple model) are taken to be the predictor of perceived texture segregation.

Linear filtering followed by a rectifying nonlinearity has been proposed by Grossberg & Mingolla (1985), Chubb & Sperling (1988), and Bergen & Adelson (1988). Grossberg and Mingolla (1985) have proposed a model containing the three stages of the complex-model plus additional processes, and have suggested that their model accounts for perceived segregation in patterns such as ours. Their demonstrations, however, involve only filterings sensitive to the higher harmonics of the pattern (small receptive fields relative to the pattern periodicity). On the basis of the findings reported in Section 2.3.5 (page 18), we believe that it is unlikely that higher harmonic information is the major determinant of perceived segregation. The trade-off between area and contrast also suggests that the low frequencies matching the period of the pattern are important in texture segregation.

The complex channel model and the effects of light adaptation appear able to account qualitatively for all our discrepancies. Specifically, let's examine in some detail how the complex channel model explains the finding that the greater the size difference between squares, the greater the minimal segregation rating. Consider a complex channel in which the first filtering is sensitive to a very high spatial frequency while the second filtering (after the nonlinearity) is sensitive to a spatial frequency near the fundamental of the pattern. Such a complex channel can respond to what might be called "low-spatial-frequency patterns of high-spatial-frequency elements". For our example, we will consider the channel where both stages are sensitive to

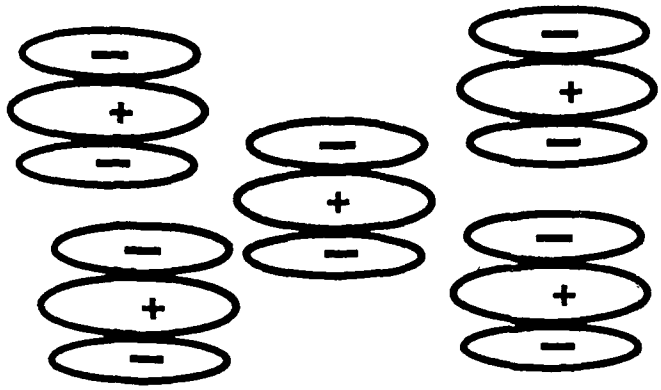

First Stage

A linear filter,
e.g. horizontal and of
high spatial frequency

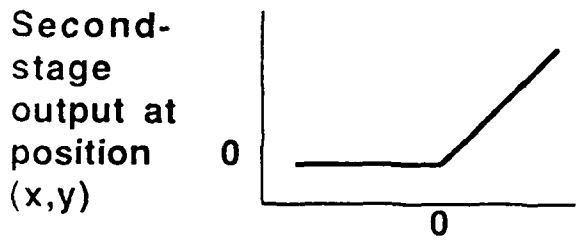

Second Stage

A point-by-point
nonlinearity,
dramatic near zero,
e.g. a rectification

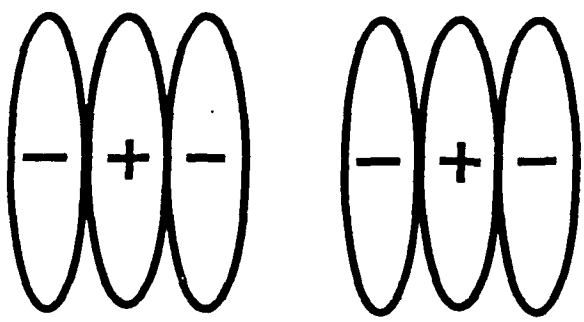

Third stage

A linear filter,
e.g. vertical and of
low spatial frequency

A Complex Channel

FIGURE 24

vertical orientations. The first high-frequency filtering extracts the edges of the squares as illustrated by the narrow dark and light bands in the right panels of Figures 3 and 4. The nonlinearity then changes below-zero first-stage outputs (dark bands in Figures 3 and 4) either to zero outputs (if half-wave rectification or something similar is assumed) or to above-zero outputs (if full-wave rectification or something similar is assumed). Since the large squares have longer edges than do the small squares, the second-stage filter (which is sensitive to the fundamental of the pattern and to vertical orientations) will have greater outputs where there are columns of large squares than where there are columns of small squares, when the contrasts of the squares is equal. Remember that the area of squares increases quadratically with edge length. Therefore, at the contrast ratios where area x contrast of the large and small squares are equated, the edge-length x contrast of the small square will actually be greater than that of the large square. The amount by which it is greater will be larger for 16 and 8 pixel squares, for example, than for the 16 and 12 pixel squares. In general, when both edge lengths and areas count, as in the complex channels model, the edges should attenuate the dip in the u-shaped function more for larger size discrepancies between squares (as long as lower sensitivity to smaller size does not cancel out the greater size difference).

A consequence of our hypothesis is that if lines (rectangles) are the texture elements (a rectangle's area increases linearly with edge-length), the minimum texture segregation should be the same for different area-ratios of the rectangles. When the area x contrast of the large and small rectangles are equated (and the first-stage filterings sensitive to the fundamental show little modulated activity), the edge-length x contrast is also equated so the complex channel also shows little modulated activity. Figure 10 compares the texture segregation of patterns composed of 4 area-ratios of squares (top panel) and lines (bottom panel). For textures composed of squares, the greater the size difference between the squares the shallower the trough, i.e., the minimum segregation was greater. For textures composed of lines, the size difference of the lines did not yield different minimum segregation ratings.

The cross-over of the functions for different fundamental frequencies in Figure 12 (right panel) may also be explained by the complex channels model. Consider the 1 c/deg and 4 c/deg fundamental frequencies. Because the higher harmonics of the 4 c/deg patterns fall in a range of low contrast sensitivity, the perceived segregation of these patterns is primarily determined by initial filtering at the fundamental frequency. Thus, when the area x contrast of the large and small squares is equated, the rated segregation in Figure 12 (right panel) is close to zero. For the 1 c/deg patterns, however, the higher harmonics are in a more sensitive range of the contrast sensitivity function and can

contribute to perceived segregation. According to the complex-channels model, the influence of the squares' edges (picked up by the initial filtering at the higher-harmonic frequencies followed by rectification and refiltering at the fundamental frequency) will attenuate the dip in the u-shaped function. As one moves away from the point of equal areal contrasts, the differences in the outputs of the initial filtering increase more rapidly for the patterns having a fundamental of 4 c/deg than of 1 c/deg because 4 c/deg is closer to the optimum of the contrast sensitivity function. Thus the curves should cross.

It is interesting to note that a condition where the area-ratio of large and small squares was 4:1 while the sizes of the squares varied appears both in the density experiment (Figure 11 bottom panel) and the scaling experiment (Figure 12 right panel). In the density experiment, however, the period of the pattern was kept constant while in the scaling experiment, the period increased proportionately to the sizes of the squares. In both cases, the minimum ratings increased as the sizes of the squares (and thus the difference between the sizes) increased. However, the cross-overs occurred only when the fundamental frequency changed. This suggests that it is the changing contribution of edges due to their weighting by contrast sensitivity, rather than the smaller size differences between the squares that produces the cross-overs in Figure 15 (right panel).

2.7 Comparison of perceived segregation and perceived lightness

A striking finding reported by Beck, Sutter, & Ivry (1987) suggested that squares of equal size differing clearly in lightness failed to yield good perceived segregation. The observations of the experimenters further suggested that equal lightness differences yielded very different degrees of segregation depending on the background luminance. When the background luminance is above that of the objects, lightness is agreed to be a logarithmic function of reflectance or relative luminance to a first approximation, i.e., the ratio of the luminance of the square to the luminance of the background or to the average luminance (Judd & Wyszecki, 1963; Helson, 1964). Figure 25 (from Beck, Sutter, and Ivry, 1987) gives mean perceived segregation ratings as a function of the ratio of the luminances of the two squares (top panel) and as a function of the ratio of the contrasts of the two squares (bottom panel). [For this figure, contrast was actually computed as the difference between the square luminance and the mean luminance of the whole pattern divided by the mean luminance--that is, an extension of the quantity called Rayleigh contrast by Shapley and Enroth-Cugel (1985) for periodic patterns.] Different curves represent different ratios of the background to the higher of the two square luminances. The different curves coincide when plotted against contrast ratio (bottom panel) but not when plotted against luminance ratio (top panel). Since it is luminance ratio that is thought to determine lightness, this suggests that the

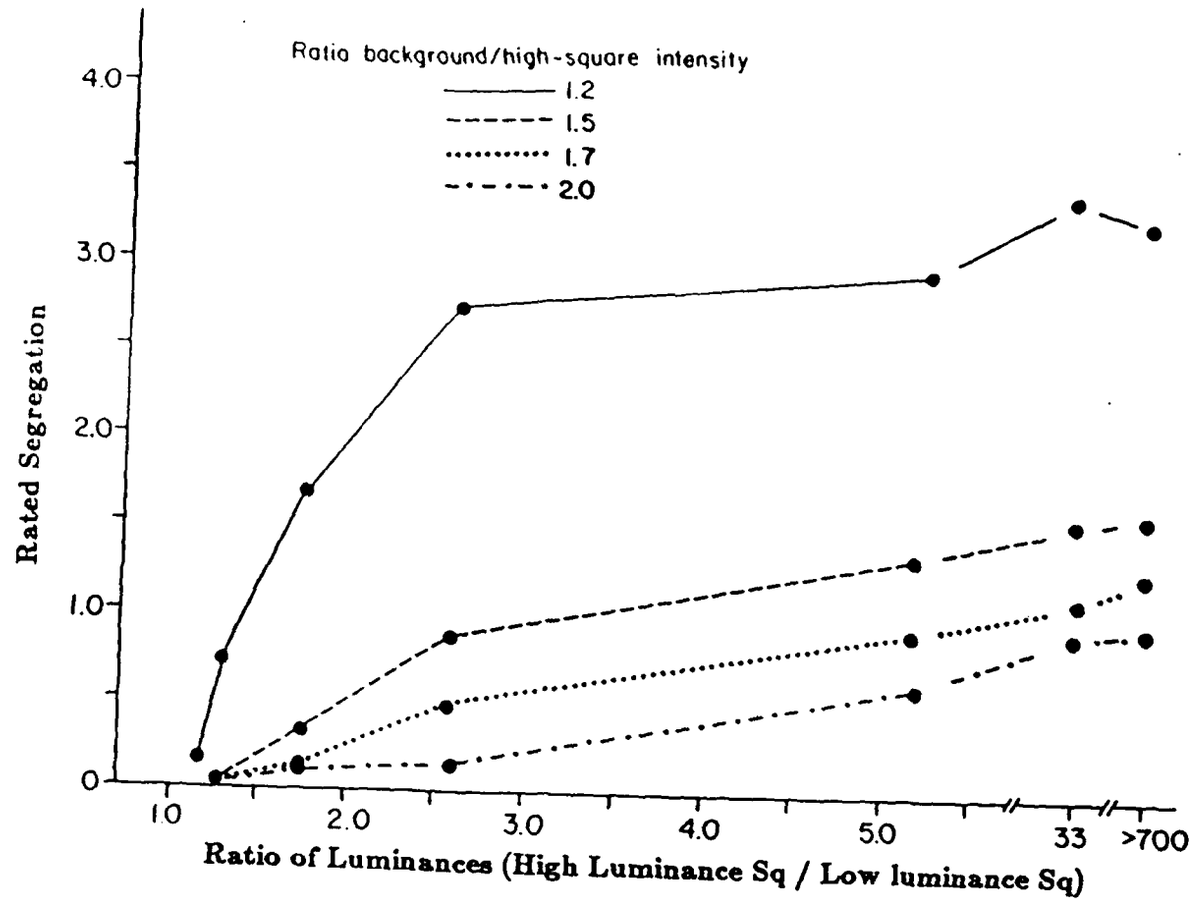
Ratio background/high-square intensity
1.2
1.5
1.7
2.0
Rated Segregation
4.0
3.0
2.0
1.0
0
1.0
2.0
3.0
4.0
5.0
33
>700
Ratio of Luminances (High Luminance Sq / Low luminance Sq)

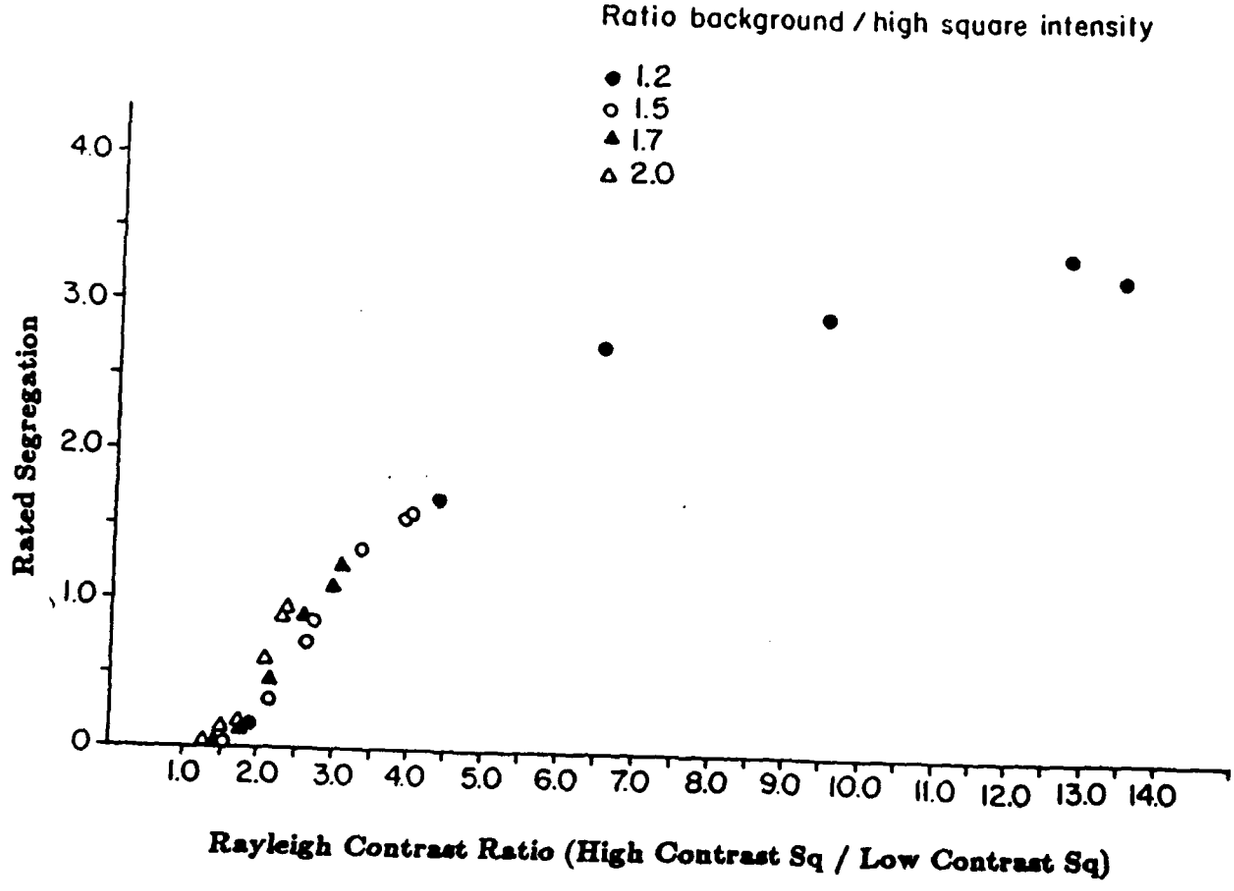
Ratio background / high square intensity
1.2
1.5
1.7
2.0
Rated Segregation
4.0
3.0
2.0
1.0
0
1.0
2.0
3.0
4.0
5.0
6.0
7.0
8.0
9.0
10.0
11.0
12.0
13.0
14.0
Rayleigh Contrast Ratio (High Contrast Sq / Low Contrast Sq)

FIGURE 25

strength of perceived texture segregation is not determined by the magnitude of the lightness difference between squares.

Lightness Matches-- Two experiments were conducted in which subjects both rated the perceived texture segregation of a pattern and also matched the lightnesses of each of the two kinds of squares composing a pattern to chips of varying Munsell lightness values (Beck, Sutter & Graham, 1988). In the first experiment, the background was the same for all the patterns (30 ft.-L.), and the squares were always darker than the background. Figure 26 shows the segregation ratings plotted against the difference between the lightness-match values for the two squares in the pattern. Clearly, equal lightness difference lead to different segregation judgement depending on the ratio of the background luminance to the higher square luminance.

Figure 27 shows the rated segregations (top row) and the differences between the lightness matches (bottom row) plotted as a function of the ratio of the luminances of the two squares (left column) and of the ratio of the Weber contrasts of the two squares (right column). Different curves in the upper left and lower right show results for different rations of background luminance to the higher square luminance. In the upper right and lower left panels the results all fell on the same function (within experimental error) and so are not distinguished. In short, perceived texture segregation appears to be a single-valued function of the ratio of the contrasts of the two squares while the difference between the lightness matches appears to be a single-valued function of the ratio of the luminances of the two squares.

In a second experiment, three backgrounds were used: a black background (.99 ft.-L.), a gray background (16.1 ft.-L.), and a white background (40 ft.-L.). The squares were always above the black background, above and below the gray background (opposite-sign-of-contrast, and below the white background. The results were similar to the first experiment. The functions describing the lightnesses of the squares differed from the functions describing the texture segregation of the patterns. Perceived texture segregation tended to be a monotonic function of the contrast ratio of the squares. With the gray background (opposite-sign-of-contrast squares whose contrast ratio was always 1), perceived segregation decreased when the luminances of the squares were close to the background. The perceived lightness of the squares was a monotonic function of the ratio of the luminances of the squares.

Is perceived lightness computed independently of and/or at a later stage from the stage controlling perceived texture? In some sense, the answer seems likely to be yes. For lightness is clearly seen as a property clearly-perceived squares and each square is seen as of uniform lightness. Yet in our models of

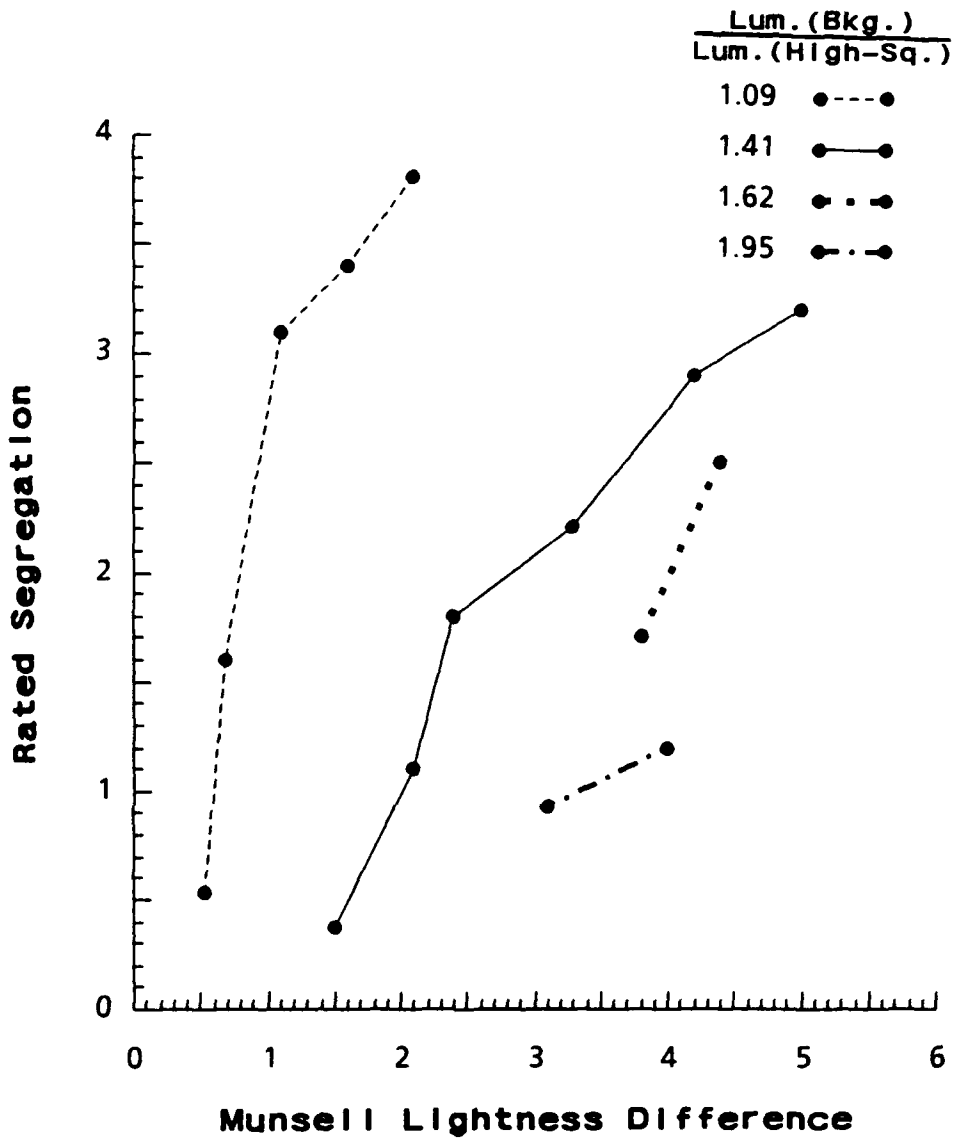
Lum.(Bkg.)
Lum.(High-Sq.)
1.09
1.41
1.62
1.95
Rated Segregation
0
1
2
3
4
0
1
2
3
4
5
6
Munsell Lightness Difference

FIGURE 26

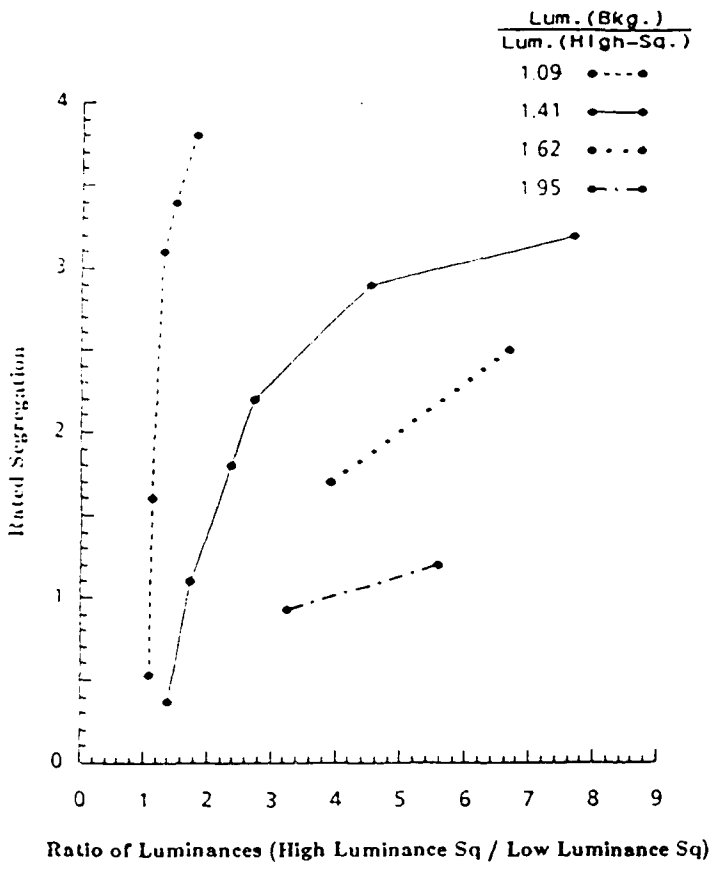
Lum.(Bkg.)
Lum.(High-Sq.)
1.09
1.41
1.62
1.95
Rated Segregation
Ratio of Luminances (High Luminance Sq / Low Luminance Sq)

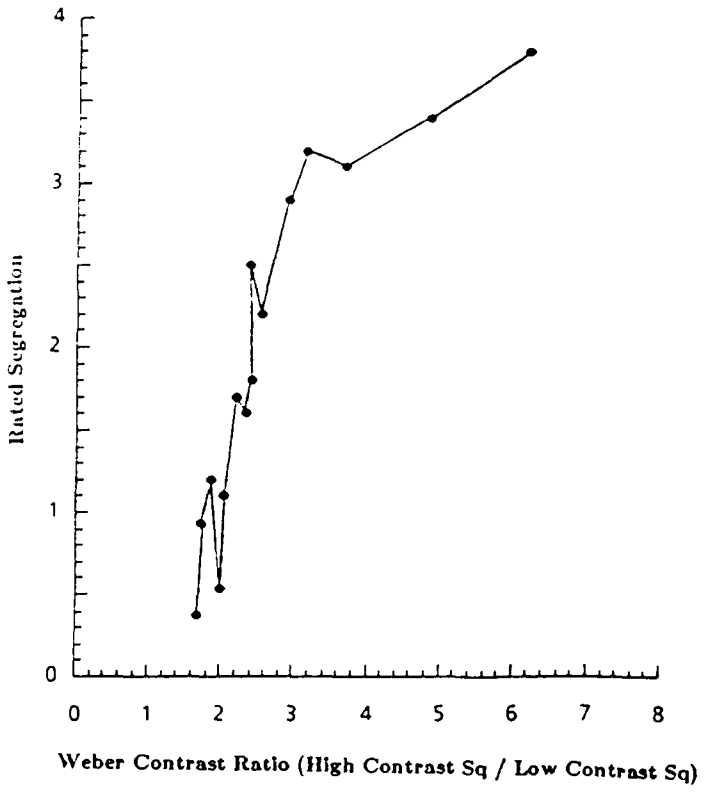
Rated Segregation
Weber Contrast Ratio (High Contrast Sq / Low Contrast Sq)

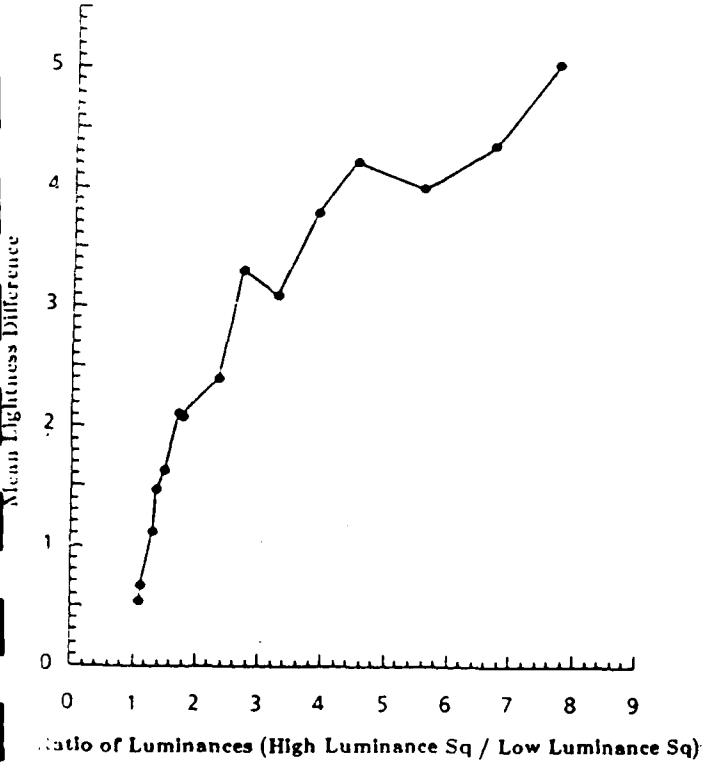
Mean Lightness Difference
Ratio of Luminances (High Luminance Sq / Low Luminance Sq)

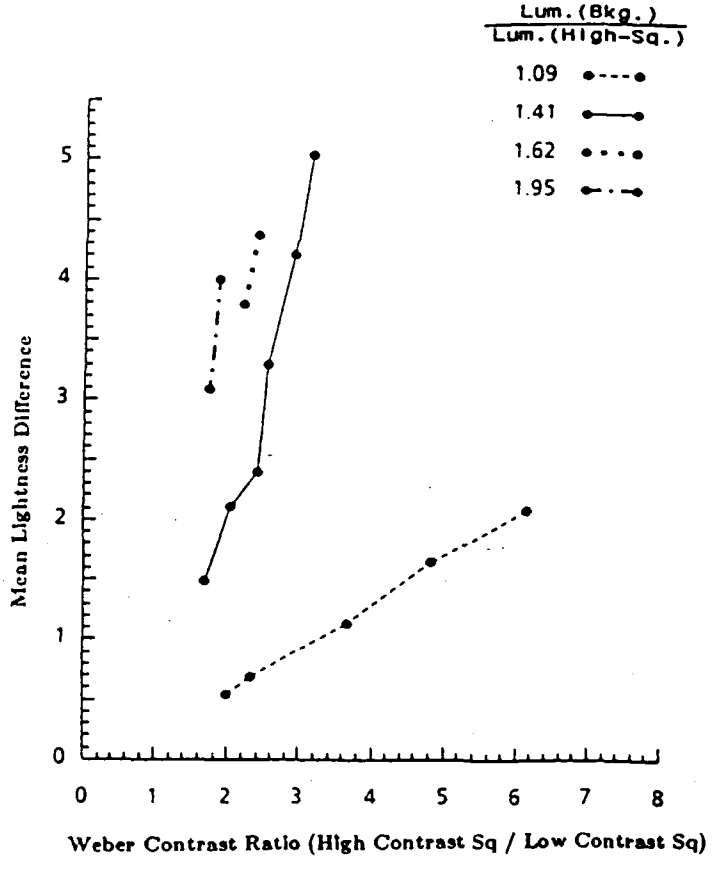
Lum.(Bkg.)
Lum.(High-Sq.)
1.09
1.41
1.62
1.95
Mean Lightness Difference
Weber Contrast Ratio (High Contrast Sq / Low Contrast Sq)

FIGURE 27

perceived texture segregation, low-level channels are primarily responsible for perceived texture segregation and these channels do not have the right properties to signal the presence of homogeneously-illuminate "squares"in the pattern. On the other hand the fact that both perceived texture segregation and perceived lightness are functions of related stimulus properties (at least through some range of conditions) suggests a closer relationship of some sort. The similarity of the contrast computations to the weighting functions of the receptive fields suggests that they are computed first and that the luminance ratio determining perceived lightness is computed from them. Neurally, the contrast computations can be interpreted as comparing the excitation produced by a patch with a base firing rate. For a square on a larger background,one can assume that the base rate is set primarily by the background. The contrast calculation computes how much the firing rate due to the luminance of a square deviates from the base rate set by the luminance of the background. It is the relevant computation for determining the perceived strength of texture segregation. Perceived lightness is determined to a first approximation by the ratio of the luminance of a square to the luminance of the background. It is based on what proportion of the base rate set by the luminance of the background is the firing rate of an object. This can be computed by adding 1 to the contrast computation. (The value of 1 represents neurally the firing rate of the background expressed in terms of the background firing rate as the unit of measurement.) Thus, the luminance ratio determining perceived lightness can be computed neurally from the firing rate signaling the luminance difference between a square and the background by adding the firing rate of the background and comparing it to the background firing rate. This calculation assumes that there are cells in the visual system that are not zero balanced, i.e., the excitatory and inhibitory responses do not cancel each other. In a uniform field, a *Ganzfeld*, such cells respond with a maintained discharge.

We recognize that our conjecture is highly speculative. However, we find it suggestive and hope that by pursing it we will better come to understand how perceived lightness is related to the outputs of spatial-frequency channels.

2.8 Global popout

We have been examining the global popout of lines and curves. By global popout, we mean the rapid, preattentive perception of a global configuration such as the dotted line in Figure 28. Treisman & Gormican (1988) have done pioneering work in popout but she has concentrated on looking for a single target amidst many distractors. She has shown that a single feature can be detected preattentively and in parallel while a combination of features requires serial search and focussed attention.

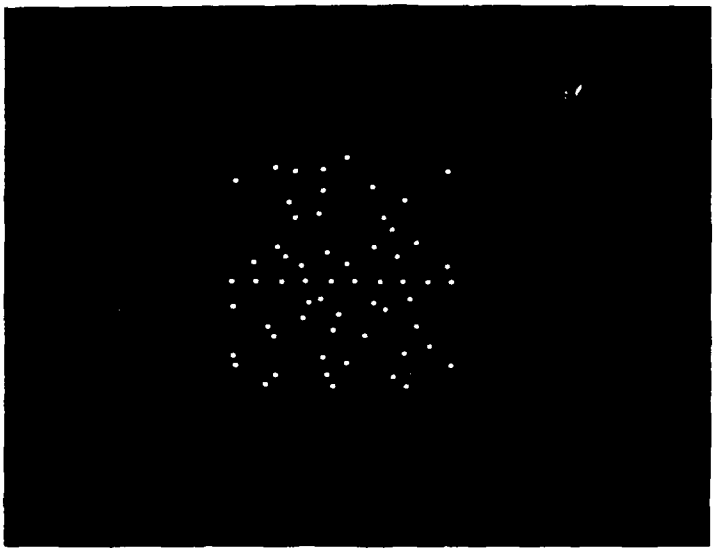

FIGURE 28

2.8.1 *Comparison of texture segregation and the popout of lines*

Beck, Rosenfeld, Ivry, & Navab (1988) have studied the factors affecting the rapid detection of a line composed of disconnected shapes embedded in a background of the same shapes. Figure 28, shows a dotted line embedded in a background of dots. The line is seen immediately and effortlessly. It is possible that the spatial frequency mechanism involved in the discrimination of texture regions also detect the line. For example, differences in the outputs of filters in the line region and in neighboring regions above and below the line may control the rapidness of line detection.

This kind of computation does not appear able to account for the detection of the lines. We have examined whether the filtered output in a 10 pixel strip about the line differs from the filtered output in the background (40 pixel strips above and below the line region) for the data reported by Smits, Vos and Oeffelen (1985). Figure 29 shows the strip about the line and the top and bottom background strips superimposed over a filtering of the pattern. There was no significant correlation between differences in either the means, standard deviations, or maximum outputs of the filters in the line and in the background strips, and the rapidity with which a line was detected. The maximum Spearman rank correlation was .21 when we summed the differences across all filters and .30 for individual filters.

2.8.2 *Popout experiments*

Why do spatial frequency channels predict texture segregation but fail to predict line detection? Before turning to this question I want to report three studies that we have conducted.

In one experiment, we investigated how the alignment and misalignment of edges affected line detection Four sizes of squares were investigated. The stimuli were scalings of one another. Square size, the spacing between the squares in the line, and the lateral displacement of the misaligned squares were increased proportionally. Figure 30 shows examples of stimuli with aligned and misaligned squares. Stimuli were flashed for 150 msec and subjects were required to judge whether the line was vertical or horizontal. We recorded both reaction time and errors. The two measures agreed closely and we shall report only reaction times.

The X axis in Figure 31 plots the square sizes in pixels and the Y axis the mean reaction times. There is a striking difference between the collinear and misaligned squares. For the misaligned squares, reaction times remained constant with increasing square size and scaling of the stimuli. If the visual system is detecting the density of squares in a particular direction, reaction time would be expected to remain constant since density remains constant

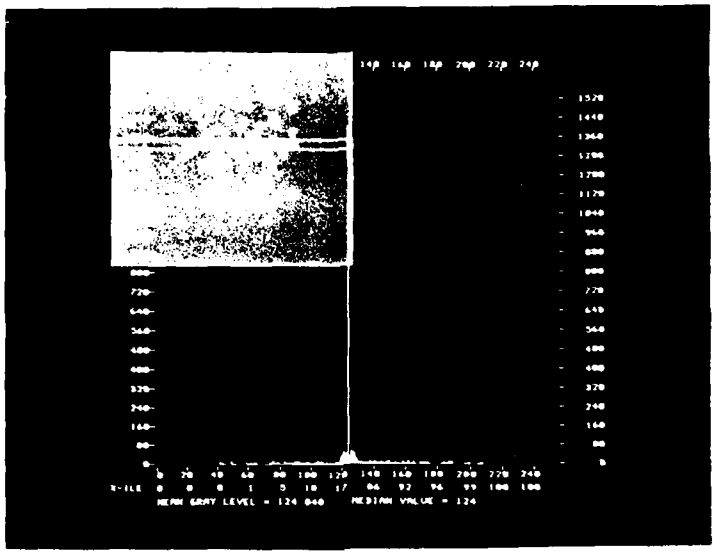

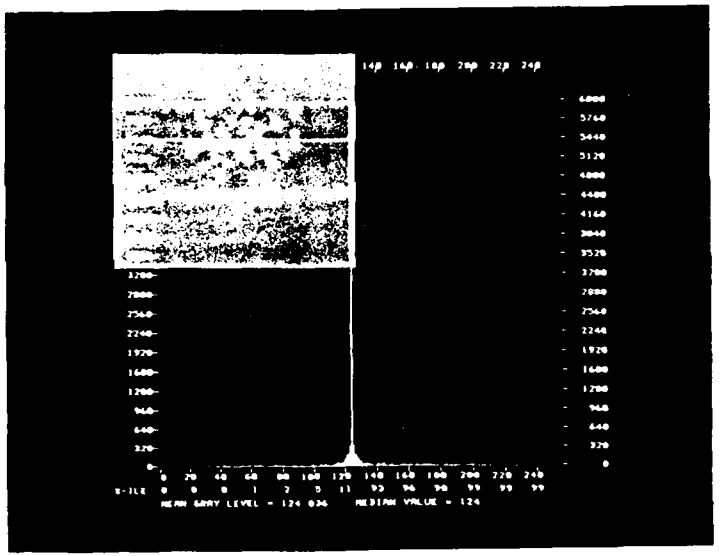

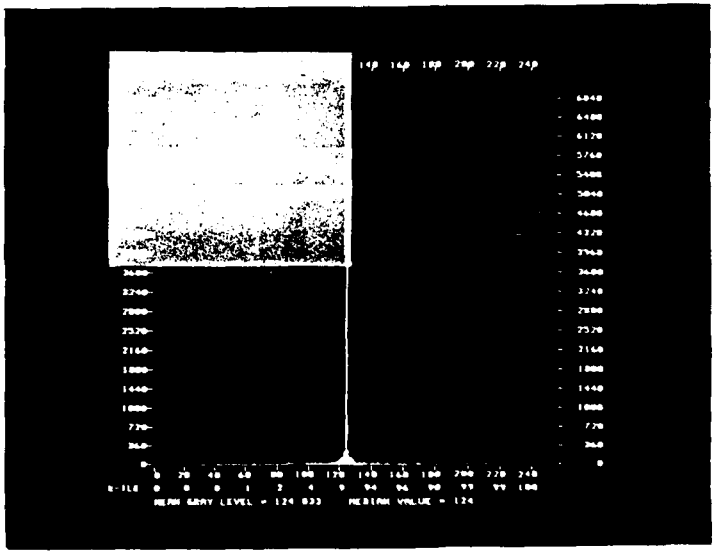

FIGURE 29

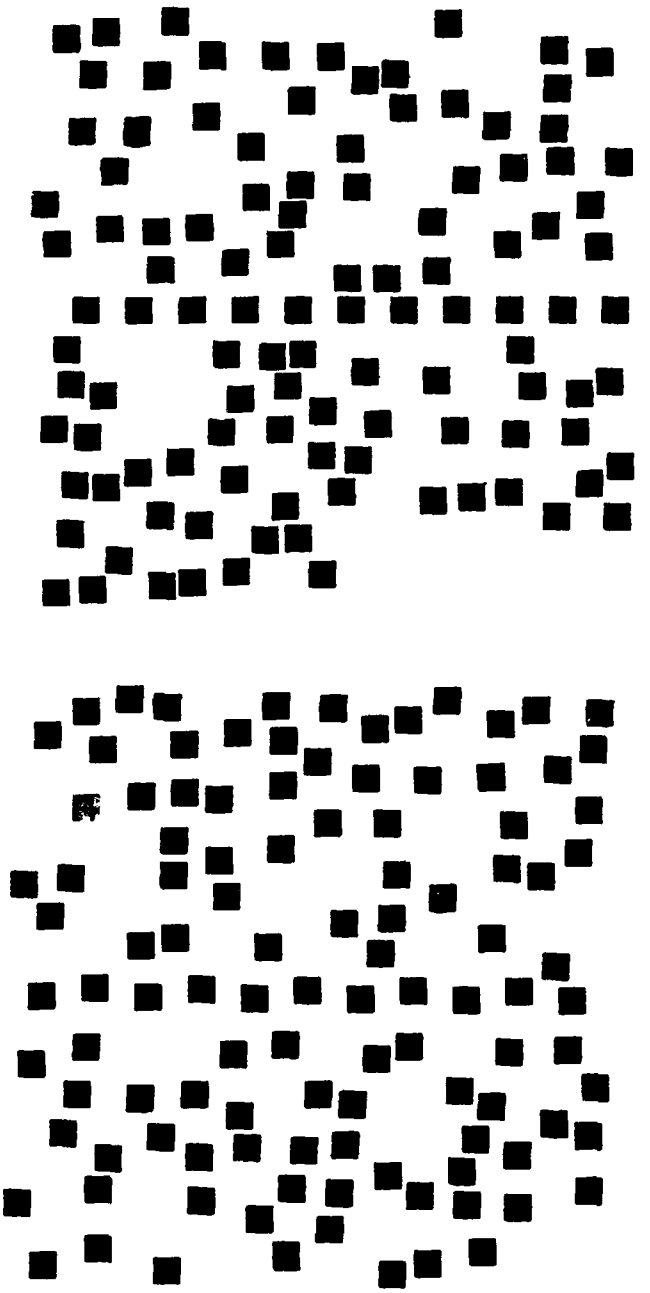

FIGURE 30

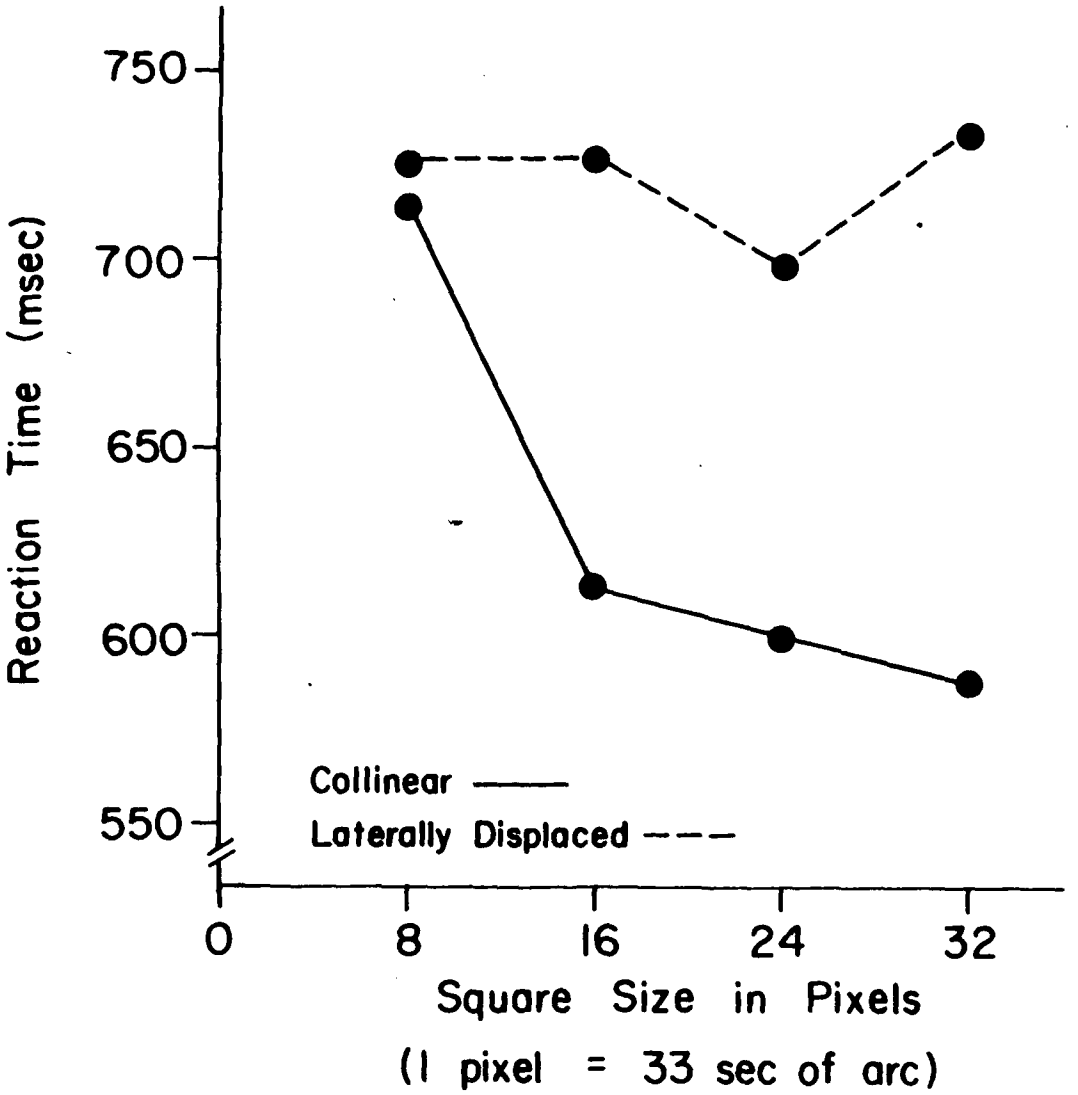
750
700
650
600
550
Reaction Time (msec)
Collinear
Laterally Displaced
0
8
16
24
32
Square Size in Pixels
(1 pixel = 33 sec of arc)

FIGURE 31

if size and spacing is increased proportionally. For the aligned squares, the reaction times decreased with increasing square size and scaling of the stimuli. Increased edge alignment facilitated detecting the line.

Two further experiments demonstrate the importance of edge alignment. The stimuli were composed of 8 and 16 pixels on a side and were scalings of one another. Figure 32 shows the reaction times. As in the previous experiment, the larger squares were detected more rapidly and than the smaller squares. This occurred at all luminance levels even when the areal contrast (area x contrast) of the smaller square was much greater than the areal contrast of the larger square. The length of the squares was more important than the areal contrast of the squares for detecting the line. A third experiment compared solid squares with outline squares. The squares were 10 and 20 pixels on a side and were scalings on one another. Figure 33 shows that the outline squares were detected as rapidly as the solid squares. Filtering the displays showed that the difference between the filtered output of the line region and the outputs of the background region was for the outline squares 60 percent of that of the solid squares.

2.8.3 *Difference between texture segregation and line detection*

What is the difference between the texture patterns and the line displays? For preattentive pattern vision such as immediate effortless texture segregation and line detection, we believe perception is a direct function of lower-level analyzers. We propose that preattentive pattern vision is a function of the information from 3 types of analyzers: bar detectors, spot detectors, and edge detectors. The large bar detectors provide information about the overall changes in luminance. The spot detectors and the small bar detectors give information for the size and orientation of the elements of a pattern. The edge detectors give information for the arrangement of the edges in a pattern.

The spot and edge detectors provide no information for segregating the texture regions in Figure 1. The spot detectors tell us that there are two populations--large and small squares. There is ,however, no spatial differentiation as a result of their outputs. The centroids of the populations of large and small squares are the same. There is also no information from the edge detectors. Though there is more alignment of the squares in the top region than in the center region, there is a strong alignment signal coming from both regions. The only spatial differentiation is from the large bar detectors which signal differences in the overall pattern of luminance changes in the top and center regions. In the top region the changes of overall luminance occur in the direction of the X axis and in the center region in a direction 45 degrees to the X axis. The large bar detectors are not sensitive to edge alignment and we have found that, unlike the line displays, perceived segregation in our texture displays is not affected by

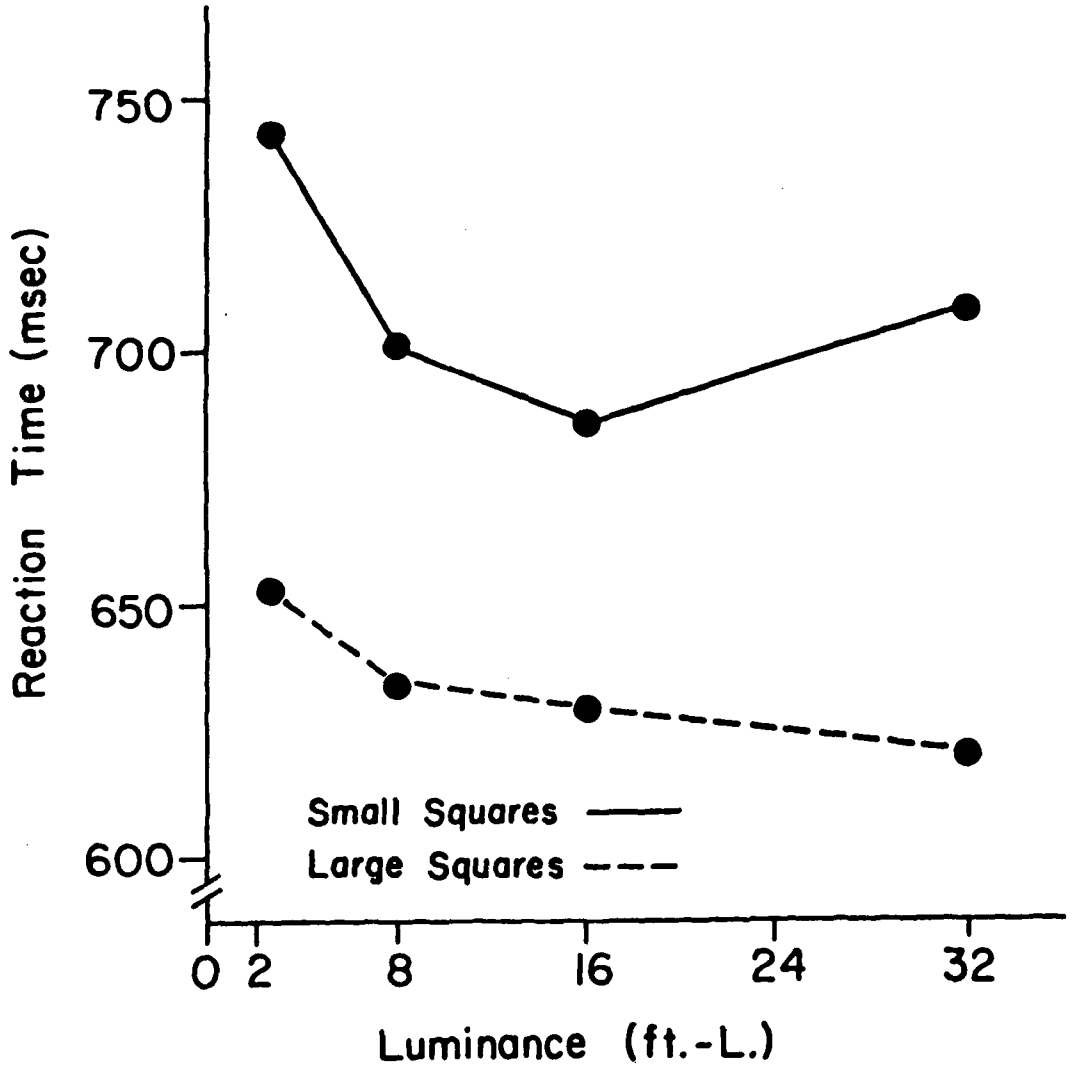
750
700
650
600
Reaction Time (msec)
Small Squares
Large Squares
0
2
8
16
24
32
Luminance (ft.-L.)

FIGURE 32

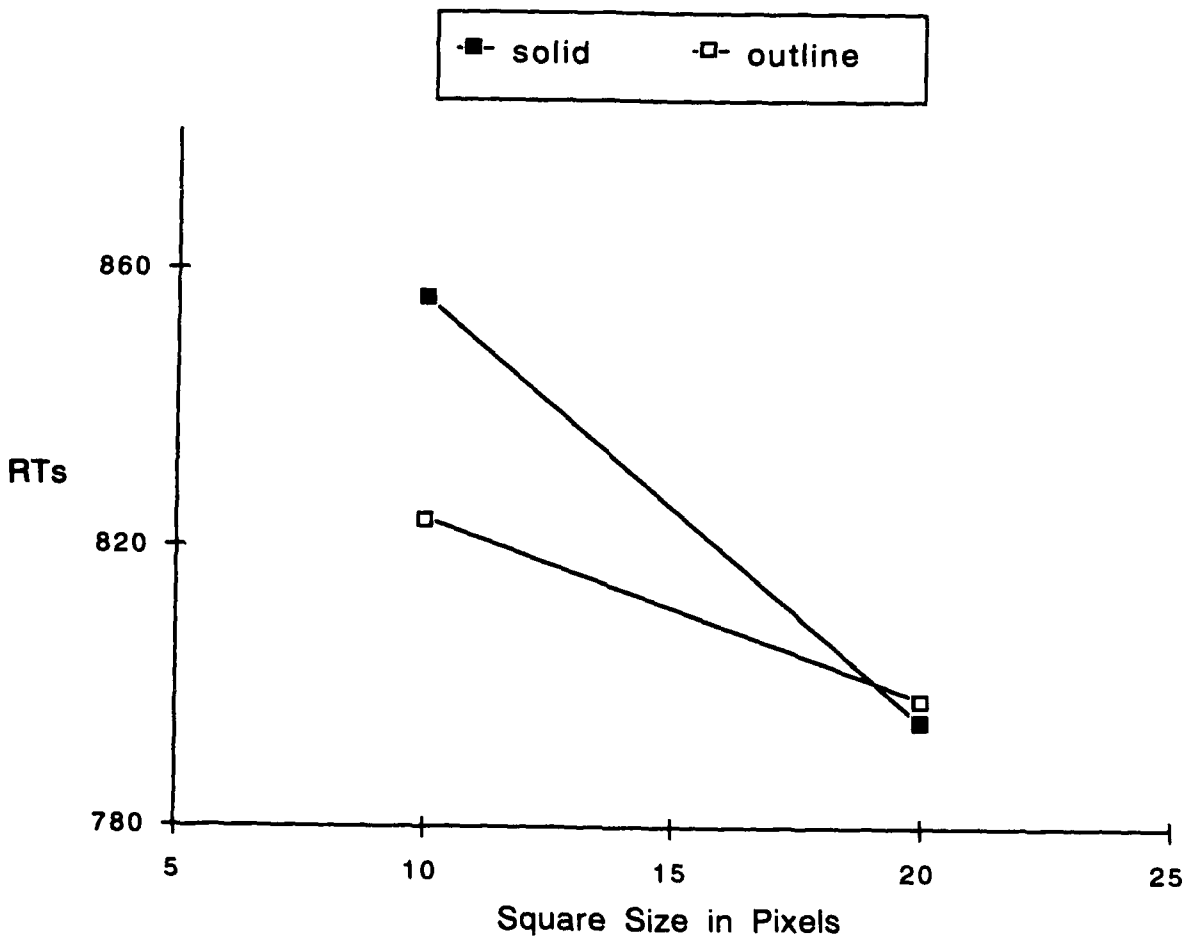
solid
outline
860
820
780
RTs
5
10
15
20
25
Square Size in Pixels

FIGURE 33

either the absence of aligned edges or the misalignment of edges.

The long line in the line displays consists of elements having the same size, contrast, and orientation as the background elements. Line detection can not be explained in terms of differences in the response of large spot or bar detectors. The line does not occupy a separate region of the display. As illustrated in Figure 34, the bar detectors become wider as they become longer and a detector long enough to fall on 3 dots of the line (upper right image) will also fall on many background dots. The small bar detectors spot detectors, and edge detectors give similar responses to elements in the line and in the background. What is suggested is that line detection is not the result of differences in the outputs of large spot or bar detectors (detectors falling on 3 or more elements of the line) but results from local operations on the outputs of small detectors. The relevant properties of the outputs of spot detectors are color, contrast, size and possibly sign of contrast. The outputs of bar detectors have in addition the properties of orientation and elongatedness. The outputs of edge mechanisms are oriented edge segments. The local operations that detect a line may be of various kinds. There may be a linking of similar outputs. Aligned horizontal squares may link to form a long line. The length of the long line is an emergent feature that makes it stand out from the surrounding region. Local operations may also direct a fast search process. Search is focused by straight edges. Short edges, however, do not focus search as well as long edges. For misaligned elements a sharp focus does not help. Rapid line detection occurs because search is focussed by local operators that compute a greater element density in a given direction.

We are investigating these possibilities.

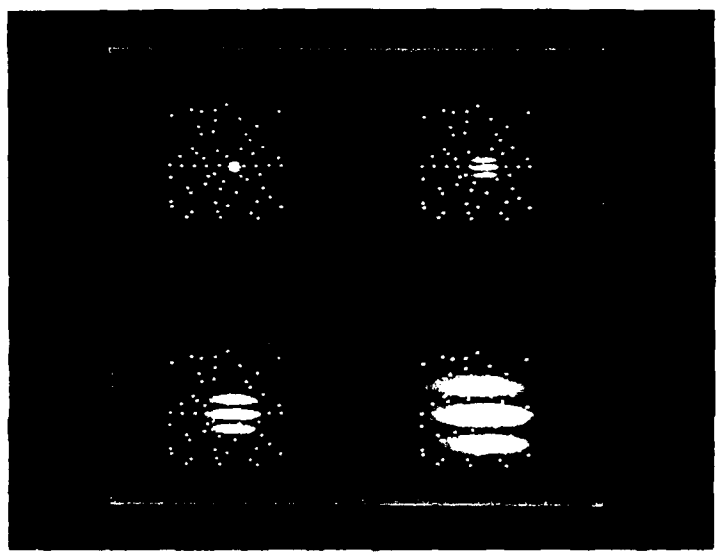

FIGURE 34

3. PUBLICATIONS (reporting AFOSR research, 1985-1989)

Beck, J. 1985. Perception of transparency in man and machine. *Computer Vision, Graphics, and Image Processing*, 31, 127-138.

Beck, J. & Halloran, T. 1985. Effects of spatial separation and retinal eccentricity on two-dot vernier acuity. *Vision Research*, 25, 1106-1111.

Beck, J. 1986. The perception of transparency: a reply to Brill. *Computer Vision, Graphics, and Image Processing*, 35, 272-273.

Moravec, L. & Beck, J. 1986. Amodal Completion: simplicity is not the explanation. *Bulletin of the Psychonomic Society*, 24, 269-272.

Beck, J., Sutter, A., & Ivry, R. 1987. Spatial frequency channels and perceptual grouping in texture segregation. *Computer Vision, Graphics, and Image Processing*, 37, 299-325.

Beck, J. 1987. Perception: the search for projection invariants. A review of Perception with an eye for for motion by J. E. Cutting. *Contemporary Psychology*, 33, 38-39.

Beck, J. & Ivry, R. 1987 On the role of figural organization in perceptual transparency. *Perception and Psychophysics*, 44, 585-594.

Beck, J., Sutter, A. & Graham, N. 1988. Comparison of perceived segregation and perceived lightness in texture segregation, In preparation.

Beck, J., Rosenfeld, A, Ivry, R. & Navab, Nassir. 1988. *Global popout of lines*, In preparation.

Graham, N. 1988. Low-level visual processes and texture segregation, *Physica Scripta*, In press.

Graham, N., Sutter, A., & Beck, J. 1988. Contrast and spatial variables in texture segregation: testing a complex spatial frequency model, In preparation.

Sutter, A. 1987 The interaction of size and contrast in perceived segregation: a spatial frequency analysis. Unpublished doctoral dissertation, University of Oregon.

Sutter, A., Beck, J., & Graham, N. 1988. Contrast and spatial variables in texture segregation: testing a simple spatial frequency channels model, submitted for publication.

4. PROFESSIONAL PERSONNEL

Principal Investigator Jacob Beck

Senior Research Investigator: Norma Graham

Graduate students: Richard Ivry, Nassir Navab, Anne Sutter, James Tanaka

Undergraduate students: Kirk Helms, Dorte Poulsen

5. MEETINGS (reporting AFOSR research, 1985-1988)

Third Human and Machine Vision Workshop, Boston,Massachusetts, 1985, "Spatial filtering, features,and grouping in texture segregation."

Eleventh Annual Interdisciplinary Conference, Whistler, British Columbia, 1986, "Spatial filtering, features, and grouping in texture segregation."

Center for Visual Science Symposium on Computational Models in Human Vision, Rochester, New York, 1986, "Unresolved issues in texture segregation."

First International Conference on Computer Vision, London, England, 1987, "Visual image processing in texture segregation."

Optical Society of America Meeting on Color Appearance, Annapolis, Maryland, 1987, "On the role of figural organization in perceptual transparency."

Meetings of the Psychonomic Society, New Orleans, Lousiana, November, 1987, "On the role of figural organization in perceptual transparency".

First Annual Workshop on Goals for Machine Vision, U.C.L.A., James E. West Center, Los Angeles, California, 1987, "Human and machine image processing in texture segregation."

AFOSR Meeting on Visual Information Processing, Annapolis, Maryland, 1987, "Visual image processing in texture segregation."

Colloquia: University of Maryland (Department of Psychology, 1986) Boston University (Center for Adaptive Studies,1986),Hebrew University (Department of Computer Science, 1987,1988), University of Haifa (Department of Psychology, 1987), University of Pennsylvania (Department of Computer Science, 1987), Rutgers University (Department of Psychology, 1987), National Institutes of Health (Department of Applied Mathematics,

1988), University of Massachusetts (Department of Computer Science, 1988)

6. REFERENCES

Beck, J. 1972 Similarity grouping and peripheral discriminability under uncertainty. *American Journal of Psychology*, 85, 1-19.

Beck, J. 1982. Textural segmentation. *In Organization and Representation in Perception*. In J. Beck Ed. Hillsdale, N.J.: Erlbaum, 285-317.

Beck, J. 1983. Textural segmentation, second-order statistics, and textural elements. *Biological Cybernetics*, 48, 125-130.

Beck, J., Prazdny, K., & Rosenfeld, A. 1983. A theory of textural segmentation. In *Human and Machine Vision* J. Beck, B. Hope, & A.Rosenfeld, Eds. New York: Academic, 1\-38.

Beck, J., Sutter, A. & Ivry, R. 1987. Spatial frequency channels and perceptual grouping in texture segregation. *Computer Vision, Graphics, and Image Processing*, 37, 299-325.

Beck, J., Sutter, A. & Graham, N. 1988. Comparison of perceived segregation and perceived lightness in texture segregation. In preparation.

Bergen, J. R. & Adelson, E. H. 1988. Early vision and texture perception. *Nature*, 333, 363-364.

Caelli, T. 1982. On discriminating visual textures and images. *Perception & Psychophysics*, 31, 149-159.

Caelli, T. 1985. Three processing characteristics of visual texture segregation. *Spatial Vision*, 1, 19-30.

Chubb, C. & Sperling,G. 1988. Processing stages in non-Fourier motion perception. *Supplement to Investigative Ophthalmology and Visual Science*, 29, 266.

Daugman, J.G. 1985. Uncertainty relation for resolution in space, spatial, frequency, and orientation, optimized by two dimensional visual cortical filters. *Journal of the Optical Society of America A*, 2, 1160-1169.

Daugman, J. C. 1987. Image analysis and compact coding by oriented 2D Gabor Primitives, *S.P.I.E. Proceedings*, 758, 19-30.

Gagalowicz, 1981 A new method for texture field synthesis: applications to the study of human vision. *IEEE Transactions on Pattern Analysis and Machine Intelligence*, 3, 520-533.

Ginsburg, A.P. 1984 Visual form perception based on biological filtering. In *Sensory Experience, Adaptation, and Perception.* L. Spillman & B.R. Wooten, Eds Hillsdale N. J.: Erlbaum, 53-72.

Graham, N. 1980. Spatial frequency channels in human vision: detecting edges without edge-detectors. *In Visual coding and adaptability*. C.S. Harris, Ed. Hillsdale N.J.: Erlbaum. 215-262.

Graham, N. 1981. Psychophysics of spatial frequency channels. In *Perceptual Organization*. M. Kubovy & J. R. Pomerantz Eds. Hillsdale N. J.: Erlbaum, 53-72.

Graham, N. 1985 Detection and identification of near-threshold visual patterns. *Journal of the Optical Society of America A*, 2, 1468-1482.

Graham, N. 1988. Low-level visual processes and texture segregation, *Pysica Scripta*, In press.

Graham, N., Sutter, A. & Beck, 1988. J. Contrast and spatial variables in texture segregation: suggesting a complex spatial frequency model. In preparation.

Grossberg, S. 1987. Cortical dynamics of three-dimensional form, color, and brightness perception: monocular theory. *Perception & Psychophysics*, 41, 87-116.

Grossberg, S. & Mingolla, E. 1985. Neural dynamics of perceptual grouping: textures, boundaries, and emergent features.*Perception & Psychophysics*, 38, 141-171.

Helson, H. 1964. *Adaptation Level Theory*. New York: Harper and Row.

Hochstein, S. & Spitzer, H. 1985. One, few, infinity: linear and nonlinear processing in the visual cortex. In *Models of the Visual Cortex*. D. Rose & V.G. Dobson Eds. New York: Wiley, 341-350.

Judd, D.B. & Wyszecki, G.W. 1963. *Color in Science, Business, and Industry*. New York: Wiley.

Julesz, B. 1975 Experiments in the visual perception of texture. *Scientific American*, 232, 34-43.

Julesz, B. 1981 Textons, the elements of texture perception and their interactions. *Nature*, 290, 91-97.

Klein, A. & Tyler, C.W. 1986. Phase discrimination of compound gratings: generalized autocorrelation analysis. *Journal of the Optical Society of America A*, 3, 868-879.

Marr, D. 1976. Early processing of viual information. *Philosophical Transactions of the Royal Society*, London B275, 483-524.

Shapley, R. & Enroth-Cugell, C. 1985 Visual adaptation and retinal gain controls. In *Progress in Retinal Research Volume 3* N.N. Osborne & G.J. Chader Eds., New York: Pergamon, 263-346.

Spitzer, H. & Hochstein, S. 1985a. Simple-and complex-cell response dependences on stimulation parameters. *Journal of Neurophysiology*, 53, 1244-1265.

Spitzer, H. & Hochstein, S. 1985b. A complex-cell reptive-field model. *Journal of Neurophysiology*, 53, 1266-1286.

Sutter, A. 1987. The interaction of size and contrast in perceived segregaton: a spatial frequency analysis. Ph.D. Thesis, University of Oregon, Eugene, Oregon.

Sutter, A., Beck, J., & Graham, N. 1988. Contrast and spatial variables in texture segregation: testing a simple spatial frequency channels model. In preparation.

Treisman, A. & Gormican, S. 1988. Feature analysis in early vision: evidence from search asymmetries *Psychological Review*, 95, 15-46.

Turner, M.R. 1986. Texture discrimination by Gabor functions. *Biological Cybernetics*, 55, 71-82.

Victor, J. D. & Brodie, S.E. 1978. Discriminable textures with identical Buffon-needle statistics. *Biological Cybernetics*, 31, 231-234.

Watson, A.B. 1983. Detection and recognition of simple spatial forms. In *Physiological and Biological Preprocessing ofImages*. O.J. Braddick & A.C. Sleigh, Eds. New York: Springer-Verlag, 110-114.

Wertheimer, M. 1923. Untersuchungen zur Lehre von Der Gestalt II. *Psychologische Forschung*, 4, 301-350.

PART II (Stevens)

CONTENTS

ABSTRACT

We have conducted research into the perception of texture, concentrating on the earliest levels in the extraction of geometric structure. The work has involved a computational and psychophysical study of the role of retinal and cortical spatial frequency filters in the extraction of contour information. The specific areas reported concern: i) the differential roles of radially-symmetric and elongated receptive fields on the Café wall illusion, a pattern that is useful for the induction of illusory brightness bands and orientation, ii) a strategy for parsing of band-pass filtered images to differentiate line-like versus edge-like luminance changes, iii) asserting orientation between discrete items, and iv) connecting contour fragments across luminance gaps. Across these areas one common theme is the importance of spatial gating nonlinearity.

1. INTRODUCTION

1.1 The Problem Areas

The overall goal of our research is to understand the visual representations and processes involved in texture perception. Towards that end we have recently investigated some early aspects of contour and form perception. We first sketch the path of investigation that has lead us to these areas. Earlier we examined problems of *bootstrapping*, i.e. of initiating the extraction of texture descriptions (Stevens & Brookes 1987). The bootstrapping study was a direct extension of (Stevens 1978) where parallelism, a primitive geometric property of texture, was examined in terms of dot patterns. We pursued the basic question of whether orientation (defined e.g. by a pair of adjacent dots) is extracted by "symbolic" virtual lines or more directly measured by elongated receptive fields that summate luminance energy. As recognized by the Gestalt investigators and later formulated computationally (Marr 1976, 1982), at some point perceptual grouping constitutes associations (such as pairings) between perceptual wholes. For example, virtual lines might represent pairwise groupings between similar place tokens. It would be significant to show that such grouping processes occur at an early stage of texture processing. Evidence was presented that supports the virtual line hypothesis (discussed in detail later). In part the argument hinged on a broad assumption about the linearity with which luminance signals are spatially summated, which on close examination led to our returning to question the symbolic grouping hypothesis for early texture processing. As we report in section 2.3, while some grouping phenomena (such as a preference for color and contrast similarity) still suggest symbolic pairings, receptive field mechanisms are strongly implicated as the underlying orientation detection mechanism. At about that time we also were pursuing the role of the concave cusp in determining local geometric evidence for form boundaries (Stevens & Brookes 1988; reported first in the previous final report). As part of the extension of that work, we sought to examine their occurrence in natural images, which entailed implementing an edge detection operator that differentiated edge- from line-like luminance changes. Consideration of extensions of Watt and Morgan's (1985) one-dimensional theory to two-dimensional images led to work reported in section 2.1. Experience with actual images led to developing a parsing operator that incorporated strong nonlinearities. This behavior was then recognized to have a possible counterpart in the nonlinearity exhibited by cortical cells, for which we suggest a functional purpose. Both themes, the distinction of luminance changes of different type and the use of spatial nonlinearity were also pursued in a study of the familiar Café wall illusion (section 2.2). The final topic we review is the characterization of form extraction as the compilation of local contour evidence. This work, which is in an early stage, is also found to implicate receptive fields (section 2.4).

1.2 Summary of Current Working Hypotheses

The work we report is performed within a larger view towards texture and form perception, which is outlined in the following discussion.

Form Perception as Construction: A visual form is a perceptually coherent whole that is distinguished as figure against its immediate background. A major aspect of the extraction of visual form involves localizing and organizing its outline or silhouette contours. It is well accepted that the extraction of visual form begins with the detection of local edge or contour information along the boundary, and concludes with the construction of a distinct perceptual entity. The *Gestalt* investigators made a series of fundamental observations that together establish the essentially constructive aspect of form perception: forming associations among the component parts of a visual form. The associations or groupings seemingly involve some type of conjoining primitives (sometimes referred to as a perceptual glue[1]) and rules for how perceptual parts can be conjoined, and at least some general rules for the application of these rules (instructions for assembly).

Preattentive versus Attentive Processing: The construction of a form is achieved substantially in parallel and preattentively. To determine the correct closure or connectivity (e.g., across substantial gaps or contrast reversals) is an intrinsically difficult computation and probably requires sequential processing, and hence focal attention. Natural vision requires assembling a form with little prior knowledge of what that form might correspond to physically, hence much of the initial aspects of the assembly process must be achieved in a bottom-up manner. One aspect of form perception that we find particularly challenging is how the process is initiated.

We suspect that many researchers have underestimated considerably the combinatorics of possible forms posed by a natural image. An image presents a very large number of different forms that might be constructed purely on the basis of an *a priori* reasonable scheme of rules for generating wholes from local collections of fragments. We believe that actually very little form perception is performed beyond a very modest initial stage of organization, and that the complexity of theoretically-possible forms that might be extracted from an image poses an intrinsically insurmountable complexity barrier, one that *tacitly defines the distinction between preattentive and attentive, or scrutinous, vision.* That is, the visual system uses attentive processing (e.g. intrinsically-sequential computations) for form detection problems that cannot be

---

[1] Some researchers, notably Treisman and Julesz, propose that this glue requires attentive processing. We suggest that the attentive aspects they address experimentally concern search and discrimination processsing that is more difficult and performed later than the early aspects of form perception we address here.

solved preattentively. Not all of form perception, however, requires focal attention: isolated, closed forms can be extracted immediately and preattentively.

The interplay between psychophysics and computational models: The specific problems we address concern the earliest precursors of visual form, and include the binding together, or conjoining, of contiguous (or nearly contiguous) contour fragments, selecting particular structures of contours as figure versus ground, and the subsequent perception of figural properties such as location and overall orientation. Each of these problems can be treated at various levels of specificity: from the understanding the basic visual strategies to providing progressively detailed proposals regarding the underlying neural mechanisms. Most frequently, we find ourselves using visual phenomena to infer basic computational issues, such as how orientation is imposed on discrete visual items, or how observers preattentively decide which side of a contour is the more likely associated with figure versus ground. What has been more difficult, but is becoming increasingly tractable, is the mapping between strategies and implementations, i.e. demonstrating the involvement of specific neural processes. These notions are sketched in the following, and pursued in more detail in subsequent sections.

Observable Behavior and Neurophysiology: Understanding the internal representation of a perceptual grouping, even that corresponding to the simple perceived grouping of two adjacent dots into an apparent pairing, is in fact an extraordinarily challenging research issue. What internal quantities might we assume underlie the dot pairing? First, and most uncontroversially, the dot pair has an apparent orientation corresponding to that of the line segment connecting the two dots. The orientation of the dot pair, as we will return to discuss in detail, is likely measured by orientation-selective receptive fields (RF's). While that is probably unsurprising, it has proven quite difficult to attribute other aspects of perceptual grouping behavior, such as similarity preferences, to local receptive fields. Although it is feasible to conclude that orientation is measured by a specific receptive field mechanism, it is quite another matter to understand how those measurements are selected and used to extract a visual appreciation for the structure implicit in the pattern. There are as yet hard limits on the feasibility of relating perceptual grouping behavior to underlying neural mechanisms. Nonetheless, the known neurophysiology can be used to constrain our computational proposals, as discussed below.

Discrete (and Symbolic) versus Continuous (and Analogical) Processing: How might the visual system achieve the effect of perceptual grouping? The association of fragments into a perceptual whole does not necessarily require discrete representations for the individual fragments and a subsequent discrete act of generating a symbolic grouping assertion. There has been persistent difficulty in deciding upon a formal way of describing perceptual groupings, i.e. to have a description that captures the salient aspects of seeing discrete items as associated perceptually, and yet is biologically implementable. Mathematically, a

grouping among n items might be characterized formally by an n-ary relation and represented by an n-tuple whose referents are pointers to the representations of the constituent fragments. But how this abstraction is implemented neurally remains obscure. Nonetheless, the visual system shows ample evidence of being able to operate selectively on subpopulations of visual items, pulling out of a complex display the structures that carry biologically meaningful organization. One is then aware of the discrete items that comprise the apparent pattern and organization. The perceptual groupings are likely achieved by neural mechanisms that individually (in single-cell recordings) exhibit graded and continuous behavior. How they affect such discrete behavior in concert is still unknown.

Nonlinearity and Visual Strategies: The extraction of a visual form requires discrimination of its boundary from the background (and the interior details of the form) and assembly of the constituent parts into a whole. These operations are intrinsically nonlinear, of course, and presumably are implemented by gating (or veto) and selection nonlinearity mechanisms. Shunting inhibition within a feedback network can achieve such strongly nonlinear behavior, as well as more continuous forms of nonlinearity, e.g. in gain control and signal-to-noise enhancement (McCulloch & Pitts 1943; Grossberg 1982). The nonlinearity in form perception is usually associated with later stages, e.g. the bistability of figure-ground decisions. Moran and Desimone (1985) have shown evidence of gating suppression in extrastriate cortex driven by selective attention But the earliest stages of contrast processing in striate cortex are generally expected to be approximately linear (Hubel & Wiesel 1962, 1968; Bishop, Coombs & Henry 1971; Bishop & Henry 1972). The major deviations from linearity is expected in length and width summation (Heggelund, Krekling & Skottun 1983; Henry, Goodwin & Bishop 1978; Webster & DeValois 1985), presumably due to a Gaussian-shaped weighting envelope, such as modelled by a Gabor filter (Daugman 1985) (see also Movshon, Thompson & Tolhurst 1978 regarding superposition).

There is evidence for gating nonlinearity as early as simple cells. Hammond and MacKay (1981, 1983a) recently showed that length summation in simple cells is highly dependent on contrast. For stimuli having constant contrast along their lengths, length summation was found to be substantially linear. Additions of line gaps of reduced (background) contrast lowered the response of the cell by an amount predictable by length summation considerations. However, reduction of contrast below background (reversed contrast) produced an unpredictably large response decrement. The term "gating" inhibition was given to this phenomenon to distinguish it from simple removal of excitatory drive, and appears to be a property of complex cells as well (Hammond & MacKay 1983b, 1985).

There would be computational advantage to having an operator act as a linear device when presented with appropriate stimuli, and be shunted when presented with a configuration for which the measurement would be meaningless. We are examining the strategic utility of this principle in early

aspects of form perception. Selection, or enhancement, nonlinearity, on the other hand, is likely more generally pervasive throughout early visual processing. At one extreme, selection might be involved in contour detection as early as the LGN, and at the other, to underlie the local bistability of figure-ground decisions. Grossberg and his colleagues have elucidated the computational principles of nonlinear systems and shown their predictive value e.g. in boundary contour detection and brightness reconstruction (Grossberg & Mingolla 1985). Specific instances of nonlinear behavior are extraordinarily difficult to describe, however, because the observed nonlinearities reflect the *purposes* of the computation, which must first be understood prior to modelling the source of the nonlinearity. Our approach is to use psychophysics to further reveal the fundamental strategies underlying geometric form perception, with the proviso that understanding the implementation of these strategies is a secondary concern.

2. RESEARCH RESULTS

2.1 Parsing Luminance Changes

Two prototypical luminance features are the step edge and bar (where a line is the limiting case of a bar of zero width). An ideal bar in an image would correspond to pair of opposite-polarity edges in very close proximity. Note that the definition of a bar feature in the image presumes a given scale. As bar width increases the component edges of the bar separate until for some arbitrary width dependent upon the design of the visual system, the two edge events are no longer labelled as coupled, and the bar is no longer seen as a unitary image event.

Psychophysically, certain perceptual phenomena such as the Chevreul illusion and the Mach band exhibit a strong degree of scale sensitivity, which suggests that bar- and line-like luminance changes might well be implemented by spatially organized receptive fields. (Kulikowski & King-Smith 1973 ; Shapley & Tolhurst 1973; Daugman 1985). The neurophysiology supports the general distinction of bar versus edge in terms of even- versus odd-symmetric simple cell receptive fields, respectively. The receptive field of appropriate orientation measures the approximate tangent to the contour. Wilson (1986), for example, using a family of orientation-tuned receptive fields of different sizes, has shown how a variety of curvature-related tasks can be subserved by elongated receptive field (RF) organizations (see also Gelb &Wilson 1983 and critique in Morgan & Ward 1985).

As contour curvature is further increased relative to the overall scale of the luminance change, the prototypical description is a closed blob, a convex region that typically corresponds to a local maximum or minimum in the luminance field. As the diameter of the feature is further reduced, the blob becomes point-like. Unlike the apparent correspondence between elongated receptive fields for processing bars and edges, it is not clear what the neural counterparts are for localizing and distinguishing blob-like luminance changes. There are many non-orientation selective cells found in cortex, such as those in the so-called anatomical blob regions, recently revealed by cytochrome oxidase (CO) labelling in V1 (Wong-Riley 1978; Horton & Hubel 1981; Livingstone & Hubel 1984; Hendrickson 1985; Hubel & Livingstone 1987). CO resides in blob-like regions that are found in regular arrays throughout V1 and is absent from intervening (interblob) regions. The blobs lie in the center of ocular dominance columns, but unlike columns, are seen only in laminae II-III and V-VI. Current speculation is that these structures are involved in color but not form processing (Livingstone & Hubel 1987, Ts'o et al. 1986a).

Figure 1. Two locations were chosen to demonstrate the complex cross-section profiles of the luminance signal in a natural image. The blue line with the white dot indicates the location of the cross-section. These locations are used in figure 2 to illustrate the corresponding convolution values after DOG filtering.

As Koenderink (1984) observes, it is mathematically possible to describe an image purely in terms of blobs of varying scales and shapes (see also Koenderink & van Doorn 1987). This leads to an elegant, unified treatment for describing images, but we are pursuing the conjecture that the visual system specifically distinguishes within this general scheme a small set of scale-dependent image features. Features such as edges and bars would have associated attributes or properties such as location, blur, size. In culminating a progression of studies on contour curvature, blur, and spatial primitives, Watt and Morgan (1985) presented a theory for distinguishing edge versus bar luminance waveforms that is more predictive of human performance than earlier models based on zero-crossings (Marr & Hildreth 1980). Watt and Morgan's model, however, is difficult to implement for waveforms that have substantial sustained activity (Stevens, in preparation). Their model incorporates an internal estimation of noise, which, when subtracted from the waveform, is expected to produce regions of zero activity. The parsing of the waveform into edges versus bars is then based on the arrangements of regions of activity bounded by regions of inactivity. Our experience with natural images, however, revealed that regions of nonzero response are quite common.

There is apparently no local means to estimate this local "noise" (the nonzero signal is not entirely noise, but also a consequence of nonlinear shading gradients which introduce nonzero second partial derivatives over extended regions). Our early implementations of the Watt and Morgan parsing strategy had only limited success, because of the strict requirement for zero-bounded regions. We further recognized that the biological signals providing the input to such parsing can be expected to have a substantial, and unpredictable, sustained component that is roughly related to absolute luminance (Barlow & Levick 1969; Marrocco 1972; Stone & Fukuda 1974). The introduction of sustained response into both the on- and off-center channels poses a major difficulty to strategies that are expecting to bound regions of activity.

Stevens (in preparation) derived a new model for the component activity in the receptive fields that effectively distinguish edge from bar, which does not require returns to zero activity. Specifically, the strategy is to localize a region of relatively enhanced activity in the on-cells that is coincident with a relatively depressed region of activity in off-cells. For a zero-balanced signal only the on- or the off- system would be expected to be active. An ideal edge would correspond to a region of on-cell activity spatially adjacent to a region of off-cell activity. The regions of activity would lie astride the zero-crossing that marks the location of the ideal edge. See e.g. (Glunder 1986) for a suggested neural implementation of Watt and Morgan's (1985) theory. But with sustained activity one can expect both the on and off systems to have substantial activity. Hence we suggest measuring the relative proportion of activity across the two systems at the same spatial location with the RF. That is, while the cross-section of an odd-symmetric (edge) RF is traditionally modelled as adjacent on-center and off-center subfields. Our extension would expect antagonistic input (inhibitory input of opposite-polarity) to each subfield. As a first Boolean approximation to an implementation that would eventually use algebraic summation and veto nonlinearity), an edge would be marked by a region of not merely on-activity, but *ON-and-not-OFF* activity (meaning much more on-cell activity than off) spatially adjacent to a region of opposite polarity, namely *OFF-and-not-ON*. This constitutes a superposition of mutual antagonism of the opposite sign channels to each subfield of the overall RF. As will be developed further in later sections, this corresponds well to the observed behavior in simple and complex cells found by Hammond and MacKay (1981, 1983a, 1983b, 1985).

Receptive fields incorporating spatial adjunctions of this type were implemented in a fast algorithm using our AFOSR-funded digital convolver (32-pixel diameter kernel) on the Symbolics 3675 Lisp Machine. Using natural images, we examined the method's success in marking line and edge features (see figures 1 through 3). In this algorithmic study, various curious observations were made. First, the scheme is remarkably resilient over spatial imbalance between the on and off system (as would arise in P-cells). Second, it is sufficient to examine only the sign of the convolution values (using a "trinarizing" method that differentiates positive, negative, and deadband zones of activity, where the deadband is typically

5-10%, i.e. on the order of the sensitivity expected of P-cells). Third, it is sufficient to use a small spatial zone of coincidence for localizing edges and bars: the precise localization of central moments (as Watt and Morgan, 1985, propose) is not particularly essential for the localization task. Fourth, we found that spatial localization in two dimensions can be effectively finessed by INCLUSIVE-ORing the detection of an edge or bar in four or so independent orientations. That is, we find that excellent bar and line positional marking can be achieved by *non-oriented receptive fields*.

Figure 2. The result of convolving the image in figure 1 with a DOG having ratio of excitatory and inhibitory space constants of 1:5. Note that the profiles correspond to the locations used in figure 1. The convolution profile represents several closely-spaced edge and line features.

Another observation from the earlier implementation study is the dramatic reduction in complexity of potential forms that results from making an early decomposition of the image into separate bar and edge descriptions. Compared e.g. to the plethora of undifferentiated zero-crossing contours resulting from

convolution with a small DOG operator (few of which correspond to form boundaries), the edge segments seen in the absence of the lines and bars make for a much more readily interpreted collection of forms.

We find it significant that while edge detection is generally expected to be accomplished by elongated receptive fields, which incorporate orientation selectivity, it is possible in principle to dissociate the problem of localizing an edge (or bar) from the problem of computing its orientation, blur, contrast, or other attributes. We do not expect that the biological system follows this strict function division, i.e. using separate mechanisms for edge localization than for measuring orientation, and so forth. Elongated RF's are likely used for both measuring curvature and for spatial localization, as modeled recently (Wilson 1986; Dobbins, Zucker & Cynader 1987). But it is nonetheless noteworthy that two-dimensional detection of edge or bar location can be finessed with *radially-symmetric* operators. The neurophysiological prediction would be the detection of RF's that are sharply tuned to phase (e.g. even versus odd symmetry) but *independent* of the orientation of the bar or edge.

Figure 3. Demonstration of our line/edge parser, where edges and lines (thin bars) are emphasized. This output was generated using one free parameter, namely a threshold representing contrast sensitivity of 5%. The implementation uses a digital convolver for the DOC convolution.

2.2 The Café Wall as Evidence for Parsing

The Café Wall is composed of alternating black and white tiles separated by narrow horizontal mortar lines of intermediate grey (figure 4). Two effects are associated with the pattern. The horizontal edges of the individual tiles appear slightly tilted, causing them to appear wedge-shaped, and overall, one receives the impression that the mortar lines are not parallel.

The Café Wall effect appears to involve several early aspects of edge detection: irradiance, brightness induction, orientation detection, edge localization, and contour completion. These effects derive from phenomena associated with the mortar, both within the mortar and at the borders between the mortar and the tiles above and below. The horizontal white and black edges that border on the mortar line appear to intrude diagonally into the mortar, producing a succession of wedge-shaped tiles. And within the mortar itself, rather than a uniform grey one sees alternating light and dark diagonal bands, a so-called "twisted cord" (Fraser 1908). The twisted cord has been shown to induce an illusion of overall tilt in this and other patterns (Fraser 1908), presumably from interactions among orientation-tuned cortical units that construct extended continuous contours (Moulden & Renshaw 1979; Grossberg & Mingolla 1985).

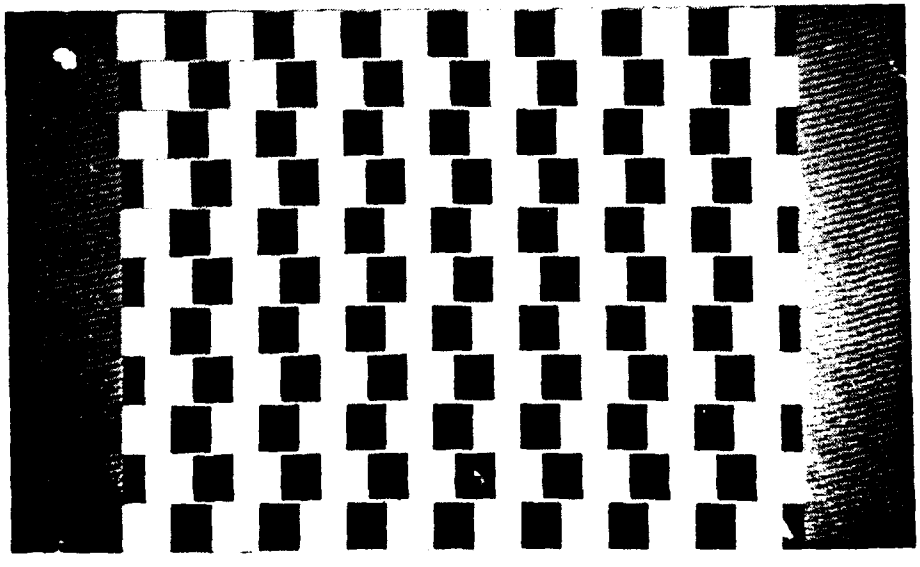

Figure 4. The Café Wall pattern.

Gregory and Heard (1979) propose that the intrusion of the tiles into the mortar is a consequence of the failure of an hypothesized "border locking" process, whose purpose is to constrain the spread of lightness to within regions bounded by contrast edges. They suggest that in those regions where tiles of opposite contrast overlap vertically, the border-locking process does not localize the edge boundaries correctly; lightness then migrates across the mortar to form the illusion. Gregory and Heard (1979) further suggest a relationship between edge contour shifts and irradiance, which Moulden and Renshaw (1979) also show strongly contributes to the tilt distortion in the related Münsterberg illusion. McCourt (1983) has shown that brightness induction also contributes to the effect by inducing an alternating pattern of elongated diagonal light and dark strands within the mortar.

Morgan and Moulden (1986) examined the spatial frequency content of twisted cords, by convolving the Café Wall pattern with a Laplacian operator that resembles the center-surround operator found in the retina (Rodieck & Stone 1965; Wilson & Bergen 1979; Marr & Hildreth 1980) They show that Laplacian filtering retains, and even accentuates, the apparent twisted cords in the Café Wall and Münsterberg patterns. The extrema (ridges and troughs) in the Laplacian-convolved image correspond quite directly to the light and dark strands of the apparent twisted cord. Foley and McCourt (1985) show that such center-surround operators can induce opposite-phase brightness into narrow fields, as is the case for a difference of Gaussians (DOG) operator of diameter somewhat larger than the mortar width. In addition to attributing small-scale brightness induction effects to retinal DOGs, irradiance-type shifts in apparent edge location along the mortar (Moulden & Renshaw 1979; Gregory & Heard 1979) may also have a partly retinal origin, e.g. by a compressive transform at luminance transduction (Morgan, Mather, Moulden & Watt 1984; Mather & Morgan 1986). The tilt effect in the Café Wall seems therefore to originate in part as perturbations or artifacts induced by the spatial filtering performed at the retina, and in part from cortical processes that measure the orientation and position of these perturbed luminance changes.

In addition to the local origins of tilt in the pattern, there is need to explain the overall impression of convergence along the alternating rows of tiles. As Fraser (1908) originally conjectured, the global aspects of the illusion likely emerge from integrative interactions along the length of the mortar. Support has been given for this conjecture, phrased in terms of facilitatory interactions among orientation-tuned cortical units that construct extended continuous contours (Moulden & Renshaw 1979; Grossberg & Mingolla 1985).

We examine here quantitatively the extent to which fine-scale Laplacian-like (DOG) filtering at the retina induces the topographic features associated with the twisted cords. We find that the smallest proposed DOG operator makes satisfactory predictions regarding the presence and extinction of induction-like features

in the bandpass image, providing further support for the ideas described by Morgan and Moulden (1986). We report a reversal of the traditional Café Wall effect that is dependent upon mortar width.

We also examine the involvement of orientation-selective units (e.g. simple cells) in extraction of the local tilt. Hammond and MacKay (1981, 1983a, 1983b, 1985) demonstrated a dramatically non-linear property of striate cells: suppression when a bar is augmented with a small dot of opposite contrast. The cell appears to be gated-off by the addition of the small dot of opposite contrast. We have found that by inserting points of opposite contrast at strategic locations where even-symmetric receptive fields might be expected to align locally with the ridges or troughs in the Café Wall pattern, there is a corresponding disruption of the tilt illusion.

The Influence of Circular-Symmetric Operators

Morgan and Moulden (1986) observe that the light and dark bands within the twisted cord correspond to the ridges and troughs (local extrema) in the Laplacian-convolved image. Using a zero-balanced difference of Gaussians, with ratio of excitatory to inhibitory space constants of 1:5 (or larger), we examined the behavior of the extrema in the convolution values as a function of the relative size of the operator and the mortar width.

Gregory and Heard (1979) varied mortar width and found that the illusory tilt was maximal at the smallest width they tested (1′), and that it weakened with increasing mortar width, until little distortion was observed for a 10′ width[2]. We find that this behavior is likewise reflected in the amplitude and shape of the extrema in the DOG-convolved image as mortar width is increased. We assume that the smallest DOG operator in the central fovea has a central excitatory diameter ω of about 1.3′ (Marr, Poggio & Hildreth 1980; Richter & Ullman 1982)[3] . The quantitative behavior of a DOG operator of this size as a function of mortar width suggests to us that this scale of operator governs both the appearance, and the gradual disappearance, of the local tilt in the Café Wall patterns seen in sharp focus. When the mortar width is on the order of ω, the extrema in the resulting convolution values resemble twisted cords, as Morgan and Moulden (1986) report. The convolution values within the mortar are also modulated periodically, in accordance with the brightness induction observed by McCourt (1983). Specifically, while the mortar is a

---

[2] This result was obtained for patterns presented in sharp focus; the illusion can also be seen over a larger range of scales when blurred optically or viewed somewhat peripherally (Moulden & Renshaw 1979; Gregory & Heard 1979).

[3] Marr et al. (1980) include the optical point spread function in the effective diameter of this operator. This proposed operator size would represent the smallest expected diameter of DOG operator, as based on the density and diameter of cones in the central fovea, and presumes that the excitatory input derives from a single cone (Richter & Ullman 1982).

uniform neutral grey, the contrast within the convolved mortar alternates in reverse phase relative to the contrast of the bordering tiles: where bounded above and below by white tiles the convolved mortar is darker, and vice versa (see figure 4a). For mortar of width ω or slightly larger, the convolved values within the mortar show a gradient tilted from the horizontal, which, as noted, corresponds well to the apparent twisted cord. But as mortar width further increases, the DOG receptive fields with centers that fall within the mortar receive decreasing contribution to their surrounds from the tiles above and below the mortar. The brightness induction effect thus diminishes until, for sufficient mortar width, the tile/mortar margins are essentially isolated edges. The progressive diminution of the induced twisted cords is predicted rather well by assuming the DOG operator has an ω of about 1.3′. An operator much larger would have preserved the twisted cord beyond the limits observed by Gregory and Heard (1979). This is further quantified by Experiment 1.

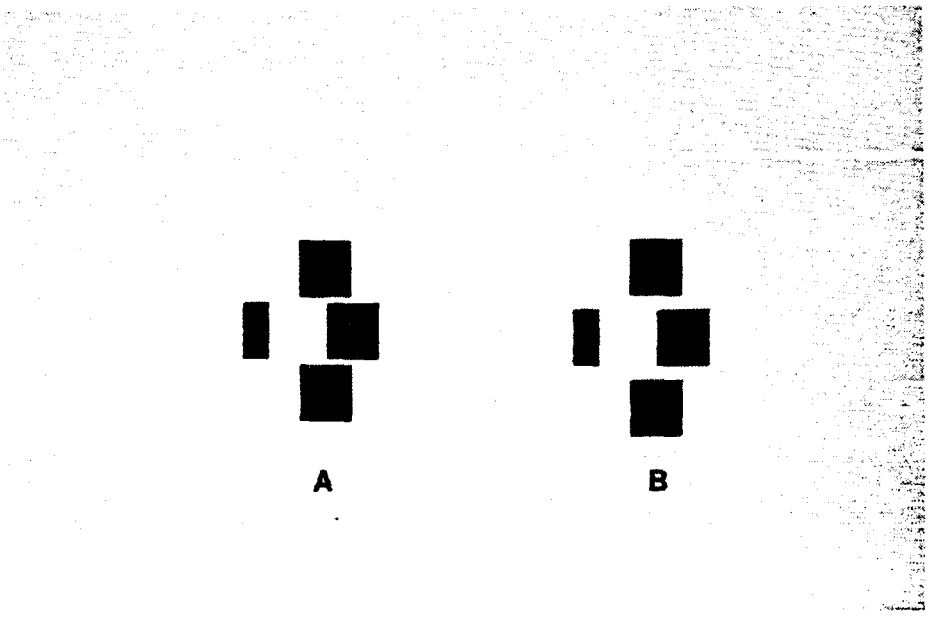

Figure 5. Two example stimuli from experiment 1, to be viewed at normal reading distance (i.e. approximately 50 cm) with central fixation. In *a* the wedge distortion in the central row appears to narrow to the left. In *b* the mortar is wider and there is slight impression of distortion in the opposite direction.

In the following (Lulich & Stevens, submitted) we will describe a brightness-induction effect in the Café Wall pattern that arises with large mortar widths. One can contrive to have the bands of induced brightness reverse the apparent direction of tilt in the Café Wall. The reversal effect can be seen in figure 5b. Notice that in the small-width pattern (figure 5a) the mortar lines appear to deviate from the horizontal, as expected in the traditional Café Wall effect. The two lines do not appear parallel, but rather, to define a shallow wedge that narrows toward the left. In figure 5b, where the mortar width is increased, there is a slight impression of a wedge pointing in the opposite direction, that is, with the right narrower than the left. We examined this change in apparent orientation as a function of mortar width.

As in Morgan and Moulden's (1986) study, this reversal effect can be shown to be objectively present in the bandpass-filtered image (see figure 7). It thus lends further support to the notion that the local tilt illusion in the Café Wall is introduced largely by artifacts of retinal processing. But furthermore, close examination of the topography of the bandpass-filtered image raises questions concerning the measurement of orientation, as distinct from spatial localization, of luminance changes.

Experiment 1

Method

Subjects: Three subjects took part in the experiment; all had normal or corrected to normal visual acuity. These subjects had participated in a variety of experiments in our laboratory and were familiar with the techniques and methods required. All were naive to the purposes of this experiment.

Stimuli: Café Wall patterns of varying mortar width were generated using a Symbolics 3600 Lisp Machine and displayed on a high-resolution CRT (Tektronix 634, with P45 phosphor and 0.21 mm spot size). The patterns were viewed from a distance of 203 cm using natural pupils. The patterns were constructed with varying combinations of tile size and mortar width (see representative stimuli in figure 5). Two tile sizes were chosen, 7.1′ and 14.2′. For the stimuli based on the smaller tile size the pattern consisted of three rows of six columns of alternating black and white tiles. The stimuli made up of the larger tile size consisted of three rows of four columns. The patterns were embedded in a background grey equal to the grey of the mortar. This grey was balanced to one-half the luminance difference between the black and white tiles. The luminance of the white tiles were 42 ft/L, the black tiles 0.1 ft/L, and that of the mortar and background was 22 ft/L. For each size of tile, stimuli were presented at one of ten different mortar widths. Mortar width was varied from 0.35′ to 3.5′ in increments of 0.35′.

The overall height of each pattern was dependent upon the size of the tiles and the particular mortar width. The overall shape of the patterns were made rectangular by cropping the left and right vertical borders. Cropping primarily insured that the patterns did not extend beyond the central foveal region (the overall patterns subtended about 28′ by 43′). It served to remove a distracting effect wherein the central row would otherwise protrude past the top and bottom rows by a half-tile, forming an overall arrow-like configuration pointing to the left or right.

Procedure: Using a forced-choice design, subjects viewed Café Wall stimuli presented for 200 msec. Subjects were told to fixate and attend to the center of the pattern. It was their task to decide the direction of apparent convergence in the pattern, i.e. whether the vertical separation between the two mortar lines appeared to narrow towards the left versus right side the pattern. They indicated their choice by pressing a left or right labeled button; no feedback was given regarding their responses. The patterns were presented randomly as a mirror reflection of the original pattern. Overall, 120 displays were presented in random order, corresponding to 3 repetitions of combinations of the 10 mortar widths, 2 sizes of tile, and 2 conditions of mirror reflection.

Results and Discussion

The impression of overall tilt in the Café Wall pattern reversed orientation for all subjects at approximately the same mortar width. This result is plotted for both tile sizes in figure 6. Both curves are sigmoidal with a zero-crossing in the vicinity of 1.75′ mortar width. There was no significant effect of tile size on the reversal effect. In each case larger standard deviations were found for the larger mortar widths, consistent with the subjects' reported impression that the reversal effect was weaker than the original Café wall illusion.

Numeric convolution of these patterns, for correspondingly scaled mortar widths and DOG sizes, reflect these results. In figure 4 the pattern dimensions in the experimental stimuli are scaled so that the DOG (corresponded to the smallest physiologically-predicted DOG of 1.3′) had a central excitatory diameter of 11 pixels. The 7.1′ tiles of the pattern correspond to 60 pixels in the scaled pattern. The DOG operator was zero-balanced (the amount of inhibition equaled the amount of excitation), and had a ratio of center to surround space constants of 1:5. Figure 7a corresponds to the convolution of a Café Wall pattern with narrow mortar, which induces the traditional effect; figure 7b shows the convolution for a larger mortar width, where the reversal is observed.

It is noteworthy that the induction effects in these stimuli are so strongly scale dependent. Since the data were gathered for mortar widths near the size of the smallest predicted physiological DOG operator, the observed transition point for the reversal (1.75′) corroborates the prediction that the smallest operator

has a central excitatory diameter of about 1.3′ (Marr et al. 1980). Furthermore, the observed brightness induction-like effect is consistent with Morgan and Moulden's (1986) conclusion that it is a consequence of bandpass filtering.

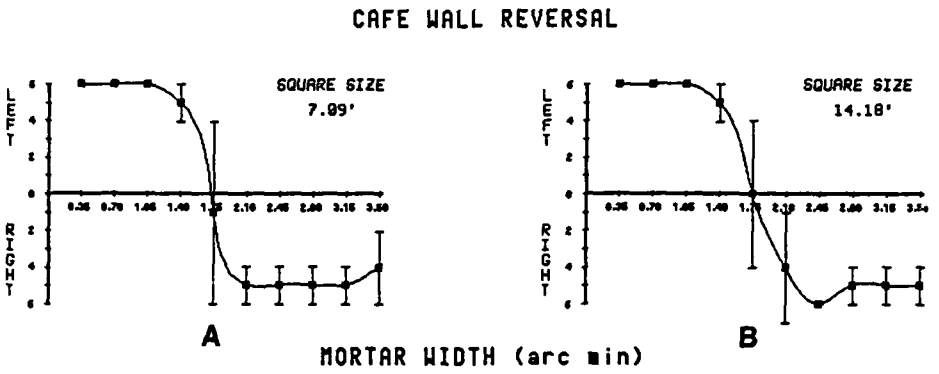

Figure 6. Graphs of tilt direction judgements, for small tiles in *a* and large tiles in *b*. In each case subjects experienced a reversal in the direction of apparent convergence for mortar approximately 1.75′.

With reference to figure 7a, a mortar width of 9 pixels (equivalent to 1.0′), results in a convolution where the dark and light bands of Fraser's twisted cords are apparent in the mortar, in accordance with Morgan and Moulden's (1986) observation. The light ridges are tilted slightly from the horizontal and span diagonally across the mortar to connect the corners of the white tiles above and below the mortar. Likewise, the dark ridges in the mortar span diagonally between corners of the black tiles. For a wider mortar of 18 pixels (equivalent to 2.0′), and convolution with the same diameter DOG, the traditional twisted cord arrangement of bands is extinguished, and replaced by a fainter induction effect. Light bands appear now span the mortar between the black tiles (and likewise dark bands between the white tiles). These induction bands or bars are seen at a steeper angle to the horizontal than those induced at smaller mortar widths. As mortar widths is further increased the induction effects spanning the mortar is further diminished and becomes negligible for mortar widths about twice the size of the DOG operator.

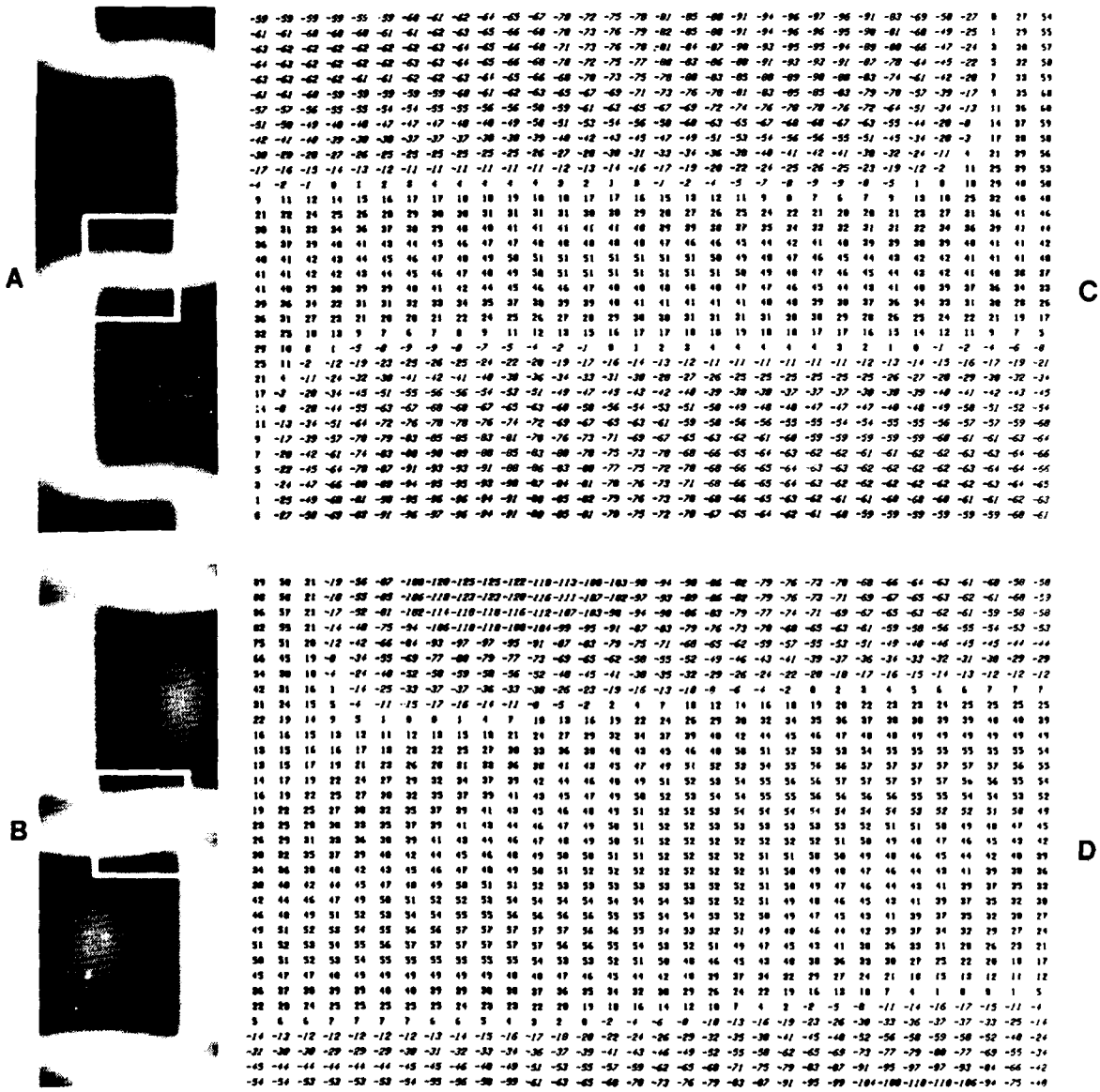

Figure 7. DOG convolution of a Café Wall pattern where the mortar is narrower (in *a*) and wider (in *b*) than the DOG central excitatory diameter. Numeric values in *c* and *d* correspond to regions indicated by rectangles in *a* and *b*.

The Influence of Elongated Receptive Fields

A DOG operator of appropriate scale produces a distribution of convolution values that is distorted in a manner that resembles the apparent twisted cords. Specifically, the geometry of the convolution values, particularly the induction of diagonal gradients into the mortar corresponds well with the impressions of illusory tilt. But how is the geometry detected? The ridges and troughs Morgan and Moulden (1986)

discuss are initially implicit in the DOG-convolved image. While there is rather broad consensus on how to model the circular-symmetric operators at the retina, there is no correspondingly quantitative model available of the measurement and encoding of tilt. It is generally expected, but still conjectural, that simple cells perform the encoding, for example.

There are many distinct ways to compute the orientation of a ridge or trough within a two-dimensional field or array of values. One approach is to locate the points of instantaneous local maximum or minimum according to some spatial criterion and to subsequently fit a line or curve through these points. Watt and Morgan (1985) propose measuring the central moments, however their proposal is restricted to a one-dimensional signal; the extension to an arbitrary two-dimensional signal is not straightforward. But where the luminance signal is approximately one-dimensional, such as midway along a ridge-like strand of the twisted cord the luminance signal could be approximated as a bar. The orientation of the ridge or trough would be the local tangent to the locus of local maximum or minimum activity (i.e. zero-bounded regions of activity). Another computationally distinct method is to summate the convolution values within elongated (orientation-selective) receptive fields of varying orientation, and to select that receptive field having maximum response (e.g. Tyler & Nakayama 1984). Clearly this latter computation would benefit from using antagonistic even-symmetric subfields, so that the operator would produce zero net response in a constant field. The relationship between this computational method and cortical receptive fields is rather apparent. The former method, based on a local extremum (or centroid) operator, is less easily related to neurophysiology.

Since simple and complex cells of the striate cortex are the first cells in the visual pathway to demonstrate orientation selectivity (Hubel & Wiesel 1962), it is reasonable to suspect that they are involved in the determination of the orientation of Fraser's twisted cords and the mortar line (Morgan & Moulden 1986). The following experiment further supports the suggestion that striate cells underlie the orientation measurement.

Experiment 2

Hammond and MacKay (1981, 1983a) have shown that length summation in simple cells is highly dependent on contrast along the axis of the receptive field. For stimuli having constant contrast along their lengths, length summation was found to be substantially linear. Additions of line gaps of reduced (background) contrast lowered the response of the cell by an amount predictable by length summation considerations. However, reduction of contrast below background (reversed contrast) produced an unpredictably large response decrement. The term "gating" inhibition was given to this phenomenon to

distinguish it from simple removal of excitatory drive, and appears to be a property of complex cells as well (Hammond & MacKay 1983b, 1985). Brookes and Stevens (1988) have used this effect to examine the role of striate cells in gating the signalling of orientation in groups of dots. We have modified the Café Wall patterns by adding tiny dots of opposite contrast to Fraser's twisted cords. The prediction is that these dots would gate-off the units that would otherwise assert the orientation of the cords in the unmodified pattern.

Method

Subjects: Forty naive subjects participated in this experiment. All subjects had normal or corrected to normal visual acuity.

Stimuli: Two different displays (stimuli 1 and 2) were constructed using the same apparatus used in the previous experiment. For both stimuli the background was a neutral grey that matched the luminance of the mortar line (8.2 ft/L). The individual Café Wall patterns in both types of display were composed of seven columns by six rows of alternating black and white tiles, each 10.3′ on a side. Each Café Wall pattern subtended 72.1′ horizontally by 61.8′ vertically. The width of the mortar in all patterns was 1′. The luminance of the white tiles was 15.2 ft/L and the black tiles was 4.1 ft/L. The Michelson contrast across the tiles was 57.5%.

Some Café Wall patterns had white or black dots positioned in the mortar. Each dot was a rectangle 1′ by 1.5′ and positioned at the center of the region of overlap between tiles of similar contrast. Stimulus 1 presented a traditional Café Wall pattern and two variants on the basic pattern induced by the included dots, so that subjects could rank-order the relative strength of the illusions as a function of the variation we introduced. Stimulus 2, shown in a subsequent series of presentations, provided a follow-on to the basic result provided by stimulus 1.

Stimulus 1 was arranged as in figure 8 and contained three Café Wall patterns (1a, 1b and 1c). Café Wall pattern 1a contained mortar dots of the same contrast sign as the tiles above and below them. The white dots had a luminance of 22.2 ft/L and the black dots 4.1 ft/L. The Michelson contrast between the white dots and the white tiles was 18.5%. The Michelson contrast between the black dots and the black tiles was 11.8%. Café Wall pattern 1b used mortar dots of opposite contrast compared to those in pattern 1a. The luminance of the white and black dots was the same as pattern 1a. The Michelson contrast between the white dots and the black tiles was 68.7% and between the black dots and the white tiles was 90%. Café Wall pattern 1c contained no dots.

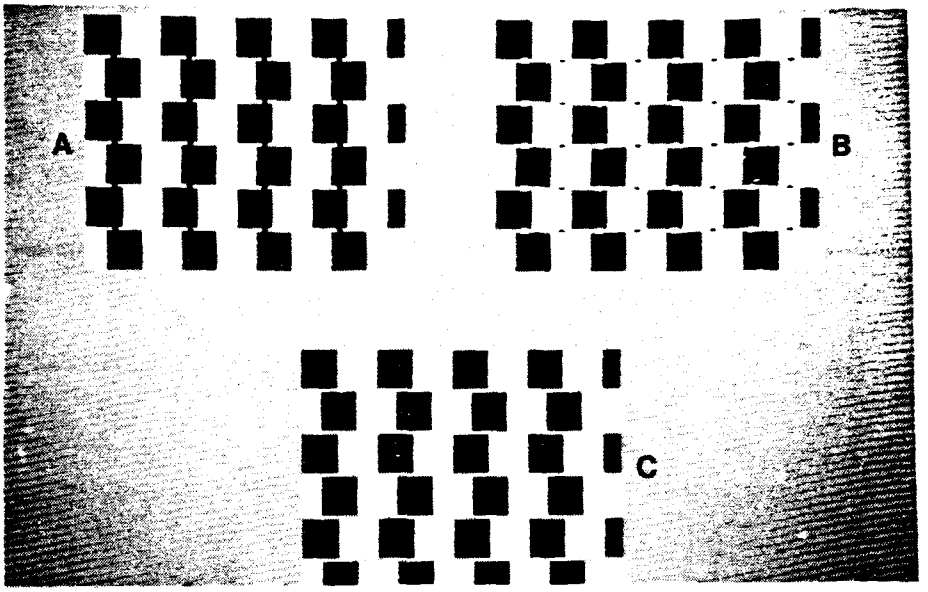

Figure 8. Stimulus1 of experiment 2.

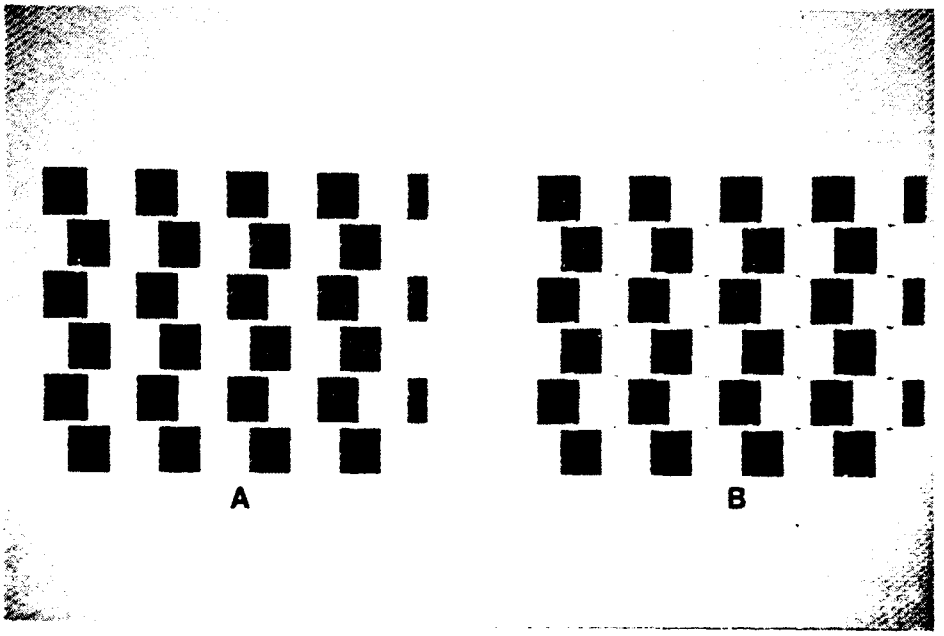

Figure 9. Stimulus 2 of experiment 2.

Stimulus (2), as shown in figure 9, was composed of two Café Wall patterns (2a and 2b). The Café Wall pattern (2a) was the conventional pattern and contained no dots, while pattern (2b) had dots in the opposite contrast configuration. The luminance of the black and white dots equalled that of the black and white tiles. The Michelson contrast between the white dots and the black tiles was 57.5% and between the black dots and the white tiles was 61.7%.

Procedure: Twenty subject viewed stimulus I and twenty different subjects viewed stimulus 2. Each subject was seated 120 cm from the stimulus display. To introduce the illusion, each subject was first shown the Zöllner illusion and asked to describe the figure. When the subject mentioned the apparent convergence of the parallel lines, it was explained that convergence of the mortar lines in the Café stimuli would similarly be seen, to varying degrees. Next the subject observed the stimulus (1 or 2) and was instructed to rank order apparent convergence of the mortar lines in the presented Café Wall patterns. Each subject was given as much time as necessary, but asked to perform the task quickly and to rely primarily on initial impressions.

Table 1: Stimulus 1

Rank orderings

Case	Most	Mid	Least	Total
A	0	0	20	20
B	16	4	0	20
C	4	16	0	20
Total	20	20	20	

Table 2: Stimulus 2

Rank orderings

Case	Most	Least	Total
A	0	20	20
B	20	0	20
Total	20	20	

Results and Discussion

Table 1 shows the rank-ordering of frequency data for the three different versions of the Café Wall in stimulus 1. Chi-squared analysis showed that the null hypothesis (i.e. the convergence strength of each pattern is equal) could be rejected ($\chi 2 = 81.5$, $p < .001$, d.f. = 4). A $\chi 2$ of 81.5 demonstrates a highly significant effect. Notice that Café Wall pattern (1a), the pattern with dots of like contrast always ranked as having the weakest convergence illusion. Café Wall pattern (1b), the pattern with dots of opposite contrast, was ranked as the strongest 80% of the time. Table 2 show the rank-ordered data for stimulus two. A strong effect is clear. Chi-squared analysis showed that the null hypothesis could be rejected ($\chi 2 = 40$, $p < .001$, d.f. = 1). Notice that lowering the contrast of the dots resulted in a perfect preference ordering.

With the addition of dots of opposite contrast to the center of Fraser's twisted cords, the overall impression of tilt of the mortar lines was significantly weakened. In addition, the presence of a dot of like contrast but higher luminance enhanced the impression of tilt. McCourt (1983) produced similar effects on apparent convergence by manipulating the contrast sign along extended segments of the mortar. His stimuli were designed to distinguish between the contributions of brightness induction and those of Gregory and Heard's (1979) border locking notion. McCourt found that the Café Wall convergence effect is weakened when the mortar is darkened in the segments bounded above and below by black tiles and lightened where bounded by white tiles (leaving neutral grey in the transition regions where tiles have opposite contrast). While this reduces the potential for brightness induction in those regions, it also removes the bar-like features that provide (piecewise) contour continuity along the mortar. In our stimuli the introduction of point-like contrast reversals are likewise highly effective in disrupting the contour organization along the mortar. The facilitatory effect provided by point-like contrast enhancements is similarly consistent with McCourt's (1983) findings using extended mortar segments. While global continuity of contrast along the mortar is not necessary, as Fraser (1908) originally observed, continuity of contrast within the individual bar-like segments that comprise the braided strands of the twisted cord is important. That is, to disrupt the overall effect it is sufficient to disrupt the contrast continuity within the individual white or black bar-like segments (those bounded above and below by tiles of same contrast). As Hammond and MacKay found, contrast reversal along the length of the bar is much more potent than a simple gap. The results of experiment 2 thus suggests that mechanisms with a gating non-linearity similar to that observed in striate cells contribute to the piecewise measurement of tilt and underlie their integration along continuous contours.

2.3 Asserting Orientation between Discrete Items

One can readily see structure in patterns made up of discrete points where the structure comes from the spatial relationships of the points in the pattern. For example, figure 10 shows a simple dot pattern known as a Glass pattern (Glass 1969). Glass patterns are constructed by superimposing onto a random dot pattern a copy that has been transformed, *e.g.* by scaling or rotation. Each dot and its transformed counterpart in the superimposed copy defines a dot pair. The radial pattern in figure 10, for example, is the result of a scaling transformation. In order for the global organization to emerge from such patterns the orientation corresponding to the lines defined by the dot pairs must be found.

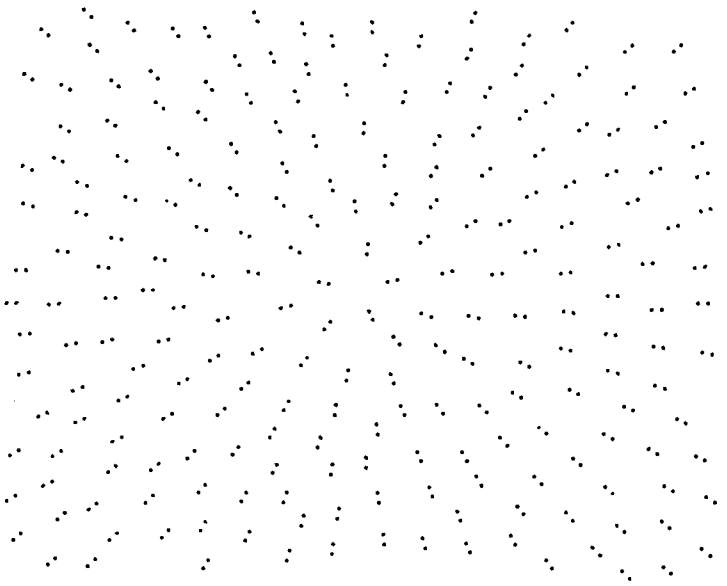

Figure 10. A Glass pattern used for examining the detection of local pairing orientation.

There is no general consensus on how this orientation is extracted. Several competing theories have been proposed, differing primarily in terms of the extent to which the component dots are treated as individual elements. The Gestalt investigators described perceptual grouping in terms of individually

marked items that are grouped explicitly on the basis of their attributes, proximity and their spatial arrangement. The notion of establishing discrete grouping tokens was tacit, by and large, in the Gestalt demonstrations of similarity grouping (Wertheimer 1923; Koehler 1929; Koffka 1935). Later, it was specifically proposed that groupings involved "place markers" (Attneave 1974) or "place tokens" Marr (1976, 1982), which individually carry information about position and attributes such as contrast, color, size and orientation (see also Ullman's (1979) grouping tokens for motion correspondence). Pairings between adjacent place tokens are represented by "virtual lines" (Attneave 1974; Marr 1976, 1982; Stevens 1978). Similarly, Caelli and Julesz (1978) discuss "local dipoles" between neighboring dots in texture discrimination. Virtual lines are not illusory lines in the sense that subjective contours are illusory intensity edges; they do not exhibit contrast phenomena. Instead, perceived pairings make explicit the orientation, position, and separation of the similar and adjacent elements. Attneave (1955, 1974) has demonstrated position and orientation judgements that seem mediated by place tokens, and Beck and Halloran (1985) similarly suggest that virtual lines underlie some vernier acuity judgments. It is not clear, however, whether the position markers in attentive judgments of relative position and orientation under focal scrutiny are the same "place tokens" that have been proposed for early visual processing of texture.

The alternative model for grouping is that the individual dots contribute to the local orientation only implicitly, in terms of their spatial proximity and their luminance energy. A closely-spaced pair of dots, or a chain of collinear dots, has a power spectrum similar to that of an isolated line segment for spatial frequencies less than 1/s, where s is the dot spacing. Low spatial frequency filtering would therefore provide a means for extracting the local orientation signal, presumably using cortical cells tuned to both orientation and spatial frequency (Ginsberg, 1973). Recently, a model for dot grouping, based on Gaussian blur, has also been proposed that shares similarities with earlier models operating in the luminance domain (Smits & Vos 1986).

The even-symmetric cortical simple cell has been specifically proposed as responsible for the local orientation measurement: the dot pair would be roughly equivalent to a continuous line of equal total energy presuming a linearly summating receptive field. The structure of the dot pattern would emerge without need for explicitly marking the constituent dots as tokens. Glass proposes that the local orientation is derived by correlating the activity of simple cells over small neighborhoods (Glass 1969; Glass & Perez 1973; Glass & Switkes 1976; Glass 1979). Zucker (1983) proposes a cooperative computation whereby the broad orientation tuning curves of individual receptive fields can be sharpened by combining the outputs of individual cells over local neighborhoods. Simple cells whose receptive fields are oriented with the dot pairs would presumably respond more vigorously, on average, than those cells at other orientations, so that local correlation (or a similar computation) of their activity would reveal the orientation of the dot pairs in each vicinity. Similarly, Caelli and Julesz (1978) suggest that linear arrangements of dots in texture are

detected by neural units with elongated receptive fields applied to the retinal image, either "a single neural feature extractor of the Hubel and Wiesel type", or a unit that "measures the quasicollinearity of adjacent dipoles by combining single neural units of a retinal neighborhood with slightly different orientation sensitivity" (Caelli & Julesz 1978, p. 172; see also Caelli *et al.* 1978; Julesz 1981). Prazdny (1984) also suggested that the dot pairings in Glass patterns are detected by "... measurements in the spatial and energy domain rather than logical operations on symbolic descriptions" (see also [Prazdny 1986]).

The simple cell model, while attractive in its ability to relate a grouping effect to underlying neural mechanisms, seemingly cannot account for certain effects. Two effects merit discussion, the first concerning spatial frequency filtering and the second grouping on the basis of contrast and color similarity. Both effects, which are contrary to the simple cell model, are reviewed in the following.

In (Stevens & Brookes 1987) we presented various arguments against using existing models of simple cells for dot grouping. The first of these arguments concerns the theory that organization is carried exclusively by low spatial frequencies. It has been shown by Carlson *et al.* (1980) and Janez (1984) that dotted-line organization can be seen in high-pass spatial frequency filtered patterns. They conclude that some process "more abstract" than low spatial frequency-tuned channels is involved. In a similar paradigm, we generated dot patterns with only high spatial frequency content (Stevens & Brookes 1987). The individual items were 3x3 pixels on a side, each a black-and-white checkerboard with the center pixel the same grey value as the background grey. The argument against simple cells is that the stimuli have insignificant power in the range of spatial frequencies at which a correspondingly scaled simple cell would respond. Using energy balanced checkerboards we found that the impression of local pairings and parallelism is apparent when the correlated dots were separated by as much as 30 arc min which is beyond the range that simple cells are believed to exist foveally. In a similar experimental design, Prazdny (1984) reported, contrary to our finding, that when a Glass pattern is composed of individual Laplacian-like dots (e.g. a central white point surrounded by a ring of darker points) that the apparent organization of the pattern is lost when the mean luminance of the Laplacian-like dots match the background grey. We likewise found this effect, but attribute the problem to the weak energy of the tiny Laplacian-like features used, particularly when presented in the parafovea where they could barely be resolved. When we scaled the Laplacian-like features linearly with eccentricity, we found that the organization of the Glass pattern was successfully preserved when the mean luminance of the individual features matched the background (Stevens & Brookes 1987). This evidence, at the time, convinced us of a non-simple cell contribution to the preattentive extraction of structure among tokens in texture.

The second line of evidence against the simple cell model for dot grouping concerns the preference for similarity among the items that are grouped. Similarity preference, first described by as a Gestalt

organizing principle, was demonstrated by Stevens (1978) in rivalrous Glass patterns. Dot triples were presented rather than mere dot pairs, where two of the three dots were of similar contrast but dimmer than the third. Contrary to contrast summation models, observers saw the organization carried by pairings of low contrast dots. This general finding was replicated and extended to color similarity in (Stevens & Brookes 1987), further strengthening the argument for token-based grouping in texture, rather than a process that operates purely in the luminance-energy domain.

The above two lines of argument against simple cells constituting the underlying grouping mechanism are ultimately based on assumptions about the linearity with which contrast energy is summated by simple cells (Hubel & Wiesel, 1962; Bishop, Coombs & Henry, 1971; Bishop & Henry, 1972). The major deviation from linearity is expected in length and width summation (Heggelund, Krekling & Skottun 1983; Henry, Goodwin & Bishop 1978; Webster & DeValois 1985), presumably due to a Gaussian-shaped weighting envelope, such as modelled by a Gabor filter (Daugman 1985) (see also Movshon, Thompson & Tolhurst 1978 regarding superposition). We will summarize this view of the simple cell as assuming linear-weighted spatial summation.

Recent neurophysiological results show that simple cells are not strictly linear summation devices. Heggelund et al. (1983) showed that excitation and inhibition in simple cells varied nonlinearly across the receptive fields. Their results indicated that there is some overlap of the excitatory and inhibitory fields. Hammond and MacKay (1983) found that while a long bar will stimulate a simple cell, the same bar, with the addition of a point of opposite contrast anywhere along the bar, will not. The effect is more like a logical gating than summation since a small point will turn off the response of even a very long bar. This property was found in each simple cell that was tested. The term "gating" inhibition was given to this phenomenon to distinguish it from simple removal of excitatory drive, and appears to be a property of complex cells as well (Hammond & MacKay 1983b, 1985).

This gating property of simple cells provides a novel way of testing the role of simple cells in dot grouping processes. If simple cells are involved in grouping then we should be able to nullify that grouping by placing a point of opposite contrast between each pair of points in the pattern. This is not conclusive evidence that simple cells are the mechanism involved, but since other cells, such as complex cells were not found to have this property it would constitute very strong evidence. The following experiment (Brookes & Stevens, in preparation) shows that dot groupings can in fact be nullified by exploiting this property.

Method

Stimuli: The stimuli consisted of three types of modified Glass patterns, each made up of triples of dots. In each case the triples were a pair of white dots and a single black dot, all presented against a grey background. The dot pairs were oriented either in radial, concentric or random orientation relative to the pattern center. For each of these three global organizations there were two possible positions for the opposite-contrast (black) dot associated with each pair of white dots. Manipulating the position of the opposite-contrast dot was intended to control for the possibility that these dots might simply be distractors or noise. In the first case, the black dot was placed midway between the two white dots of each pair, the analogue to the stimuli used by Hammond and MacKay. In the second, the black dot was placed adjacent to the pair at a distance of half the spacing of the pair. In this control case the opposite-contrast dots were displaced to lie adjacent to, rather than between, the paired dots of like contrast. The separation between dot triples was approximately 34' with the individual dot pairs separated by approximately 9'. Each Glass pattern was constructed from an underlying set of points of homogeneous density with no discernible structure (see Stevens 1978 for method). Thus the overall pattern consisted of an organized collection of dot triples, each consisting of two white dots in either radial, concentric or random organization, and the third black dot in either the between or adjacent position relative to the pair. The stimuli are shown in figure 11. The stimuli were generated by a Symbolics 3675 Lisp Machine and displayed on a Tektronix 690SR monitor.

Procedure: Eight subjects participated. All but one were naive to the purpose of the experiment. The subjects were seated 2m from the stimulus display. A trial consisted of the presentation of one of the six conditions (three types of dot patterns with 2 possible positions of black dots each) chosen randomly, and the task was to decide which of the three patterns was present. Initially, a small fixation cross was presented for 1 sec, after which the dot stimulus was presented for 200 msec without masking. Subjects were to respond to this stimulus by pressing one of three buttons on a mouse pointing device. Each was given 20 repetitions of the 6 stimuli, for a total of 120 trials.

Results

Table 3 shows the data for the eight subjects. In most cases there was a strong tendency to see the pattern correctly for stimuli in which the opposite contrast dot appeared adjacent to the dot pairs. In this case the mean percentage of correct responses was 94% for the concentric case, 78% for the radial case and 92% for the random case. For the condition where the opposite contrast dot appeared between the paired dots these means were lowered to 28% for the concentric, 31% for the radial. For the random case the mean in this case was 85%.

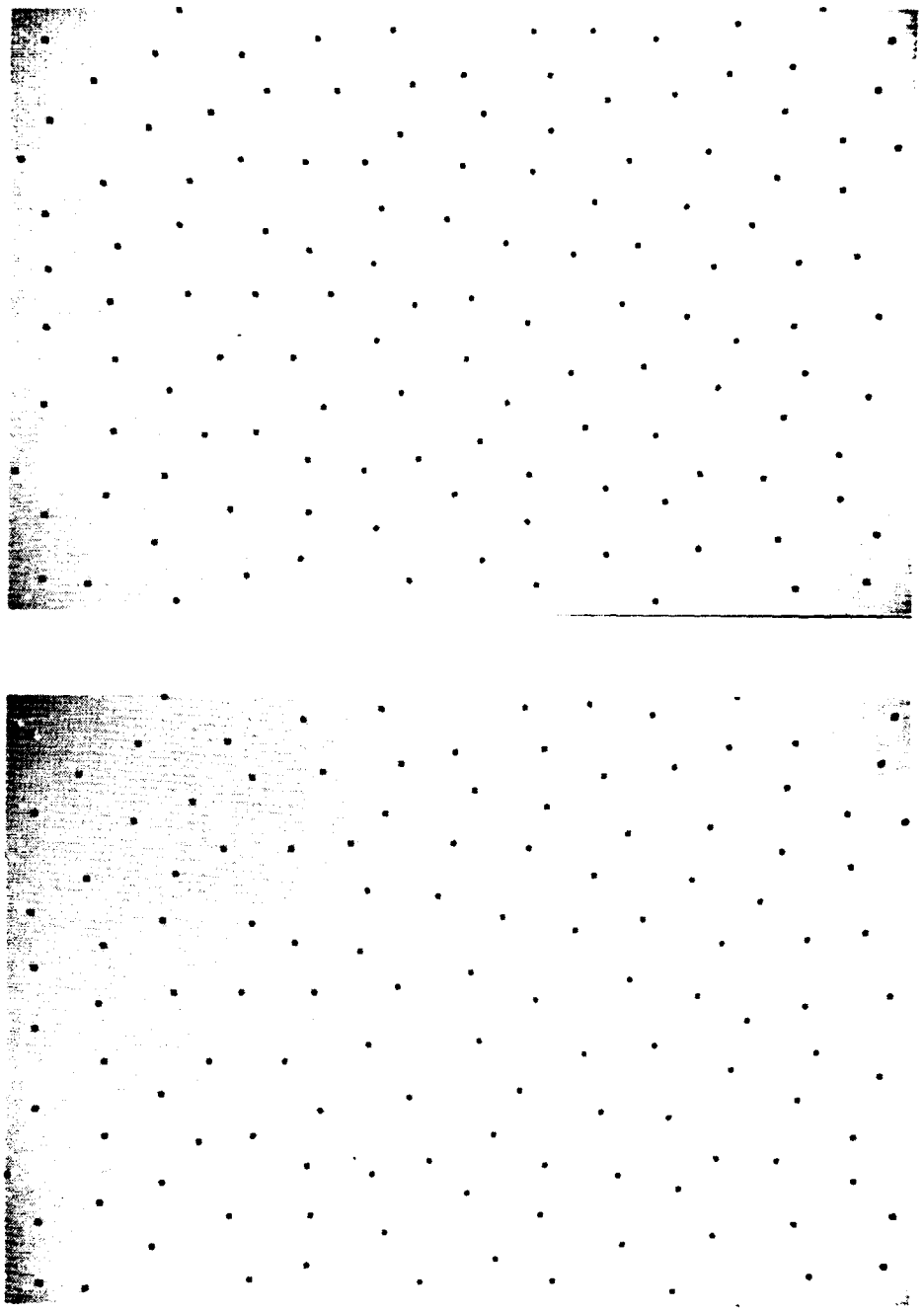

Figure 11. Experimental stimuli for examining effect of contrast reversal in dot pairing.

An ANOVA was performed to test the significance of this data.. The dot-between and dot-adjacent cases were found to be significantly different ($F(7, 1) = 37.3$). There was also a significant difference between Glass pattern types ($F(14, 2) = 11.8$) indicating that the difference was due to the concentric and radial patterns. There also appears to be a secondary effect for most subjects. In many instances of the dot-

between condition induced a reversal, where subjects indicated the radial pattern when the concentric pattern was presented and the concentric pattern when the radial pattern was presented. In some cases this constituted an almost complete perceptual reversal. In others simply a greater number of responses in the direction of the reversal than for the correct pattern.

Discussion

Despite the earlier evidence against the model that dot groupings are performed by simple cells, this experiment provides, we believe, strong evidence that implicate their involvement, in much the manner originally proposed by Glass and Prazdny. The extinction of apparent organization among the white dots by the inclusion of black dots at the midpoint between each pairing is consistent with the gating nonlinearity finding reported earlier and, as yet, has not been associated with any other mechanism.

In addition, there is a secondary effect of apparent reversal, such that a radial Glass pattern may appear concentric when the opposite contrast dots are placed between the original dot pairs, and vice versa, for most observers we tested. This shows that is there not only a gating or suppression of the output of striate cells by the opposing contrast but also a facilitation of the perpendicular orientation. This is similar to the subtle effect shown in (Glass & Switkes 1976) in which paired black and white dots are perceived as having a roughly orthogonal organization to that suggested by the pairings. Glass (1979) proposes that those simple cells positioned between the black and white dots and oriented perpendicularly to the dot pair may be weakly stimulated. While perpendicularly oriented receptive fields may contribute to the phantom impression of orthogonal orientation, we should note that more is likely involved since it the experiment we found that few subjects experienced complete reversals in apparent organization. But overall, we conclude that manipulation of apparent organization by the position of the opposite contrast dots is strong evidence implicating contrast-summation receptive fields in the extraction of the local orientation mechanism.

We are still faced with the rather convincing arguments reported earlier against simple cells being the mechanism used for grouping discrete points. These, recall were the demonstrations of apparent organization in energy-balanced dot patterns (e.g. made of Laplacian-shaped luminance features) and the observed preference for similarity in dot groupings.

		dot in triple			dot not in triple		
subject		con	rad	ran	con	rad	ran
1	con	20	0	0	2	8	10
	rad	1	14	5	12	7	1
	ran	1	0	19	1	0	19
2	con	20	0	0	1	19	0
	rad	0	20	0	16	1	3
	ran	0	0	20	1	0	19
3	con	18	1	1	7	5	8
	rad	0	19	1	7	8	5
	ran	0	1	19	0	2	18
4	con	17	1	2	4	0	16
	rad	0	6	14	10	3	7
	ran	0	0	20	0	0	20
5	con	20	0	0	2	17	1
	rad	1	15	4	20	0	0
	ran	1	1	18	2	3	15
6	con	19	1	0	0	11	9
	rad	0	16	4	16	3	1
	ran	1	1	18	1	1	18
7	con	20	0	0	16	0	4
	rad	0	18	2	6	12	2
	ran	1	4	15	1	5	14
8	con	16	1	3	12	3	5
	rad	1	16	3	1	16	3
	ran	1	0	19	2	5	13

Table 3. Raw data for experiment. Rows represent responses for a particular pattern.

We have already cited neurophysiological evidence that simple cells do not perform strict linear summation when presented with opposite contrast within their excitatory subfields. The energy-balanced dot pattern demonstrations rested on a similar assumption about the summation properties of simple cells. It was assumed that contrast features having only very high spatial frequency content would not provide effective input to receptive fields sufficiently large as to span two such features. While apparently valid on the basis of optimal spatial frequency tuning of cortical receptive fields as a function of their size, one cannot rule out the possibility that large cortical receptive fields receive input from very small LGN fields. If that were the case, the various demonstrations involving high spatial frequency stimuli would be invalid.

The second line of evidence concerns similarity grouping. We believe that the various demonstrations of similarity preference are valid, and this must be reconciled with the underlying role of elongated cortical cells in detecting or encoding the pairing orientation.. The preference for color similarity demonstrated by rivalrous Glass patterns (Stevens & Brookes 1987) must either be directly attributed to color specificity of corresponding cortical receptive fields or associated with later selection processes. Since pairings can also be made between dots of similar contrast, at least part of the selection would presumably be performed later.

Prazdny (1986) suggests that simple cells detect orientations within separate feature spaces. His example of feature spaces is the separation of dark and light points due to the separation of the on and off cells in the retina. This idea may account for many of the properties of dot grouping if we broaden the notion of feature spaces so that it includes each of the features that seem to control the grouping. Along with each of these feature spaces must be a mechanism tuned to that property so that it may be distinguished.

2.4 Connecting Contour Fragments across Gaps

One of the first problems in bootstrapping forms is to connect fragments of the boundary that, for one reason or another, are disconnected. It seems that the size of the gap can have a great effect on how the constituent parts are treated. For large gaps the parts are seen as separate units, while for sufficiently small gaps the parts form a single unit which in some ways is equivalent to a continuous contour. The critical size of the gap seems to scale with the size of the contour fragments. Some of the problems are: what properties are retained by the individual pieces when they are connected, which are lost, and what are the relationships of this property to oriented receptive fields?

Within a critical distance, we have found that separate pieces of contour are treated as single entities. This behavior would be expected at the limit of resolution where the gap may simply be ignored, but the property seems to scale with the size of the contour segments.

Recently, Julesz (1986) found that there are two critical distances in texture discrimination. The first, which Julesz calls delta, is the distance between texture elements. The second, epsilon, is the distance between the pieces that make up the individual texture elements. The significance of the epsilon distance is that texture elements within epsilon of each other are combined into a single element. These distances are relative to the size of the texture element and are thus similar to the property we found with regard to contour aggregation. An example of this property is shown in figure 12. In figure 12*a* the gap between the crosses is small and the figure is seen as a grid. In figure 12*b* the gap is greater than the critical distance so the figure is seen as a collection of crosses. In figures 12*c* and 12*d* the grids have been doubled in size with the gaps doubling as well. In figure 12*c* the grid is seen while in figure 12*d* the crosses are seen. Thus the critical distance scales with the size of the crosses. These demonstrations, of course, are preliminary and will require formal experiments. Tentatively, however, we conclude that the ability to group across gaps is dependent on the sizes of the constituent parts in the grouping. When the crosses are skewed so that the ends do not line up there is a similar critical distance for the gaps, so that if the gap is smaller a grid is seen, and if larger, the crosses are seen (figure 13). This distance seems to be smaller than that of the collinear crosses, but careful experiments must be performed before this is known.

Kulikowski (1969) has shown a length-dependent effect on contrast threshold for detection of a straight line up to a length of 60 arc min (and corresponding width summation up to about 6 arc min). This 60 arc min summation area is presumed to be the overall span of facilitatory interaction among collinear subunits, each about 9 arc min in length (Andrews 1967a, b; Bacon & King-Smith 1977). Thus, there is psychophysical evidence for facilitation across collinear receptive fields. This detection is degraded by gaps more than expected by linear summation (Andrews 1967b; Sakitt 1971). However, it is possible that this intolerance to gaps has no relation to the present problem since our stimuli are well above the detection threshold.

Recent anatomical and physiological work supports our findings. Gilbert and Wiesel (1979, 1983) have shown that single striate cortical cells have dendrites that are located at some distance from the cell body. Ts'o et al. (1986b) demonstrated that interactions between neurons in different cortical columns are constrained by orientation. Thus, stimuli of the same orientation but in different retinal locations mutually reinforce activity in the same groups of neurons. In some cases, parallel orientations may be reinforced, but in others, collinearity may be signalled.

The property of connecting contour fragments into a single unit is suggestive of the notion of an "emergent feature". Pomerantz et al. (1977) suggested under certain circumstances discrete items can combine into single elements and take on properties that the individual elements did not posses alone. Thus, discrimination between two elements may be facilitated when an emergent feature is present in one element but not in the other. Another way to state this is that discrimination means the detection of emergent features.

Treisman (1984) extended this work by showing that the presence of an emergent feature was sufficient to distinguish an object from a field of objects lacking that feature. She further showed that the emergent property was distinct from the individual parts that formed the feature. For example, when the visual system is overloaded by many distractors consisting of elements in the shape of a "V", the closure property can be transferred from a circle to a conjunction of features forming an illusory triangle. The independence of the property from the object suggests a separate level or map at which the emergent feature is being detected.

The demonstration above in figure 12 shows that even though the gaps between the crosses are still apparent there is a level at which the gaps are ignored, resulting in a larger connected form. This larger form acts as an emergent feature, which can be demonstrated in the same manner in which Treisman (1984) demonstrated other emergent features. Treisman showed that an object can be distinguished preattentively from a field of similar objects if the given object differs from the field in a single feature. This is true for primitive features as well as emergent features.

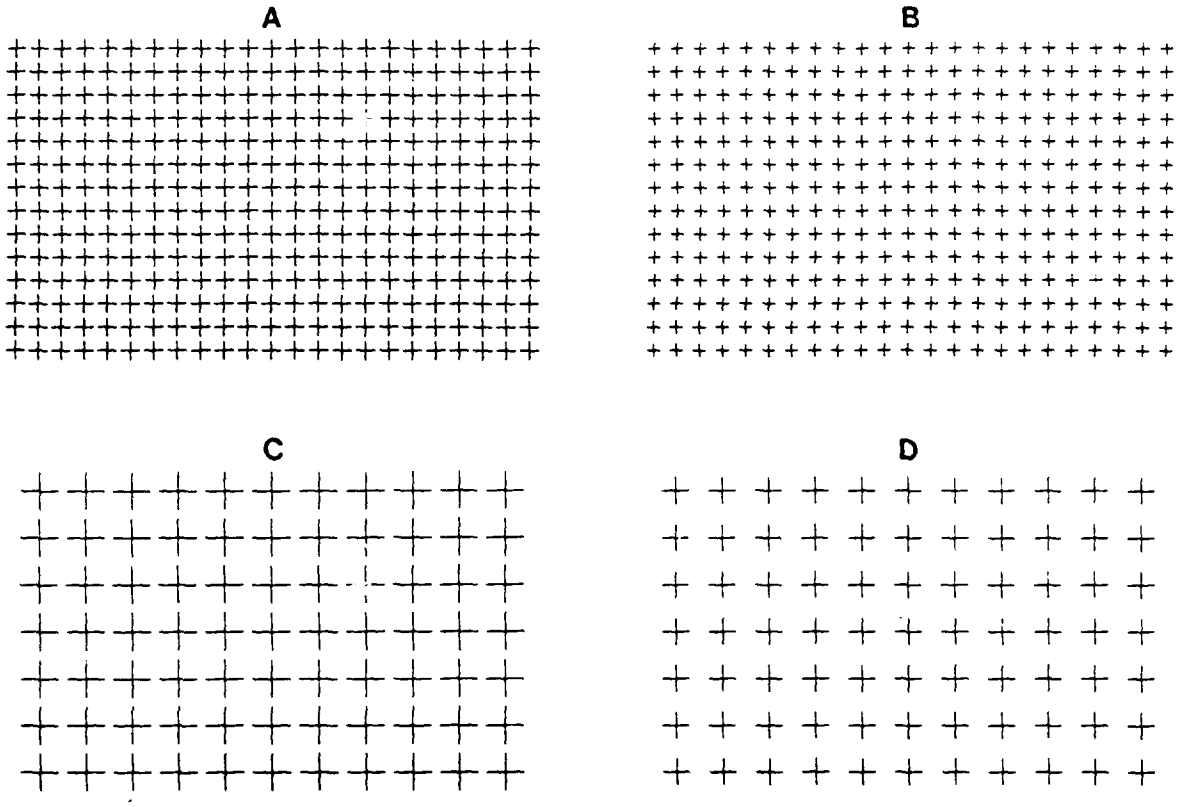

Figure 12. In a and c the gaps are small and the figure is seen as a grid. In b and d the gaps are large and the figure is seen as separate crosses.

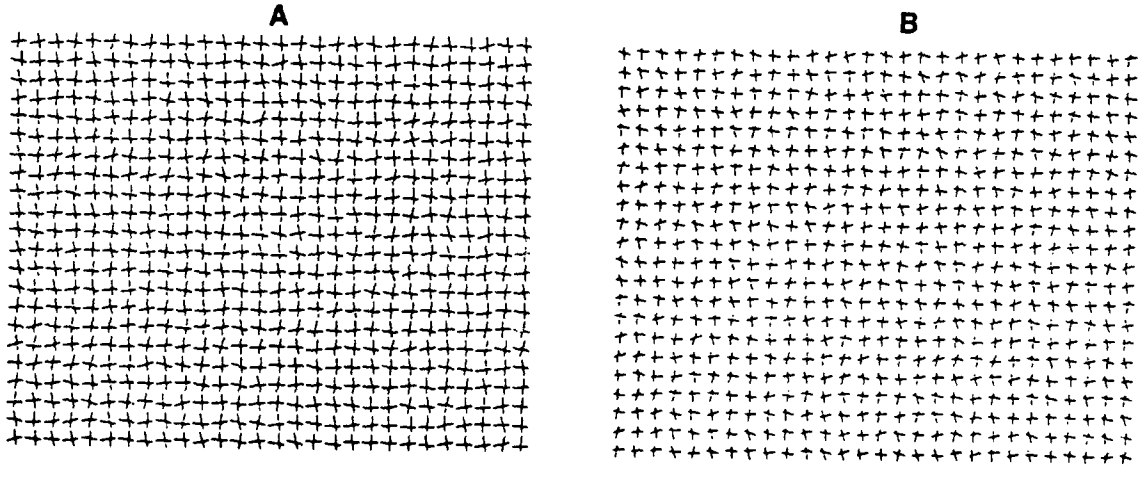

Figure 13. As in figure 12 a is seen as a grid even though the lines are skewed and b is seen as separate crosses.

3. REFERENCES

Andrews, D.P. 1967a Perception of contours in the central fovea. Part I: Short lines. *Vision Research* 7, 975-997.

Andrews, D.P. 1967b Perception of contours in the central fovea. Part I: Spatial Integration. *Vision Research* 7, 999-1013.

Atneave, F. 1954 Some informational aspects of visual perception. *Psychological Review* **61**, 183-193.

Attneave, F. 1955 Perception of place in a circular field. *American Journal of Psychology* **68**, 69-82.

Attneave, F. 1974 Apparent movement and the what-where connection. *Psychologia* **17**, 108-120.

Bacon, J. & King-Smith, P.E. 1977 The detection of line segments. *Perception* **6**, 125-131.

Barlow, H.B. & Levick, W.R. 1969 Changes in the maintained discharge with adaptation level in the cat retina. *Journal of Physiology (London)* **202**, 699-718.

Beck, J. & Halloran, T. 1985 Effects of spatial separation and retinal eccentricity on two-dot vernier acuity. *Vision Research* **25**, 1105-1111.

Bishop, P.O & Henry, G.H. 1972 Striate neurones: receptive field concepts. *Investigative Ophthalmology* **11**, 346-355.

Bishop, P.O, Coombs, J.S & Henry, G.H. 1971 Responses to visual contours: spatio-temporal aspects of excitation in the receptive fields of simple striate neurones. *Journal of Physiology (London)* **219**, 625-657.

Brookes, A. & Stevens, K.A. 1989 Symbolic grouping versus simple cell models, in preparation.

Caelli, T.M. & Julesz, B. 1978 On perceptual analyzers underlying visual texture discrimination: Part I. *Biological Cybernetics* **28**, 167-175.

Caelli, T.M., Preston, G.A.N., & Howell, E.R. 1978 Implications of spatial summation models for processes of contour perception: a geometric perspective. *Vision Research* **18**, 723-734.

Carlson, C.R., Anderson, C.H. & Moeller, J.R. 1980 Visual illusions without low spatial frequencies. *Investigative Ophthalmology and Visual Science* **19**, 165.

Daugman, J.G.1985 Uncertainty relation for resolution in space, spatial frequency, and orientation optimized by two-dimensional visual cortical filters. *Journal of the Optical Society of America* **2**, 1160-1169.

Dobbins, A., Zucker, S.W., and Cynader, M.S. 1987 Endstopped neurons in the visual cortex as a substrate for calculating curvature. *Nature* **329**, 438-441.

Foley, J.& McCourt, M.E. 1985 Visual grating induction. *Journal of the Optical Society of America* **2**,1220-1230.

Fraser, J. 1908 A new illusion of visual direction. *British Journal of Psychology* **2**, 307-320.

Gelb, D.J. & Wilson, H.R. 1983 Shifts in perceived size as a function of contrast and temporal modulation. *Vision Research* **23**, 71-82.

Gilbert, C.D. & Wiesel, T.N. 1979 Morphology and intracortical projections of functionally identified neurons in cat visual cortex. *Nature* , 120-125.

Gilbert, C.D., & Wiesel, T.N. 1983 Clustered intrinsic connections in the cat visual cortex. *Journal of Neuroscience* **3**, 1116-1133.

Ginsberg, A.P.1973 Pattern recognition techniques suggested from psychological correlates of a model of the human visual system. 1973 *IEEE Transactions of Aerospace Electronics* **9**, 625-635.

Glass, L. 1969 Moire effect from random dots. *Nature* **223**, 578-580.

Glass, L. & Perez 1973 Perception of random dot interference patterns. *Nature* **246**, 360-362.

Glass, L. & Switkes, E. 1976 Pattern recognition in humans: correlations which cannot be perceived. *Perception* **5**, 67-72.

Glass, L. 1979 Physiological mechanisms for the perception of random dot moire patterns. In *Pattern formation by dynamic systems and pattern recognition.* H. Haken, ed. Berlin: Springer-Verlag.

Glunder, H. 1986 Neural computation of inner geometric pattern relations. *Biological Cybernetics* **55**, 239-251.

Gregory, R. L. & Heard, P. 1979 Border locking and the cafe wall illusion. *Perception.* **8**, 365-380.

Grossberg, S. 1982 *Studies of mind and brain: Neural principles of learning, perception, development, cognition, and motor control.* Boston: Reidel Press.

Grossberg, S. & Mingolla, E. 1985 Neural dynamics and perceptual groupings: Textures, boundaries, and emergent segmentations *Perception & Psychophysics* **38**, 141-171.

Hammond, P. & MacKay, D.M. 1981 Suppressive of luminance gradient reversal on simple cells in cat striate cortex. *Journal of Physiology (London)* **315**, 30P

Hammond, P. & MacKay, D.M. 1983a Influence of luminance gradient reversal on simple cells in feline striate cortex. *Journal of Physiology (London)* **337**, 69-87.

Hammond, P. & MacKay, D.M. 1983b Effects of Luminance gradient reversal on complex cells in cat striate cortex. *Experimental Brain Research* **49**, 453-456.

Hammond, P. & MacKay, D.M. 1985 Influence of luminance gradient reversal on complex cells in feline striate cortex. *Experimental Brain Research* **359**, 315-329.

Heggelund, P., Krekling, S., & Skottun, B. 1983 Spatial summation in the receptive field of simple cells in the cat striate cortex. *Experimental Brain Research* **52**, 87-98.

Hendrickson, A.E. 1985 Dots, stripes, and columns in monkey visual cortex. *Trends in Neuroscience* **8**, 406-410.

Henry, G.H., Goodwin, A.W. & Bishop, P.O. 1978 Spatial summation of responses in receptive fields of single cells in cat striate cortex. *Experimental Brain Research* **32**, 245-266.

Horton, J.C. & Hubel, D.H. 1981 A regular patchy distribution of cytochrome oxidase staining in primary visual cortex of the macaque monkey. *Nature* **292**, 605-607.

Hubel D.H., & Livingstone, M.S. 1987 Segregation of form, color and stereopsis in primate area 18. *Journal of Neuroscience* **11**, 3378-3415.

Hubel, D.H. & Wiesel, T.N. 1962 Receptive fields, binocular interaction and functional architecture in the cat's visual cortex. *Journal of Physiology (London)* **160**, 106-154.

Hubel, D.H. & Wiesel, T.N. 1968 Receptive fields and functional architecture of monkey striate cortex. *Journal of Physiology (London)* **195**, 215-243.

Janez, L. 1984 Visual grouping without low spatial frequencies. *Vision Research* **24**, 271-274.

Julesz, B. 1978 Perceptual limits of texture discrimination and their implications to figure-ground separation. In *Formal theories of visual perception*. Leeuwenberg, E.L.J and Buffart, H.F.J.M. Eds. Wiley, Chichester.

Julesz, B. 1981 Figure and ground perception in briefly presented isodipole textures. In *Perceptual organization*, Koehler, W. 1929 *Gestalt Psychology*. New York: H. Liveright.

Koenderink, J.J. 1984 The structure of images. *Biological Cybernetics* **50**, 363-370.

Koenderink, J.J. & van Doorn, A.J. 1987 Representation of local geometry in the visual system. *Biological Cybernetics* **55**, 367-375.

Koffka, K. 1935 *Principles of Gestalt Psychology*. New York: Harcourt, Brace.

Kulikowski, J.J. 1969 Limiting conditions of visual perception (in Polish and English translation) *Prace Instytuto Automatyki Polskiej Akademji Nauk Warsaw* **77**, 1-133.

Kulikowski, J.J. & ..ing-Smith, P.E.1973 Spatial arrangement of line, edge and grating detectors revealed by subthreshold summation. *Vision Research* **13**, 1455-1478.

Livingstone, M. H. & Hubel, D.H. 1984 Anatomy and Physiology of a color system in the primate visual cortex. *Journal of Neuroscience* **4**, 309-356.

Livingstone, M.H. & Hubel, D.H 1987 Psychophysical evidence for separate channels for the perception of form, color, movement, and depth. *Journal of Neuroscience* **7(11)**, 3416-3468.

Lulich, D.P., & Stevens, K.A. 1988 Differential contributions of circular-symmetric and elongated receptive fields to the Cafe Wall illusion. In preparation.

Marr, D. 1976 Early processing of visual information. *Philosophical Transactions of the Royal Society of London Series B* **275**, 483-524.

Marr, D. 1982 *Vision*. San Francisco: Freeman.

Marr, D. & Hildreth, E. 1980 Theory of edge detection. *Proceedings of the Royal Society of London Series B* **207**, 187-217.

Marr, D., Poggio, T. & Hildreth, E. 1980 Smallest channel in early human vision. *Journal of the optical Society of America* **70**, 868-870.

Marrocco, R.T. 1972 Responses of monkey optic tract fibers to monochromatic light. *Vision Research* **12**, 1167-1174.

Mather, G. & Morgan, M. J. 1986 Irradiation: implications for theories of edge localization. *Vision Research* **26**, 1007-1015.

McCourt, M. E. 1983 Brightness induction and the Café wall illusion. *Perception* **12**,131-142.

McCulloch, W.S. & Pitts, W. 1943 A logical calculus of the ideas immanent in nervous activity. *Bulletin of Mathematical Biophysics* **5**, 115-133.

Moran, J.& Desimone, R. 1985 Selective attention gates visual processing in the extrastriate cortex. *Science* **229**, 782-784.

Morgan, M.J., Mather, G., Moulden, BP, Watt, RJ 1984 Intensity response nonlinearities and the theory of edge localization. *Vision Research* **24**, 713-719.

Morgan, M. J. & Moulden, B. 1986 The Münsterberg figure and twisted cords. *Vision Research* **26**, 1793-1800.

Morgan, M.J. & Ward, R.M. 1985 Spatial and spatial-frequency primitives in spatial interval discrimination. *Journal of the Optical Society of America* **7**, 1205-1210.

Moulden, B. & Renshaw, J. 1979 The Munsterberg illusion and irradiation. *Perception* **8**, 275-301.

Movshon, J.A., Thompson, I. D. & Tolhurst, D. J. 1978 Spatial summation in the receptive fields of simple cells in the cat's striate cortex. *Journal of Physiology (London)* **283**, 53-77.

Pomerantz, J.R., Sager, J. C., & Stoever, R. J. 1977 Perception of wholes and their component parts: some configural superiority effects. *Journal of Experimental Psychology: Human Perception and Performance* **3**, 422-435.

Prazdny, K. 1984 On the perception of Glass patterns. *Perception* **13**, 469-478.

Prazdny, K. 1986 Some new phenomena in the perception of Glass patterns. *Biological Cybernetics* **53**, 153-158.

Richter, J. & Ullman, S. 1982 A model for the temporal organization of X- and Y-type receptive fields in the primate retina. *Biological Cybernetics* **43**, 127-145.

Sakitt, B. 1971 Configuration dependence of scotopic spatial summation. *Journal of Physiology (London)* **216**, 513-528.

Shapley, R.M. & Tolhurst, D.J.1973 Edge detectors in human vision. *Journal of Physiology (London)* **229**, 165-183.

Smits, J.T.S. & Vos, P.G. 1986 A model for the perception of curves in dot figures: the role of local salience of virtual lines. *Biological Cybernetics* **54**, 407-416.

Stevens, K.A. 1978 Computation of locally parallel structure. *Biological Cybernetics* **29**, 19-28.

Stevens, K.A. 1989 Distinguishing line- versus edge-like luminance changes. In preparation.

Stevens, K.A. & Brookes, A. 1987 Detecting Structure by Symbolic Constructions on Tokens. *Computer Vision, Graphics, and Image Processing* **37**, 238-260.

Stone, J. & Fukuda, Y. 1974 Properties of cat retinal ganglion cells: a comparison of W-cells with X-cells and Y-cells. *Journal of Neurophysiology* **37**, 722-748.

Treisman A. 1985 Preattentive processing in vision. *Computer Vision, Graphics, and Image Processing* **31**, 156-177.

Ts'o, D., Gilbert, C.D., & Wiesel, T.N. 1986a Relationships between color specific cells in cytochrome oxidase-rich patches of monkey striate cortex. *Society for Neuroscience Abstracts* **12**, 1497.

Ts'o, D., Gilbert, C.D., & Wiesel, T.N. 1986b Relationships between horizontal interactions and functional architecture in cat striate cortex as revealed by cross-correlation analysis. *Journal of Neuroscience* **6**, 1160-1170

Tyler, CW, Nakayama K 1984 Size interactions in the perception of orientation. In: Spillman, L, Wooton BR (eds) Sensory experience, adaptation and perception: Festschrift for Ivo Kohler. Lawrence Earlbaum, Hillsdale, N.J., 529-546.

Ullman, S. 1979 *The interpretation of visual motion*. Cambridge, MA: MIT Press.

Watt R.J. & Morgan, M.J. 1985 A theory of the primitive spatial code in human vision. *Vision Research* **25**, 1661-1674.

Webster, M.W. & De Valois, R.L. 1985 Relationship between spatial-frequency and orientation tuning of striate-cortex cells. *Journal of the optical Society of America* **2**, 1124-1132.

Wertheimer, M. 1929 Untersuchungen zur Lehre von der Gestalt. *Psych. Forch.* **4**, 301-350. Abridged translation: *Principles of perceptual organization.* In *Readings in Perception*, 1958, D. C. Beardslee & M. Wertheimer, Eds. New York: D. Van Nostrand.

Wilson, H.R. 1986 Responses of spatial mechanisms can explain hyperacuity. *Vision Research* **26**, 453-469.

Wilson, H.R. and Bergen, J.R. 1979 A four mechanism model for threshold spatial vision. Vision Research 19,19-32.

Wong-Riley, M.T.T. 1978 Changes in the visual system of monocularly sutured or enucleated cats demonstrable with cytochrome oxidase histochemistry. *Brain Research* **171**, 11-28.

Zucker, S.W. 1983 Computational and psychophysical experiments in grouping: early orientation selection. In *Human and machine vision*, Beck, J., Hope, B., & Rosenfeld, A., eds. 545-567.

4. Publications, Meetings and Personnel

Refereed Publications:

Stevens, K.A. 1986 Autocorrelation has no merit in 3-D, figuratively. Review of: W.R. Uttal 1985, *The Detection Nonplanar surfaces. Contemporary Psychology* **31**, 23-24.

Stevens, K.A. 1986 3-D shape from 2-D contour. Invited paper, *Proceedings of the Annual Meeting of the Optical Society of America*, Seattle, Washington, October.

Stevens, K.A. & Brookes, A. 1987 Detecting structure by symbolic constructions on tokens. *Computer Vision, Graphics, and Image Processing* **37**, 238-260.

Stevens, K.A. & Brookes, A. 1987 Probing depth in monocular images. *Biological Cybernetics* **56**, 355-366.

Stevens, K.A. & Brookes, A. 1987 Depth reconstruction in stereopsis. *Proceeding of the First IEEE International Conference on Computer Vision*, London, June.

Stevens, K.A. 1987 Implicit and Explicit Computation. Commentary on: Neuroethology of releasing mechanisms: Prey-catching in toads, by J.E. Ewert. *Behavioral and Brain Sciences* **10:3**, 387-388.

Stevens, K.A. & Brookes, A. 1988 Integrating stereopsis with monocular interpretations of planar surfaces. *Vision Research* **28**, 371-386.

Stevens, K.A. & Brookes, A. 1988 The convex cusp as a determiner of figure-ground. *Perception* **17**, 35-42.

Stevens, K.A. 1988 Differential Coupling for Detection versus Discrimination. Commentary on: *Sensory Analysis* by D. Laming. *Behavioral and Brain Sciences* **11:2**, 310-311.

Brookes, A. & Stevens, K.A. 1988 Binocular depth from surfaces vs. volumes. *Journal of Experimental Psychology: Human Perception and Performance*, in press.

Brookes, A. & Stevens, K.A. The analogy between stereo depth and brightness. Submitted.

Brookes, A. & Stevens, K.A. Symbolic grouping versus simple cell models. Submitted.

Lulich, D. P. & Stevens, K.A. Differential contributions of circular and elongated spatial filters to the Café wall illusion. Submitted.

Book Chapters:

Stevens, K.A. 1986 Inferring shape from contours across surfaces. In *From Pixels to Predicates: Recent Advances in Computational Vision.* A.P. Pentland, ed., 93-110. Norwood, N.J.: Ablex.

Stevens, K.A. 1988 Visual object perception from a computational perspective. In *Visual object processing*, G. Humphreys & J. Riddoch, eds., 17-42. New York: Erlbaum.

Stevens, K.A. 1988 The perception of three-dimensionality across continuous surfaces. To appear as a chapter of a forthcoming book, S. Ellis, ed. New York: Lawrence Erlbaum Associates.

Technical reports:

Beck, J. & Stevens, K.A. 1986 Visual representations subserving texture perception. Final Report AFOSR Contract Number F4962-083-C-0093.

Stevens, K.A. & Beck, J. 1986 On the integration of depth information. Final Report ONR Contract Number N00014-84-K-0533.

Beck, J. & Stevens, K.A. 1988 Representing visual texture. Final Report AFOSR Grant Number AFOSR-85-0359.

Stevens, K.A. & Brookes, A. 1988 Binocular depth and the perception of visual surfaces. Technical Report 88-01, Office of Naval Research Contract Number N0014-87-K-0321

Stevens, K.A. & Brookes, A. 1988 Reconstruction of binocular depth across continuous surfaces. Technical Report 88-02, Office of Naval Research Contract Number N0014-87-K-0321

Meetings

"Localization of point-like grouping tokens". Third Human and Machine Vision Workshop. Boston, Massachusetts, November, 1985.

"Grouping tokens and attribute selection". Eleventh Annual Interdisciplinary Conference, Whistler, British Columbia, February, 1986.

"Integrating stereopsis and monocular surface interpretations". Visual Perception and Neural Computation, ONR principal investigators meeting, Endicott House, Massachusetts Institute of Technology. June, 1986.

"3-D shape from 2-D contour". Invited talk, Optical Society of America, Seattle, Washington. October, 1986.

"Local geometric evidence for figure-ground". Twelfth Annual Interdisciplinary Conference, Jackson, Wyoming, January, 1987.

"Theory of depth reconstruction in stereopsis". Invited talk, University of California, Berkeley. May, 1987.

"The perception of three-dimensionality across continuous surfaces". Invited talk, Spatial Displays and Spatial Instruments. NASA-sponsored symposium and workshop. Asilomar, California. August, 1987.

"Geometric interpretation of luminance changes". Review of Vision Research, Air Force Office of Scientific Research. Annapolis, Maryland. December, 1987.

"Integrating Stereopsis and monocular depth". Thirteenth Annual Interdisciplinary Conference, Jackson, Wyoming, January, 1988.

Personnel

Allen Brookes (Ph.D. Summer, 1988)

Daniel Lulich

Marek Lees